REGULATORY INFORMATION DISTRIBUTION SYSTEM (RIDS)

ACCESSION NBR: 8606300263 DOC. DATE: 86/06/26 NOTARIZED: NO DOCKET #
FACIL: 50-250 Turkey Point Plant, Unit 3, Florida Power and Light C 05000250
50-251 Turkey Point Plant, Unit 4, Florida Power and Light C 05000251
AUTH. NAME AUTHOR AFFILIATION
WOODY, C. O. Florida Power & Light Co.
RECIP. NAME RECIPIENT AFFILIATION
RUBENSTEIN, L. S. PWR Project Directorate 2

SUBJECT: Forwards addl info re NUREG-0737, Item II.D.1 re performance testing of relief & safety valves, in response to NRC 850714 request. "See Repts"

DISTRIBUTION CODE: A046D COPIES RECEIVED: LTR 1 ENCL 3 SIZE: 100
TITLE: OR Submittal: TMI Action Plan Rgmt NUREG-0737 & NUREG-0660

NOTES:

	RECIPIENT ID CODE/NAME		COPIES LTTR	COPIES ENCL	RECIPIENT ID CODE/NAME		COPIES LTTR	COPIES ENCL
	PWR-A ADTS		1	1	PWR-A EB		1	1
	PWR-A EICSB		2	2	PWR-A FOB		1	1
	PWR-A PD2 LA		1	0	PWR-A PD2 PD 01		5	5
	McDONALD, D		1	1	PWR-A PSB		1	1
	PWR-A RSB		1	1				
INTERNAL:	ADM/LFMB		1	0	ELD/HDS4		1	0
	IE/DEPER DIR 33		1	1	IE/DEPER/EPB		3	3
	NRR BWR ADTS		1	1	NRR PAULSON, W.		1	1
	NRR PWR-A ADTS		1	1	NRR PWR-B ADTS		1	1
	NRR/DHFT		1	1	NRR/DSRO EMRIT		1	1
	REG FILE	04	1	1	RGN2		1	1
EXTERNAL:	LPDR	03	1	1	NRC PDR	02	1	1
	NSIC	05	1	1				

TOTAL NUMBER OF COPIES REQUIRED: LTTR 31 ENCL 28

[illegible]

P. O. BOX 14000, JUNO BEACH, FL 33408

FLORIDA POWER & LIGHT COMPANY

JUN 2 6 1986

L-86-241

Office of Nuclear Reactor Regulation
Attention: Mr. Lester S. Rubenstein, Director
PWR Project Dictorate #2
Division of PWR Licensing - A
U. S. Nuclear Regulatory Commission
Washington, D.C. 20555

Dear Mr. Rubenstein:

Re: Turkey Point Units 3 and 4
Docket Nos. 50-250 and 50-251
NUREG-0737, Item II.D.1
Performance Testing of Relief and Safety Valves -
Request for Additional Information
NRC TAC Nos. 44626 and 44627

Attached is the information requested in your July 14, 1985 letter relating to NUREG-0737, Item II.D.1, Performance Testing of Relief and Safety Valves.

If you have any further questions, please call us.

Very truly yours,

C. O. Woody
Group Vice President
Nuclear Energy

COW/TCG/cab

Attachment

cc: Harold F. Reis, Esquire
Dr. J. Nelson Grace, NRC Region II

TCG5/001/1

A046
1/3

NRC REQUEST FOR ADDITIONAL INFORMATION

NUREG-0737, ITEM II.D.1

PERFORMANCE TESTING OF RELIEF AND SAFETY VALVES

Questions Related To Selection of Transients and Inlet Fluid Conditions:

Question 1

The Westinghouse valve inlet fluid conditions report stated that liquid discharge through both the safety and power operated relief valves (PORVs) is predicted for a FSAR feedline break event. The Westinghouse report gave expected peak pressure and pressurization rates for some plants having a FSAR feedline analysis. The Turkey Point Units 3 and 4 plants were not included in this list of plants having such a FSAR analysis. Nor does the plant specific submittal address the FSAR feedline break event. NUREG-0737, however, requires analysis of accidents and occurrences referenced in Regulatory Guide 1.70, Revision 2, and one of the accidents so required is the feedline break. Provide a discussion on the feedwater line break event either justifying that it does not apply to this plant or identifying the fluid pressure and pressurization rate, fluid temperature, valve flow rate, and time duration for the event. Assure that the fluid conditions were enveloped in the EPRI tests and that the time period of water relief in the EPRI tests was as long as expected at the plant. Demonstrate operability of the safety valves and PORVs for this event and assure that the feedline break event was considered in analyses of the piping system.

Response

The feedwater line break event is not a design basis event for Turkey Point. The Westinghouse Owner's Group is considering a project authorization to address this issue for plants that do not have a FSAR feedline break analysis.

Question 2

Since the Crosby 4K26 safety valve, which is used at Turkey Point Units 3 and 4, was not tested in the EPRI program, the Crosby 3K6 valve was chosen to be representative of the valves at Turkey Point. Results of the EPRI loop seal tests and steam tests on the 3K6 valve indicate that the test blowdowns well exceeded the design value of 5%. If the blowdowns expected for the plant also exceed 5%, the higher blowdowns could cause a rise in pressurizer water level such that water may reach the safety valve inlet line and result in a steam-water flow situation. Also the pressure might be sufficiently decreased that flashing occurs in the primary loop or the reactor vessel, natural circulation is interrupted, and adequate cooling for decay heat removal is not achieved. Discuss these consequences of higher blowdowns if increased blowdowns are expected.

Response

The impact on the plant safety of excessive pressurizer safety valve blowdowns (up to 14%) has been evaluated for Turkey Point Units 3 and 4. The results of this evaluation showed no adverse effects on plant safety.

Safety valve blowdowns in excess of that assumed in the Turkey Point Unit 3 and 4 FSAR will have the following effect on the events in which safety valve actuation occurs:

1. Increased pressurizer water level during and following the valve blowdown,
2. Lower pressurizer pressure during and following valve blowdown,
3. Increased inventory loss through the valve.

The impact of the increased safety valve blowdowns with respect to the above effects was evaluated for the Turkey Point Units 3 and 4 FSAR events in which the safety valve actuation occurs (i.e., Loss of External Electrical Load and Single Reactor Coolant Pump Locked Rotor).

For the Loss of External Electrical Load event, results from sensitivity analyses performed for a 4-loop plant were used for the evaluation. These analyses investigated the effects of different blowdown rates on the event. Similar results are expected for a 3-loop plant. The results of these analyses showed only marginal increases in pressurizer water volume and the maximum pressurizer water levels were well below the level at which liquid relief would occur. The Turkey Point Units 3 and 4 FSAR analysis results show that a small increase in pressurizer water volume, due to increased safety valve blowdown, would not result in liquid relief. The sensitivity analyses also showed that peak RCS pressures were unaffected by the increased blowdowns. The increased blowdowns did result in lower pressurizer pressure and increased RCS inventory loss, however, these had no adverse impact on the event and adequate decay heat removal was maintained.

For the Single Reactor Coolant Pump Locked Rotor event, increased safety valve blowdowns have little impact. As analyzed and presented in the Turkey Point Units 3 and 4 FSAR, the opening and closing of the safety valve occurs over a short time period (less than 4 seconds). As a result, there is little change in either pressurizer level or RCS inventory. Increased safety valve blowdowns would have no impact on peak pressure, peak clad temperature, or minimum DNBR as these occur prior to the closing of the safety valve.

Question 3

According to the Westinghouse valve inlet fluid conditions report, operation of the PORV at a predetermined set point pressure is employed to arrest cold overpressure transients in Westinghouse plants. According to this report, the PORVs are expected to operate over a range of steam, steam/water, and water conditions because of the potential presence of a steam bubble in the pressurizer. To assure that the PORVs operate for all cold overpressure events, explain what range of fluid conditions is expected for these types of transients at Turkey Point. Identify the EPRI test data that demonstrate PORV operability for these cases.

Response

With regard to the cold overpressure (COP) event, the maximum temperature and pressure conditions that can be achieved at the PORV inlet coincidently occur for steam bubble operation. Since pressure is normally maintained below the PORV setpoint, the maximum steam and saturated liquid pressure maintained in the pressurizer during startup and shutdown operations in anticipation of the COP event would occur at the PORV setpoint. The attached Figures 1 & 2 for Units 3 & 4 respectively show the setpoint curves for PORV opening pressures and temperatures.

EPRI test conditions for the PORVs were chosen based on expected inlet fluid conditions. Tests were limited but designed to confirm operability over a full range of expected inlet conditions. Steam, steam-to-water, and water flow tests were conducted. Results of these tests can be found in EPRI report, EPRI NP-2670-LD, volume F, Table VII-3. Although steam tests were conducted only at the higher pressures, it is expected that satisfactory operation would also result at the less severe lower pressures. This can be seen by the successful low pressure (675 psia), low temperature (105-442°F) water tests.

Questions Related to Valve Operability:

Question 4

The Crosby 4K26 safety valve, which is used at Turkey Point Units 3 and 4, was not tested in the EPRI program. According to the submittal, the Crosby 3K6 valve was chosen to be representative of the Turkey Point valve. The EPRI test results show that this valve had not achieved rated flow at 3% accumulation for loop seal tests at certain ring settings. Provide an evaluation as to whether the plant safety valves will pass rated flow at the ring settings used.

Response

EPRI test results did show the 3K6 valve had not achieved rated flow at 3% accumulation at certain ring settings. In cross referencing EPRI tables, 4-3 and 4-4 in Volume 5 of EPRI Report NP-2770-LD, however, it is found that for steam tests of the 3K6 valve where blowdown was measured to be less than 10%, flow rates of 119-122% of rated flow at 3% accumulation were reported. The EPRI tables indicate that lower than rated flows occurred at blowdowns greater than 15% for the 3K6 valve. Crosby production tests for the Turkey Point valves indicate 5% blowdown with the "as-shipped" ring settings. Since this is within the range where the 3K6 valve achieved rated flow, rated flow can also be expected at 3% accumulation for Turkey Point Safety Valves.

Question 5

The submittal does not identify the ring settings to be used on the Crosby 4K26 safety valves or what effect these settings have on valve performance in the Turkey Point installation. Provide the final ring settings selected for the Turkey Point safety valves and explain which EPRI tests on the Crosby 3K6 valve, if any, had equivalent ring settings. Identify the expected blowdowns corresponding to the ring settings used and verify that the valves will perform their safety function at the blowdown, back pressures and fluid conditions occurring at the plant.

Response

Ring settings "as-shipped" by Crosby:

Valve	Nozzle Ring	Guide Ring	Guide Ring Level
3-RV-551A	-5	-235	-204
3-RV-551B	-5	-235	-201
3-RV-551C	-5	-235	-190
4-RV-551A	-5	-230	-210
4-RV-551B	-5	-235	-213
4-RV-551C	-5	-275	-221

Please note that the ring settings given above were measured from the "highest-locked position," as noted in Crosby procedures and in the EPRI report "Definitions of Key Terms for Safety Valves". Ring settings reported by EPRI were measured from the "level position". The guide ring level position is provided as a reference.

In the past, plant procedures were written such that after maintenance, rings were returned to the "as-found" settings. During the course of several maintenance cycles, this resulted in a drift of a few notches (mostly lower) in the settings of some of the rings. These differences are expected to have negligible impact on valve performance. Regardless, the valves will be reset to the "as-shipped" settings, and applicable procedures revised so that they are consistently returned to these settings.

The as-shipped settings were established by a method which includes a steam operational test on each valve by Crosby. Blowdowns measured during these production tests were equal to, or one-half percent less than, five percent for all valves. The Crosby 3K6 valve tests done with "manufacturer's recommended ring position" had ring settings that were established by the same methods. These tests, performed on a 3K6 valve, rather than Turkey Point's 4K26 valve, may come closest of the EPRI tests to approximating how the valves will perform their pressure relief function in safely shutting down the plant.

Question 6

During an EPRI loop seal steam-to-water transition test on the Crosby 3K6 valve, the valve fluttered and chattered when the transition to water occurred. The test was terminated after the valve was manually opened to stop chattering. Justify that the valve behavior exhibited in this test is not indicative of the performance expected for the Tureky Point Units 3 and 4 valves.

Response

A response to Question 6 is not included at this time pending outcome of WOG review of the feedline break event. This is the only event for which steam-to-water flow may be applicable through the safety valves.

Question 7

NUREG-0737, Item II.D.1. requires that the plant-specific PORV control circuitry be qualified for design-basis transients and accidents. Provide information which demonstrates that this requirement has been fulfilled.

Response

Environmental Criteria

The following Nuclear Safety Related electrical equipment, required for PORV operation and/or monitoring, have been determined to be within the scope of 10 CFR 50.49 and have been qualified for the environmental conditions under which the equipment must function:

- MOV-535, 536
- Limit Switches for PORV's 456 and 455C
- Pressure Transmitters PT-455, 456, 457
- Pressure Transmitters PT-403, 405
- Temperature Element TE-430, 423A
- PORV Accoustic Flow Monitors ZT/ZS 6303 A, 6303 B,6303 C
- Electrical Cables
- Electrical Penetrations
- Electrical Splice Bits
- Conax Miniseals

This equipment can be found listed in the Turkey Point Units 3 and 4 "Environmental Qualification (EQ) list for 10 CFR 50.49". Complete records of the environmental requirements and qualifications can be found in the applicable Environmental Qualification documentation packages.

All other electrical components for indications and/or control, are determined to be outside the scope of 10 CFR 50.49 and no special environmental documentation is required.

These components have been installed taking into consideration their specification and the available environmental data to assure the adequacy of the installation for the specified environmental service.

Seismic Criteria

The PORV's, PORV's Motor Operated block valves and support equipment and systems are classified as Class I structures. Class I structures, systems, equipment and their associated supports, enclosures, piping, wiring, controls, power sources and switch gears are designed to withstand the maximum hypothetical earthquake loads simultaneously with other applicable loads, as given in the Updated Final Safety Analysis Report, Appendix 5A.

Design controls are in place to insure that the seismic integrity of equipment presently installed is maintained.

Question 8

Bending moments are induced on the safety valves and PORV's during the time they are required to operate because of discharge loads and thermal expansion of the pressurizer tank and inlet piping. Make a comparison between the predicated plant moments with the moments applied to the tested valves to demonstrate that the operability of the valves will not be impaired.

Response

From the PLAST analysis (see ref. 1) the results of the modelled run indicate plasticity in the first elbow downstream of the pressurizer and the elbow below the SRV.. The maximum moments computed in the system through the first 70 milliseconds response are shown in the attached Table 1. The table also shows the time at which the maximum moment occurs. This table also indicates the values of 70 percent of the ultimate moment carrying capacity of a pipe of this size. Refer to the response to question 17 for an explanation of the meaning of this term.

In order to compare the predicted plant moments with the moments applied to the tested valves, the following information should be noted. The safety relief valves at Turkey Points Units 3 and 4 are Crosby HB-BP-86 type 4K26. Assembly No. 51249. The seating material is Stellite 6B and the disc holder is stainless steel with stellite lands and stellite disc bushing. Three Crosby SRV's were tested by the EPRI test program (reference 2,3). These were HB-BP-86 Types 3K6, 6M6 and 6NB. The type 3K6 is chosen as the representative test valve for Turkey Point due to its orifice size and corresponding flowrate. For the tests shown on pg. 3-57 of reference 6 the tested valve was subjected to moments which ranged from 59 x 10^3 in - lb to 147.5x10^3 in - lb without impairing the valve operability.

Since the maximum test moment and 70 percent of the ultimate moment carrying capacity of the pipe exceed the calculated maximum moment it is concluded that the operability of the valves will not be impaired.

Question 9

The submittal states that the inlet piping configuration in which the test safety valve was tested was similar to that of the Turkey Point safety valve system. It does not, however, provide a comparison between the inlet piping configurations to verify this statement. Therefore, provide a comparison between the inlet piping systems used in the tests and the plant. As part of this comparison, the two inlet piping pressure drops should be compared. Provide a numerical comparison between the calculated plant pressure drop and the test pressure drop and explain how the plant pressure drop was calculated.

Response

The following is the comparison between the EPRI Test case and the Turkey Point configuration:

EPRI 3K6 SAFETY VALVE

"F" INLET PIPING CONFIGURATION

	Length, in.	I.D., in.
Nozzle	17	6.813
Venturi	38	6.813
Pipe	6	6.813
Reducer	6	6.813/3.152
Loop Seal		
Straight	54	3.152
Bends	4-90°	6 inch radius
Reducer	4	3.152/2.624
Inlet Flange	7	2.624

Inlet pressure drops

Opening: 391 psi
Closing: 194 psi

Data shown is from "EPRI PWR Safety and Relief Valve Test Program Guide for Applications of Valve Test Program Results to Plant Specific Evaluations", REv. 2, Interim Report, July 1982 (V102) Tables B-3 and B-7.

See Figure 3 for an illustration of the EPRI configuration.

TYPICAL TURKEY POINT 4K26 SAFETY VALVE

SAFETY VALVE INLET PIPING CONFIGURATION

	Length, in.	I.D., in.
Total pipe length	136.5	3.624
90° Elbows	4	
45° Elbows	1	

Inlet pressure drops
- Opening: 433 psi
- Closing: 244 psi

Calculation of inlet pressure drops was made following the procedure provided in "EPRI PWR Safety and Relief Valve Test Program Guide for Application of Valve Test Program Results to Plant Specific Evaluations", Rev. 2, Interim Report, July 1982 (V102), Appendix B. The rated capacity was obtained from Table B-1 and flow parameters from Table B-2 for the 4K26 valve. Flow of Fluids through Valves, Fitting and Pipe; Crane Co., Technical Paper No. 410 was used as a reference. The inlet pipe configuration chosen as typical is the longest one on Unit 4.

See Figure 4 for an illustration of the Turkey Point configuration.

Question 10

The block valve that is used at Turkey Point, a Velan Model B10-3054B-13MS, was tested in the EPRI/Marshall PORV block valve testing program. However, Turkey Point utilizes a Limitorque SMB-000-5 operator while a larger Limitorque SB-00-15 operator was tested. Explain how the test results for the SB-00-15 operator can be used to demonstrate operability of the smaller SMB-000-5 operator.

Response

As reported in EPRI report NP-2514-LD, "EPRI-Marshall Electric Motor-Operated Valve (Block Valve) Interim Test Data Report", two Velan Model B10-3054B-13MS valves were tested. One valve had a Limitorque SB-00-15 operator, and the other a Limitorque SMB-000-10 operator. Turkey Point utilizes a Limitorque SMB-000-5 operator. With the exception of the operators, the three valves can be considered identical. The difference in the operators reflects differences in required stroke speed. These are detailed below:

Operator	Stroke Time
EPRI SB-00-15	10 seconds
EPRI SMB-000-10	15 seconds
Turkey Point SMB-000-5	40 seconds

Since the valves tested by EPRI operated satisfactorily during the tests at very near the design stroke speeds and the Turkey Point block valves are the same except for an operator sized similarity to provide a different stroke speed, the Turkey Point block valves can be expected to also provide satisfactory operation at its design speed.

Question 11

The submittal does not provide an expected value for the plant back pressure. To assure that the expected plant back pressure was enveloped in the EPRI tests, provide a value for plant back pressure and explain how it was determined.

Response

The plant back pressure was calculated by RELAP5/MOD1 assuming simultaneous actuation of all safety valves with loop seals. The calculated back pressure is 493 psia as shown in Table 4.05 of EBASCO report (Reference 1).

EPRI tests for the corresponding CROSBY 3K6 valve (Reference 6) give back pressures in the range of 471 psia (test 525) to 557 psia (test 537). Thus the expected plant back pressure is enveloped by the EPRI tests.

Questions Related to Thermal Hydraulic Analysis:

Question 12

The submittal states that the thermal hydraulic analysis was performed using RELAP5/MOD1 and that forcing functions were calculated from RELAP5 output with the Code CALPLOTFIII. Provide verification that the latter code has produced accurate force histories for similar problems.

Response

The post-processor CALPLOTFIII was programmed to convert the transient flow conditions (calculated by RELAP5/MOD1) into transient forces on the piping system. The derivation of the governing equations are shown in Appendix B* of EBASCO report (Reference 1). The validity of the program coding was verified by comparing hand calculation results against the values computed by the program. The program was further assessed against the GE 4-inch pipe blowdown test results. Favorable comparisons were obtained in comparing the computed results against the test data.

CALPLOTFIII was also verified by running CE test 1411 for SRV actuation on RELAP5/MOD1 using the input from EPRI RELAP5/MOD1 application (Reference 13). The calculated hydrodynamic conditions were converted by CALPLOTFIII to transient forces that duplicated the forces obtained by EPRI (Reference 13).

*See Attachment D to this submittal.

Question 13

The submittal indicates that thermal hydraulic analyses were performed for simultaneous actuations of the two PORVs in one analysis and three safety valves in another. It does not, however, verify that the analyses were performed on fluid transient cases that produce maximum loading on the safety valve/PORV piping system. Provide evidence that the analyses were performed for transient conditions that produce maximum expected loading on the piping system. Identify the fluid conditions assumed including pressure, temperature, pressurization rate, and fluid range.

Response

Three cases have been considered corresponding to the following scenarios of valve actuation.

A. Two PORVs open simultaneously. SRVs closed.

B. PORVs do not open. All three SRVs open simultaneously.

C. PORVs open. Pressurizer pressure continues to increase, SRVs open when set pressure is reached.

The characteristics of the discharge are such that Case C is not a bounding case. Initially the system behaves as Case A until the pressure reaches the setpoint of the SRVs. At such time the SRVs open against a much larger backpressure than that of Case B, therefore producing lower loads.

For Case A the two PORVs opened at a pressure of 2419.75 psia (2335 psig set point + 3%) with zero pressurization rate and steam in the pressurizer at saturated temperature. At the valve inlet the water in the cold loop seal is at 120°F.

For Case B the three SRVs opened at a pressure of 2574.25 psia (2485 psig set point + 3%) with zero pressurization rate and steam in the pressurizer at saturated temperature. At the valve inlet the water in the cold loop seal is at 120°F.

The solid water case has not been analyzed for Turkey Point Units 3 and 4.

Question 14

Report the flow rates through the safety valves and PORVs that were assumed in the thermal hydraulic analyses. Because the ASME Code requires derating of the safety valves to 90% of the actual flow capacity, the safety valve analysis should be based on a flow rate of at least 111% of the flow rating of the valve, unless another flow rate can be justified. Provide information explaining how derating of the safety valves was handled.

Response

The valve flow rates were calculated by the RELAP5/MOD1 (reference 14) computer code. To generate the required flow rates adjusted flow areas have to be used as was demonstrated in EPRI RELAP5/MOD1 application (Reference 13). The actual calculated flow rate for the SRV actuation case is 356,400 lbm/hr which is 121% of the original flow rating of the valve (295,000 lbm/hr) and 111% of the updated capacity (320,000 lbm/hr as shown in Table B-1 of Reference 2). The calculated flow rate through the PORVs is 266, 400 lbm/hr, their capacity is 153,000 lbm/hr.

Questions Related to Structural Analysis:

Question 15

The submittal states that the structural analysis was performed using PIPESTRESS 2010 for elastic analysis and PLAST for plastic analysis. Provide verification that these programs have produced accurate results on similar fluid transient problems.

Response

The PLAST program has been used to perform stress analysis of piping subject to pipe rupture and water hammer problems on various nuclear projects. A discussion of two of these analyses, taken from References 7 and 8, are included as attachments A and B. Furthermore, PLAST has been compared to the well known finite element program ANSYS and to the computer program FAB. These comparisons, taken from reference 8, are shown in attachment C.

The PIPESTRESS 2010 verification may be found in references 10 and 11. Additional verification exists at EBASCO. For example, the time history version of PIPESTRESS 2010 has been compared to the finite element program ABAQUS with very good agreement being observed. The PIPESTRESS 2010 program has been used on both nuclear and fossil plants to perform the stress analysis of piping subject to fluid hammer, main steam turbine trip and hot reheat turbine trip loads.

Question 16

The submittal does not explain what loading combinations were considered in the analysis to determine acceptability of the piping system. Therefore, identify the load combinations performed together with allowable stress limits for piping and supports both upstream and downstream of the valves. The letter of September 1, 1982, indicates that the ANSI B31.1 code was used to evaluate stresses in the piping and supports unique to the PORVs. Identify all other governing codes and standards (with date of edition) used to determine piping and support adequacy.

Response

The load combinations and stress allowables which are used to determine the adequacy of the Turkey Point pressurizer relief piping system are identical to the criteria specified in the Turkey Point FSAR by which the plant was designed, specifically that is the non-seismic ANSI B31.1 (1955) criteria. An additional load combination in the FSAR accounts for normal and seismic OBE loads with an allowable of 1.2S. For normal and SSE loads the allowables are Sy (yield stress). For comparison purposes, and because thermal hydraulic load cases were not part of original design, the calculated loads which are shown in Table 4.3.1 (attached) were combined according to the EPRI recommended load combination as provided in Reference 2 and shown in Table 2. Table 4.3.1 was developed for piping upstream and downstream of the PORVs subjected to PORV actuation. The stress allowables for these tables correspond to References 4 and 5, accordingly and are included in Table 2.

The load combinations used to analyze the piping subjected to SRV actuation correspond to EPRI recommended load combinations as shown in Table 2. For piping upstream of the SRV valves the stress allowables are as shown in Table 2. For piping downstream of the SRVs and subjected to SRV actuation, the moment developed in the piping is compared to 70 percent of the ultimate moment carrying capacity of the pipe. The ASME code itself allows use of this value to satisfy integrity criteria. For a further discussion of this point see the response to Question 9.

Load combinations for supports are also shown in Table 2. These also correspond to the EPRI recommendation (Appendix E of Reference 2). FPL is analyzing the first and third load combination for supports. That analysis will be completed by 9/1/86. Support loads for both PORV and SRV transients were originally compared against support capacity and are discussed in the response to question 17.

All analyses were performed on Unit 4 due to the similarity of the Units. Unit 4 was considered to be the more limiting of the two based on its support configuration.

Question 17

The submittal states that the piping and supports unique to the PORVs have acceptable stress levels, and that all piping and supports in the safety valve and PORV systems contained in the Primary Coolant Boundary were shown to have acceptable stresses. Provide a numerical comparison between calculated piping and support stresses with allowable stresses to verify this conclusion. The submittal also states that results from PLAST analysis show the discharge piping and supports to be adequate when stress levels exceed the yield point for the following reasons:

(a) No deformation was significant enough to reduce the flow area or detrimentally impact the flow path.

(b) Piping and restraint movements were such to preclude interaction with other components.

(c) No pipe rupture was found, thereby precluding possibility of pipe whip or jet impingement.

Supply numerical results from the PLAST analysis that verify these conclusions. Finally, provide an evaluation of the effects that large deformations in the discharge piping will have on the structural integrity of the valve inlet piping and pressurizer nozzle connections.

Response

For the analysis of the pressurizer relief piping subjected to PORV actuation, the stress ratios as predicted by PIPESTRESS 2010 are shown in Tables 4.3.1 and 4.3.2. At isolated points, overstress has been recorded. Upstream, the overstress is restricted to two points (1384 & 1714) with 3% and 10% overstress. Downstream, three points (1202, 1212 & 1260) showed overstress.

For the upstream nodes, due to the well known conservatism of Generalized response method used for this calculation, it is felt such overstress is artificial and can be overriden by more refined analysis. Furthermore, these results reflect conservative combination of moments from all three orthogonal directions. For Turkey Point, the loads are only required to be combined in one horizontal and the vertical direction to gain the resultant stress.

For the downstream nodes, elastic stress ratios are shown to be as high as 50% above allowable. These ratios are of significantly smaller magnitude than those discussed below for the SRV actuation. Since these loads are enveloped by downstream loads due to SRV actuation, the discussion below is bounding.

The calculated support loads due to PORV actuation are compared to the design loads in Table 4.4. All the reactions are within the capacity of the restraint structures. As stated in Question 8's response, FPL is currently performing analyses to satisfy load combinations 1 & 3 for supports.

With regard to the pressurizer relief piping subjected to SRV actuation, the PLAST analysis (see Reference 1) indicates plasticity in the first elbow downstream of the pressurizer and the elbow downstream of the SRV. The

moment carrying capacity of the pipe has been computed for each size and material by the method of Gerber which has shown excellent agreement with experiments. For elbows, that moment is modified by dividing by the B_2 factor to account for the lesser capacity of the elbow. This approximate method has shown excellent agreement with utimate moments of elbows computed by finite element techniques. Refer to Table 1 (question 8) for tabulation of the maximum moments due to SRV actuation. The maximum moments computed in the system through the first 70 millisecond response are shown and are compared with 70 percent of the ultimate moment. As mentioned in the response to Question 16, the ASME code itself allows use of this value to satisfy integrity criteria. Clearly nowhere is the 70 percent ultimate moment exceeded.

The support reactions due to SRV actuation are shown in Table 4.4.A. All the reactions are lower than capacities of the support structures.

In response to (a), the choice of 70 percent of the ultimate moment is dictated by prior finite element analysis as discussed in Reference 12. At such a load level plastic strains in the pipe would be insufficient to change its cross section significantly enough to affect its flow characteristics.

In response to (b), the small strains (approximately 0.4%) will not cause interaction of piping with other components.

In response to (c), the limitation on the maximum bending moment to 70% of the ultimate capacity implicitly precludes pipe rupture.

Finally, in regard to evaluation of response to large deformations in the discharge piping, the response to (b) above demonstrates that with such small strain, no large deformations are produced.

Question 18

The submittal notes that high frequency pressure oscillations occurred in the safety valve piping during loop seal discharge tests.

According to EPRI results these oscillations were approximately 170-260 Hz. The submittal refers to an evaluation of this phenomenon that is documented in Westinghouse report WCAP 10105. The study discussed in the Westinghouse report determined the maximum permissible pressure for the inlet piping and established the maximum allowable bending moments for Level C Service Condition in the inlet piping based on the maximum transient pressure measured or calculated. While the internal pressures are lower than the maximum permissible pressure the pressure oscillations could potentially excite frequency vibration modes in the piping, creating bending moments in the inlet piping that should be combined with moments from other appropriate mechanical loads.

Typically the structural responses in these piping systems is due to frequencies less than 100 Hz. The piping response is limited to these lower frequencies primarily because these systems are not normally subjected to forces having frequencies above 100 Hz. With the presence of the high frequency pressure oscillations, however, the higher frequencies existing in the inlet piping could potentially be excited, resulting in significant structural response. Therefore, provide one of the following: (1) a comparison of the allowable bending moments established in WCAP 10105 for Level C Service Conditions with the bending moments induced in the plant piping by the dynamic motion and other mechanical loads, or (2) justification for other alternate allowable bending moments with a similar comparison with moments induced in the plant piping.

Response

To evaluate a bending moment in the inlet piping due to the high frequency pressure oscillation at the opening or closing of the valve a linear dynamic analysis (Generalized Response Method) of a critical portion of the pressurizer relief piping system has been performed. That portion of the system includes one loop of Class 1 piping (4 inch O.D.) and outlet portion of the valve (6 inch O.D.) down to the X,Z-directions restraints and Y-direction snubber.

High frequency sinusoidal forcing function parameters are based on selected experimental data obtained from EPRI/CE safety valve tests (ref. 6) for the Crosby HB-BP-3K6 with loop seal internals (Test #526).

Pressure oscillation amplitude is 40 psi (from peak to peak) and frequency 170 hz.

Program 2010 PIPESTRESS (Reference 10, 11) has been used for analysis. The results show that the effect of the high frequency loading is negligible.

The maximum bending moment of 1.056×10^3 in-lb. in the inlet portion of the valve is much lower than an established maximum allowable moment 1.47×10^5 in-hr.

REFERENCES

1. Turkey Point N.P.P. Units No. 3 & 4. Analysis of Pressurizer Power Operated Relief Valve and Safety Valve Discharge Piping. NRC NUREG 0737 Item II.D.1, prepared by EBASCO Services Inc., August 1982.

2. EPRI PWR Safety and Relief Valve Test Program Guide for Application of Valve Test Program results to Plant Specific Evaluations, EPRI Safety and Relief Test Program, February 1982.

3. Review of Pressurizer Safety Valve Performance as Observed in the EPRI Safety and Relief Valve Test Program by E. M. Burns et al; WCAP-10105, June 1982.

4. ASME Section III - Division 1, Subsection NB, 1980 Edition, NB-3654.2, NB-3655.2.

5. ASME Section III - Division 1, Subsection NC, Winter 1981 Addenda NC-3653.1, NC-3654.

6. EPRI PWR Safety and Relief Valve Test Program, Safety and Relief Valve Test Report, EPRI NP-2628-SR Special Report, December 1982, Prepared by Electric Power Research Institute, Palo Alto, California.

7. Florida Power and Light Company Updated FSAR, Docket 50-389, St. Lucie Plant Unit 2, Vol. 4 revision 1, 4/86.

8. Florida Power and Light Company Updated FSAR, Docket 50-335, St. Lucie Plant Unit 1, Vol. 3 revision 3, 7/85.

9. ETR-1002-P Design Considerations for the Protection from the Effects of Pipe Rupture, Part I Pipe-Whip Dynamic Analysis by J. Heifetz and R. Iotti, EBASCO Services Incorporated, October 1974.

10. Program 2010 Theory Manual for Release 3.8.1 of PIPESTRESS 2010 New Dynamic Analysis Features, EBASCO Services, August, 1981.

11. PROGRAM 2010 VERIFICATION Manual for Release 3.8.1 of PIPESTRESS 2010 New Dynamic Features, EBASCO Services., August 1981.

12. S. H. Shaaban et al, "Functional Capability of Piping Elbows", SMIRT Proceedings, August 1985.

13. 'Application of RELAP5/MOD1 for Calculation of Safety and Relief Valve Discharge Piping Hydrodynamic Loads' Interim Report, EPRI Safety and Relief Valve Test Program, March 1982.

14. RELAP/MOD1 Code Manual, Ransom V.H., Wagner, R J et al, Vol. 1 & 2, EG&G Idaho Inc., NUREG/CR 1826, EGG 2070 Draft, Revision 2, September, 1981.

15. Letter from C. S. Kent to L. Tsakiris, JPE-PTPO-83-365, dated March 7, 1983.

FI 1

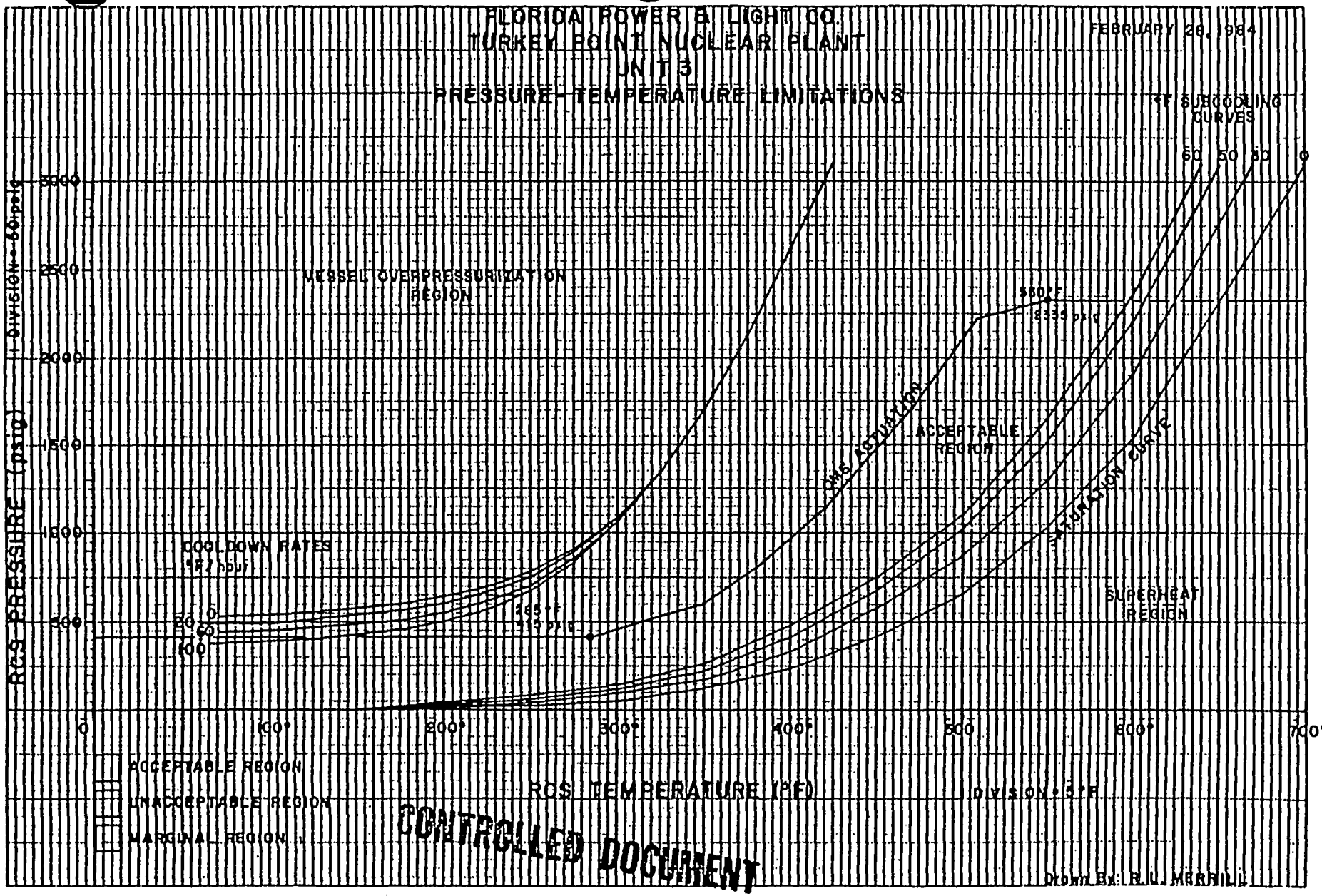

SECTION V, FIGURE 3A

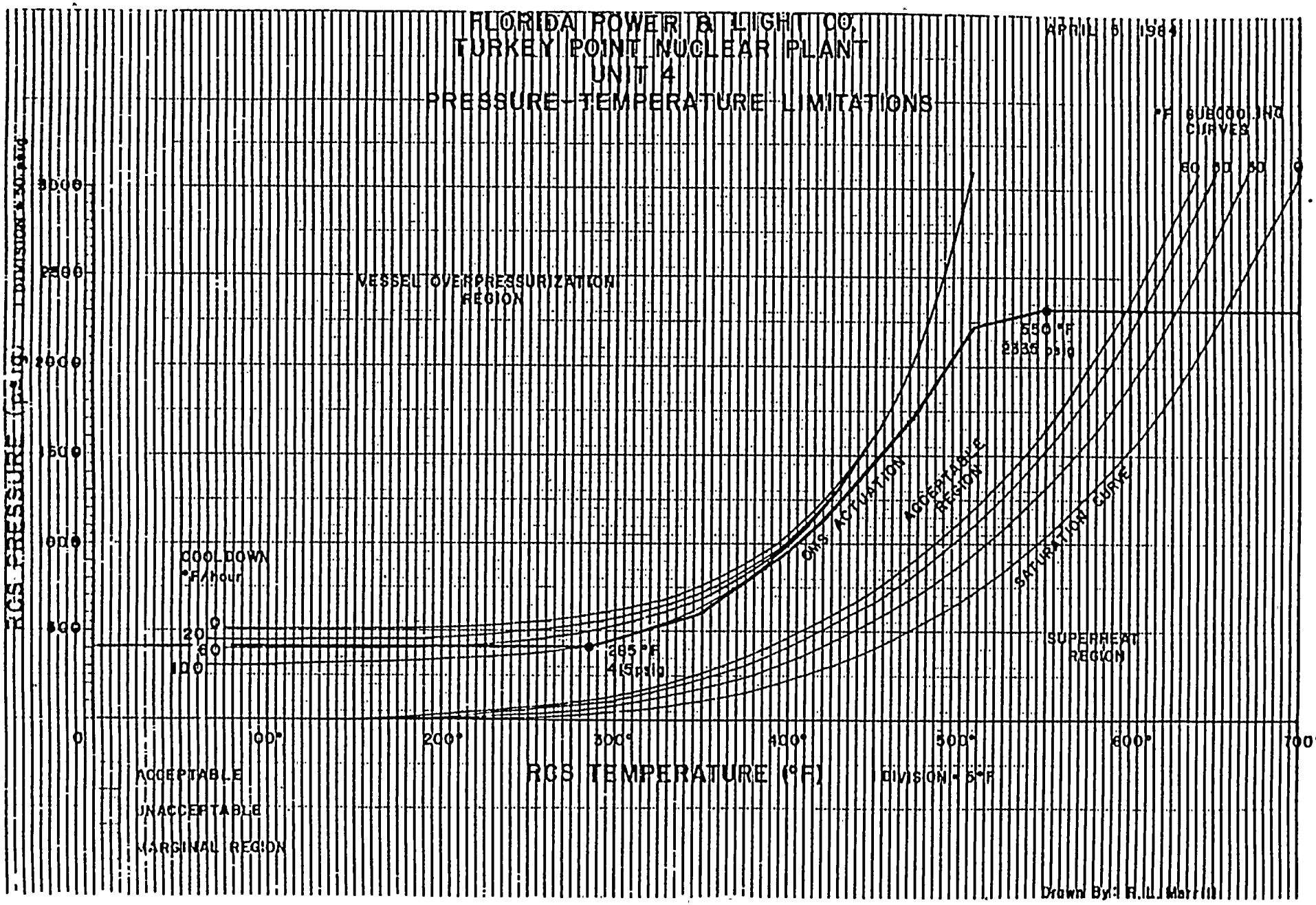

FIGURE 3

PIPING CONFIGURATION
EXTRACTED FROM EPRI NP-2770-LD
VOLUME 5

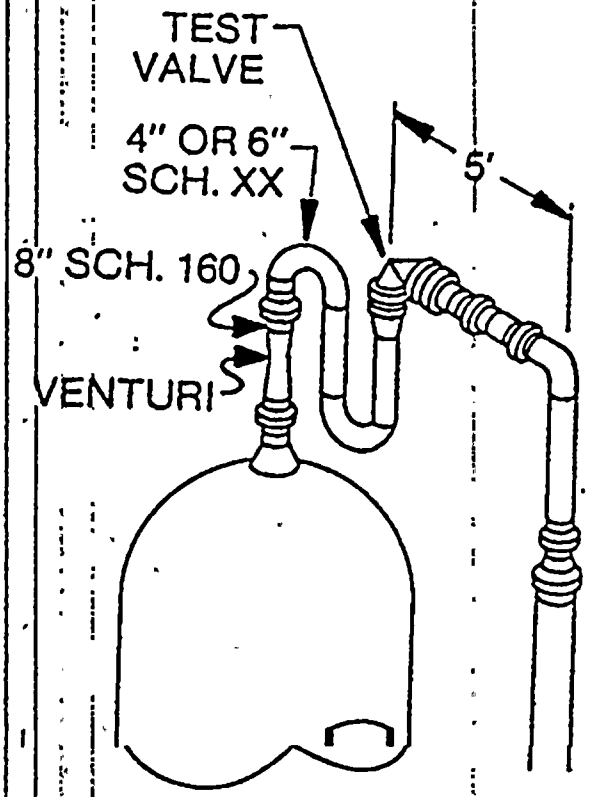

FIGURE 4

PIPING CONFIGURATION
TYPICAL TURKEY POINT

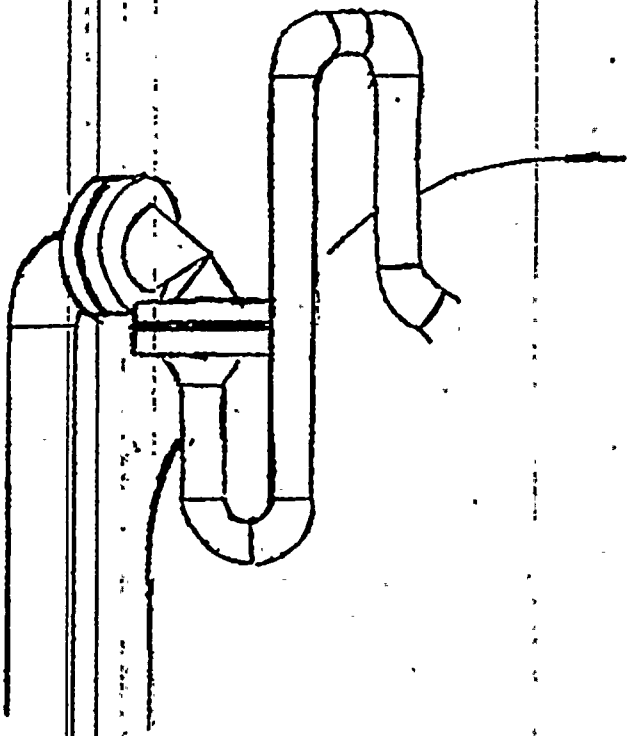

COMPARISON OF THE MAXIMUM MOMENTS

Node	Pipe Size and Sch.	70% Ult. Moment (in-lb)	Calc. Max. Moment (in-lb)	Time of Occurance (msec)	Induced *) Bending Moment Opening/Closed (in-lb)	Calculated Moment/Max Induced Bending Moment
40	4 in Sch 120	2.44×10^5	1.26×10^5	17.6	$(0.59 - 1.47) \times 10^5$	0.86
39	4 in Sch 120 Elb	1.23×10^5	7.96×10^4	13.8	"	0.54
29	6 in Sch 40	3.59×10^5	1.04×10^5	5.5	"	0.71

*) The reported values are the maximum induced bending moments on the valve discharge flange during opening or closing.

TABLE 2

GOVERNING PORV & SRV LOAD COMBINATIONS FOR PIPES & SUPPORTS

COMBINATION	PLANT/SYSTEM OPERATING CONDITION	LOAD COMBINATION	SERVICES STRESS LIMIT CLASS 1	CLASS 2
1	UPSET (PIPING)	Sustained Loads + OBE + Relief Valve Discharge Transient	$1.8S_m$	$1.8S_h$
1	UPSET (SUPPORTS)	Sustained Loads + Relief valve Discharge transient	Stress Level B	
2	EMERGENCY (PIPING)	Sustained Loads + Safety Valve $2.25S_m$	$2.25S_m$	$2.25S_h$
2	EMERGENCY (SUPPORTS)	Sustained Loads + Safety Valve discharge transient	Stress Level C	
3	UPSET (SUPPORTS)	Sustained Loads + OBE + Relief Valve Discharge Transient	Stress Level C	

NOTE:

S_m = Basic Allowable Stress Intensity = 20 ksi

S_h = Basic Material Allowable Stress at Maximum Temperature = 15 ksi

TABLE 4.3.1

STRESSES IN TURKEY POINT 3 & 4 PRESSURIZER
RELIEF PIPING FROM PORV ACTUATION

Pipestress 2010 Node Point	ASME Code Class	TYPE OF STRESS (PSI) Pressure	Weight	PORV	OBE(EDS)*	Load Combination (PSI)	Ratio of Stress to Allowable
192	2	51	5389	6477	1477	12273	0.454
254	2	35	7408	7576	2324	15198	0.563
362	1*	11481	3570	2154	2418	17374	0.483
374	1*	11481	3977	3306	2361	18912	0.525
384	1*	11481	1174	2901	1771	15656	0.436
912	2	35	18237	8338	1980	26683	0.989
954	2	35	7869	7632	1787	15639	0.579
1072	1*	11481	2197	2239	2101	16055	0.447
1082	1*	11481	2763	2399	2322	16804	0.467
520	2	35	4211	6968	2800	11558	0.428
534	2	35	8476	6540	864	15076	0.558
1202	2	35	16717	21831	4906	38894	1.440
1212	2	35	14558	21017	4187	35855	1.328
1222	2	35	7947	9611	2148	17724	0.664
1234	2	35	7143	10468	2195	17782	0.659
1242	2	35	7538	12487	2342	20196	0.748
1260	2	35	21853	18277	6338	40662	1.506

* REF. 15

TABLE 4.3.1 (continued)

STRESSES IN TURKEY POINT 3 & 4 PRESSURIZER
RELIEF PIPING FROM PORV ACTUATION

Pipestress 2010 Node Point	ASME Code Class	TYPE OF STRESS (PSI)				Load Combination (PSI)	Ratio of Stress to Allowable
		Pressure	Weight	PORV	OBE(EDS)*		
1330	1*	8930	2410	9855	5184	21820	0.606
1382	1*	11481	11936	10169	3769	33800	0.939
1384	1*	11481	14445	13371	3908	39491	1.097
1410	1*	11481	3638	3625	3300	19032	0.529
1422	1*	8930	10042	9158	9216	29601	0.823
1502	2	12	3984	8198	5340	13312	0.493
1514	2	12	3434	8064	5390	12709	0.470
1714	1*	11481	18644	6621	5164	37107	1.031
1724	1*	11481	4044	6497	6582	22984	0.639
1734	1*	11481	3259	7129	6830	22954	0.638

* Ref. 15

TABLE 4

REACTIONS ON THE SUPPORTS (lbs)

(TRANSIENT EFFECTS DUE TO OPENING OF PORV's)

ISO PT	EBASCO PT	PIPE SIZE	SUPPORT I.D. (ISO)	FUNC-TIONAL DIRECTION	*TRANSIENT (LOAD (LB)	TYPE OF SUPPORT	**)MAX DESIGN LOADS,LBS (PAGE046A-046B)		**)CAPACITY OF SUPPORT (FROM STRUCTURAL DWGS)
A4	41	12"	4-PRH-3	X	1718	Rigid Restraint	1801	-2896	8000,Tab 1
A4	41	12"	"	Z	1521	" "	N.A	N.A	7,000,Tab 1
14	140	12"	4-PRH-4	X	2094	" "	2240	-1869	N.A, Tab 2
27	270	6"	4-PRH-8	X	484	" "	580	-562	6,000,Tab 4
27	270	6"	"	Z	573	" "	606	-1285	7,000,Tab 4
B53	532	6"	4-PRH-12	Z	228	" "	2085	510	4,000,Tab 6
59	590	6"	4-PRH-11	X	389	" "	516	-731	N.A, Tab 7
59	590	6"	"	Z	349	" "	368	-2328	N.A. Tab 7
62C	620	6"	4-PRH-10	Skewed LAT Z	538	" "	318	-784	8,000, Tab 8
62D	620	6"	"	Skewed LAT X	226	" "	1095	-307	8,000, Tab 8
98	980	6"	4-PRH-9	X	368	" "	577	-904	2,000, Tab 9
98	980	6"	4-PRH-9	Z	229	" "	602	-510	7,000, Tab 9
123	1230	6"	Penetration	X	2913	" "	1546	-1787	N.A
A125	1251	6"	4-PHR-6	Z	1904	" "	1287	-1423	1,000, Tab 11
13	130	12"	4-PHR-4	Z	2630	Snubber	2016	-2016	N.A, Tab 2
A18	181	12"	4-PRH-2	Y	111	"	560	-560	10,000,Tab 3
26	260	6"	4-PRH-8	Y	742	"	572	-572	10,000,Tab 4
A61	611	6"	4-PRH-10	Y	227	" "	203	-203	10,000,Tab 8
96	960	6"	4-PRH-9	Y	1184	" "	550	-550	10,000, Tab9
125	1250	6"	4-PRH-6	Y	1184	"	464	-464	<10,000,Tab 11
138B	1384	4"	4-PRH-5	S-W	1828	"	1693	-1693	N.A., Tab 16
138C	1385	4"	"	S-W 10	4437	"	4257	-4257	N.A., Tab 12
138D	1386	4"	"	25°Vert W	3057	"	3408	-3408	N.A., Tab 12

* HOOP STRESS IS INCLUDED IN EVERY TRANSIENT LOADING

**) Document TR-5322-158, PR-2, UNIT 4
by Teledyne Engineering Services

TABLE 4.4A

REACTIONS ON THE SUPPORTS (lbs)

(TRANSIENT EFFECTS DUE TO OPENING OF SRV, "PLAST" PARTIAL MODEL)

ISO PT	EBASCO "PLAST" PT	PIPE SIZE (IN)	SUPPORT ID(ISO)	FUNCTION, DIRECTION	TYPE OF SUPPORT	SRV TRANSIENT REACTION (lbs)	TIME OF OCCURANCE (Sec)	CAPACITY OF SUPPORT (FROM STRUCTURAL DWGS. lbs)	TELEDYNE ENG. SERV. STRUCTURAL DWGS.
A4	5A	12	4-PRH-3	X	RESTRAINT	3,114	0.038	8,000	Ref.DWG. DCN-M 380- **)TAB 1
A4	5	12	4-PRH-3	Z	"	444	0.14	2,000	"
14	12	12	4-PRH-4	X	"	1,030	0.04	Design Load on Struc Dwg. +2,240;-6869	**) TAB 2
27	26	6	4-PRH-8	X	"	6,955	0.009	6,000	DWG 4-128-1,4-129 Sub. Syst.E-2388-WIC-2 **) TAB4
27	26	6	4-PRH-8	Z	"	6,902	0.009	7,000	"
26	25A	6	4-PRH-8 PSA-10, S/N=121	Y	SNUBBER	10,050	0.006	<10,000	"
13	12A	12	4-PRH-4	Z	"	1,630	0.174	N.A on Struct. DWG.(Design Loads ± 2016*)	NA
A18	14	12	4-PRH-Z PSA-10 S/N=108, S/N=104	Y	"	1,583	0.045	Snubbers assumed to be a weak link capac. of each ~10 Kips	Dwg 4-114-1,4-115 Sub Syst E-2388-WIC-6**)TAB3

*) Max design loads are taken from TR-5322-158, Rev. 2, p 046A

**) Documents are indicated as TR-5322-158, Prob. PR-2, unit 4

Attachment A

Reference 7 Discussion of a Use of PLAST

APPENDIX 3.6E

MAIN STEAM & FEEDWATER ANALYSIS

3

3.6E MAIN STEAM & FEEDWATER ANALYSIS

This appendix presents the results of dynamic analyses performed to verify the structural adequacy of the Main Steam and Feedwater pipe whip restraints.

The transient forces resulting from postulated piping failures have been generated using the RELAP computer code. Thrust forces from RELAP are used as input to the PLAST 2267 Code. The PLAST code uses these forces to determine the pipe whip restraint reaction loads by performing a dynamic structural analysis on a lumped mass parameter of the piping system. These computer codes are described in References 3.6E-1 through 3.6E-3.

Typical pipe whip restraint structures used on the Main Steam and Feedwater systems are shown in Figures 3.6D-1 and 3.6D-2. Elastic stiffness values for these restraints have been determined by two methods:

a) The bolts securing the restraints to the RCB structure were considered infintely rigid. Credit was taken only for the elasticity of the pipe whip restraint structural steel 3

b) The elasticity of the bolts was considered and a combined stiffness was calculated.

Method 2 results in stiffness values approximately 36 percent to 57 percent of the values obtained by Method 1. In addition, pullout loads have been determined for the bolt system.

Reaction loads at the pipe whip restraints have been generated by the PLAST program based on the combined stiffness values. The resulting loads were then compared with the bolt pullout loads. Typical results are tabulated in Table 3.6E-1 for selected Main Steam restraints and show that the restraints perform their design function since the reaction loads are below the bolt pullout loads.

The break locations analyzed are shown in Figure 3.6E-1 for Main Steam piping and Figure 3.6E-2 for Feedwater. These figures also represent the PLAST models for these systems. Figures 3.6E-3 and 3.6E-4 give the RELAP models for the Main Steam and Feedwater piping, respectively. The volume and junction data for Main Steam RELAP are given in Tables 3.6E-2 and 3.6E-3. The pipe whip restraint gaps used in PLAST For Main Steam are given in Table 3.6E-4. This information is tabulated for the Feedwater analyses in Tables 3.6E-5 through 3.6E-7, respectively.

Force versus time history for RELAP is presented for a typical Main Steam break in Figure 3.6E-5 and for a typical Feedwater break in Figure 3.6E-6.

REFERENCES: SECTION 3.6E

3.6E-1 "RELAP3 A Computer Program For Reactor Blowdown Analysis" by W H Rettig, G A Jayhe, K V Moore, C E Slater, M L Uptmore, Idaho Nuclear Corporation IN-1321 Issued June, 1970, Reactor Technology, TDD-4500

3.6E-2 RELAP4-MOD6, A Computer Code For Transient Thermal Hydraulic Analysis of Nuclear Reactor and Related Systems, User's Manual, EG&G Idaho, Inc., CDAPTR003, January, 1978

3.6E-3 "Design Considerations for the Protection From the Effects of Pipe Rupture", ETR-1002-P (Proprietary Version) and ETR-1002 (non-Proprietary version), by Ebasco Services, Inc. August, 1977.

3

TABLE 3.6E-1

SUMMARY OF SELECTIVE PIPE WHIP RESTRAINTS AND DYNAMIC LOADS

RESTRAINT NUMBER	RESTRAINT STRUCTURE STIFFNESS[1] (KIP/IN) PULLOUT (+x1) (-x1)	SHEAR (x2) (x3)	RESTRAINT STRUCTURE STIFFNESS[2] (KIP/IN) PULLOUT (x1)	SHEAR (x2)	BOLT PULL-OUT LOAD[3] (KIPS)	RESTRAINT REACTION LOAD (KIPS)	SOURCE RUN	BREAK LOCATION	REMARK
RE-MS-16	+38,749 -181,549	52,375 -38,993	+16,202 -90,728	+35,830 -25,547	5,187	5,160	FLO21J2MS	Slot break betn Pts 9 & 6709	
RE-MS-17	+39,304 -117,548	+37,106 -40,521	+14,288 -81,754	+23,103 -25,538	3,021	542	FLO21KLMS	Guill. at S/G Nozzle	
RE-MS-20	+28,291 -51,075	+39,126 -28,969	+16,143 -71,780	+32,025 -33,924	4,795	3,520	FLO21HMS	Guill. at Pt. 16 from Pt. 16	

Notes:

(1) Bolts rigid

(2) Bolts elastic

(3) Applied load at which first both failure occurs.

TABLE 3.6E-4

RESTRAINT GAPS USED FOR PLAST MODELS OF MAIN STEAM LINE

RESTRAINT NAME	LOCAL (1) +Y GAP (IN.)	LOCAL (1) -Y GAP (IN.)	LOCAL (1) +Z GAP (IN.)	LOCAL (1) -Z GAP (IN.)
RE-MS-24	4.00	4.00	4.00	4.00
RE-MS-21	4.25	4.00	4.00	4.25
RE-MS-20	4.50	4.00	4.00	5.50
RE-MS-19	4.00	5.25	4.00	4.50
RE-MS-18	4.00	4.25	5.75	4.00
RE-MS-17	4.00	4.50	100.0(2)	100.00(2)
RE-MS-16	4.00	4.00	4.00	6.00
RE-MS-15	5.75	4.00	4.75	4.00
RE-MS-14	6.25	4.00	99.625(2)	100.375(2)
RE-MS-13	5.75	4.00	4.00	6.500
RE-MS-12	4.00	6.75	4.00	5.750

3

NOTES:

(1) For local directions see Figure 3.6E-1

(2) Local $\pm$ Z is unrestrained for this restraint

3

TABLE 3.6E-7

RESTRAINT GAPS USED FOR PLAST MODELS OF BOILER FEEDWATER LINE

RESTRAINT NAME	LOCAL(1) +Y	LOCAL(1) -Y	LOCAL(1) +Z	LOCAL(1) -Z
	GAP (IN.)	GAP (IN.)	GAP (IN.)	GAP (IN.)
RE-BF-17	4.00	4.00	4.00	4.50
RE-BF-16	4.00	4.00	4.00	4.50
RE-BF-15	4.00	4.00	4.75	4.00
RE-BF-14	4.00	4.00	4.00	4.25
RE-BF-11	9.00	9.00	9.00	9.00
RE-BF-10	6.50	4.00	4.25	4.00

3

Note:

1. For local directions (see Figure 3.6E-2)

NOTES:

1. ◆ INDICATES THE LOCATION OF A GUILLOTINE BREAK. THE THRUST FORCE ON THE PIPING IS DIRECTED ALONG THE PIPE AXIS OPPOSITE TO THE ESCAPING JET FLOW.
2. THIS FIGURE WAS DEVELOPED USING INFORMATION FROM EBASCO ISOMETRIC NO. MS-147-1.
3. NUMBERS IN PARENTHESIS REFER TO NODE NUMBERS ON THE ISOMETRIC CITED ABOVE.
4. X_1, Y_1, Z_1 REFER TO THE GLOBAL COORDINATE DIRECTIONS.
5. X, Y, Z REFER TO THE LOCAL COORDINATE DIRECTIONS AT A PARTICULAR NODE.
6. IN THE ACTUAL PIPING THERE IS A RESTRAINT RE-MS-11 LOCATED AT NODE 34(1). THE GAPS ON THIS RESTRAINT WOULD NOT HAVE CLOSED WITH ANY OF THE BREAK LOCATIONS MODELED. AS A CONSEQUENCE THIS RESTRAINT WAS NOT MODELED.

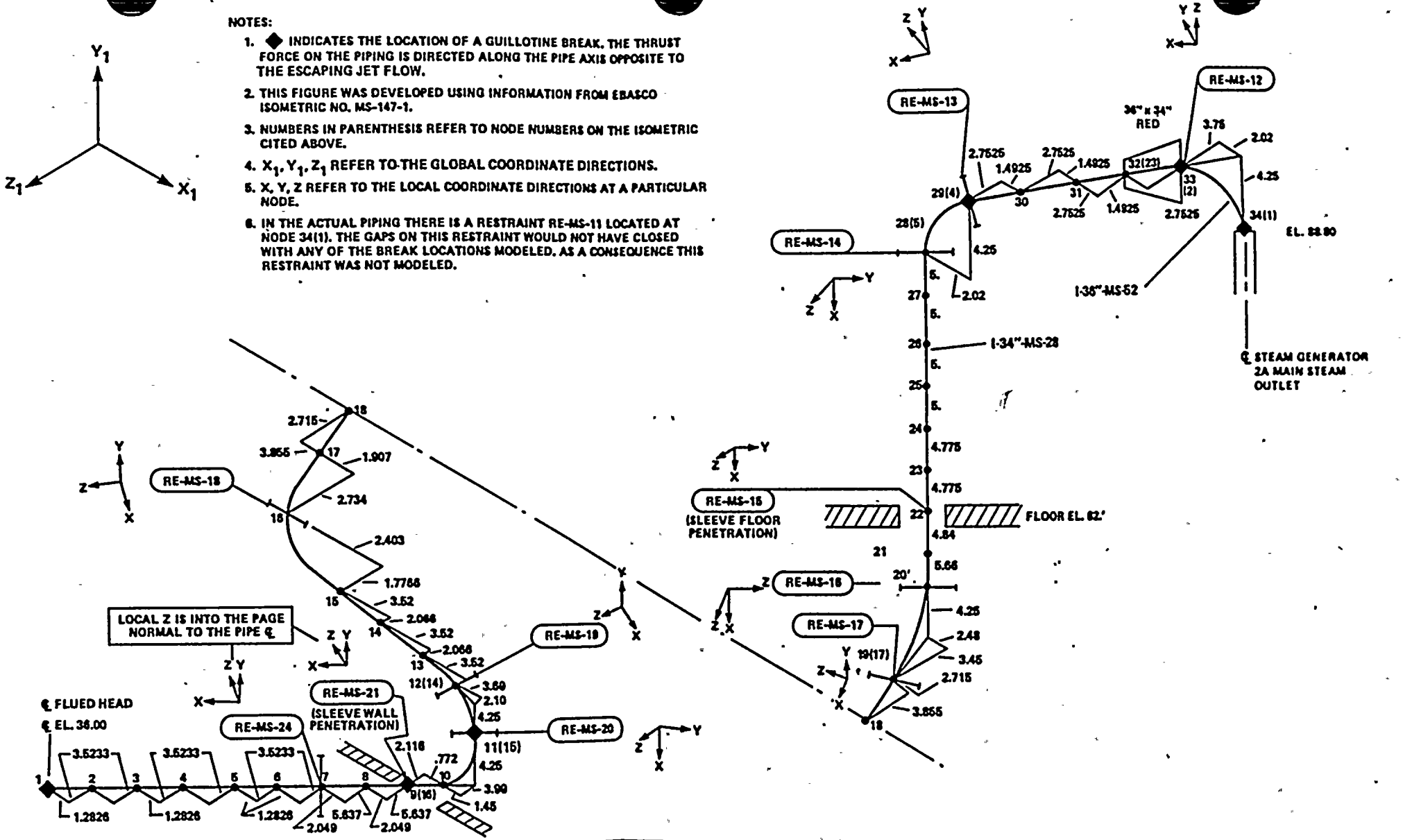

LINE NO.	PIPE O.D.	SCH. NOM. WL. THICKNESS	MATERIAL	OPERATING TEMP. °F	MODULUS OF ELASTICITY @ OP. TEMP. PSI	POISSON'S RATIO	OPERATING PRESSURE PSIG
I-34"-MS-28	34.000"	1.255	C.S.	532	26.26×10^6	.3	885.
I-36"-MS-52	36.625"	1.245	C.S.	532	26.26×10^6	.3	885.

AMENDMENT NO. 8 (8/81)

FLORIDA POWER & LIGHT COMPANY
ST. LUCIE PLANT UNIT 2

PLAST PIPE RUPTURE MODEL OF THE REACTOR BLDG. MAIN STEAM LINE

FIGURE 3.6E-1

1. RELEVANT INFORMATION FOR I-20"-BF-14 AND I-18"-BF-51

LINE NO.	PIPE O.D.	SCH. NOM. WALL THICKNESS	OPERATING TEMP. °F	OPERATING PRESSURE, PSIG	MATERIAL
I-20"-BF-14	20.00"	1.037"	440.	1050.	C.S. A106-B
I-18"-BF-51	18.00"	0.937"	440.	1050.	C.S. A106-B

MATERIAL PROPERTIES @ TEMP.					
LINE NO.	MODULUS OF ELASTICITY PSIA	YIELD STRESS PSIA	YIELD STRAIN	POISSON'S RATION	DENSITY LB_f/IN^3
I-20"-BF-14	29.75×10^6	29.75×10^3	0.05605	0.3	0.283
I-18"-BF-51	29.75×10^6	29.75×10^3	0.05605	0.3	0.283

2. FIGURE 3.6.E-20 WAS DEVELOPED FROM EBASCO ISOMETRIC NO. BF-147-1 REV 1 12-20-78.
3. ◆ INDICATES THE LOCATION OF A GUILLOTINE BREAK.

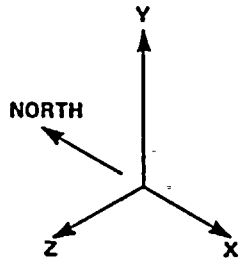

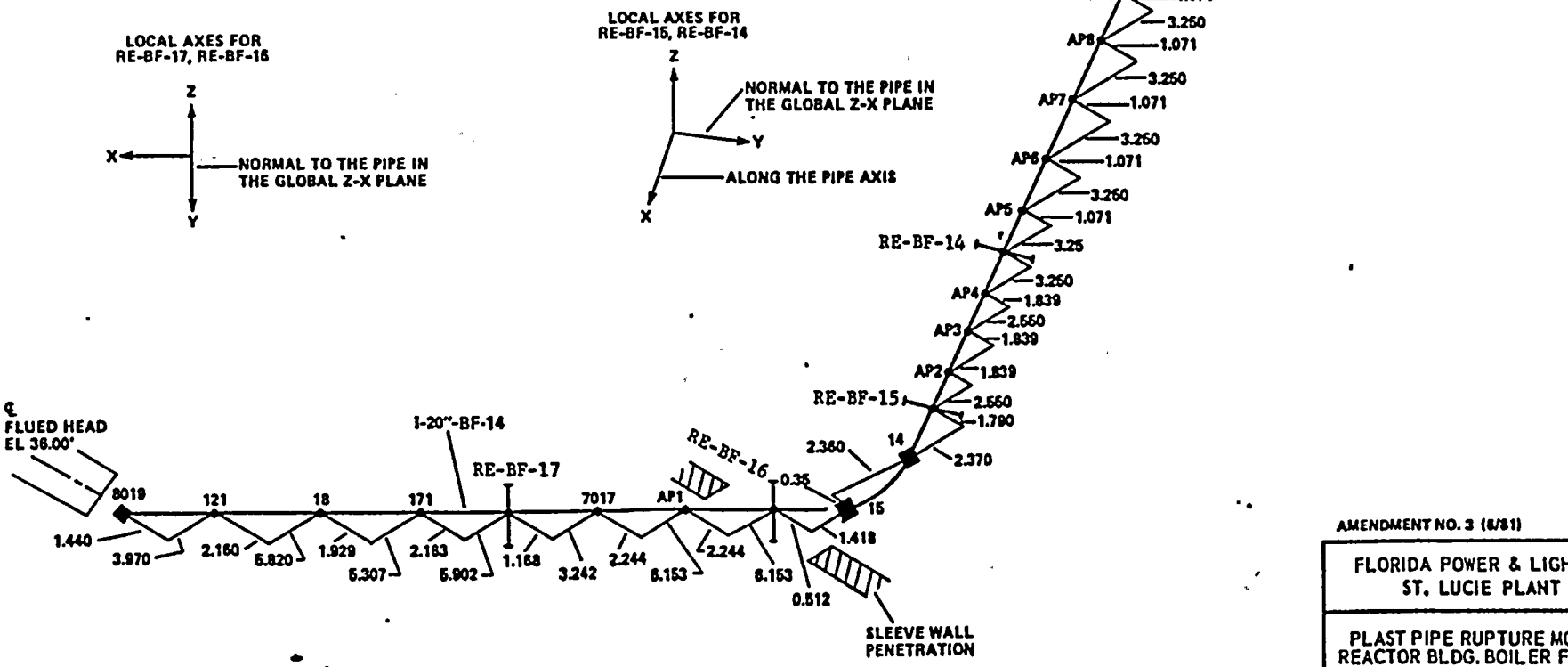

AMENDMENT NO. 3 (6/81)

FLORIDA POWER & LIGHT COMPANY
ST. LUCIE PLANT UNIT 2

PLAST PIPE RUPTURE MODEL OF THE REACTOR BLDG. BOILER FEEDWTR. LINE

FIGURE 3.6E-2

PIPE THRUST FORCE VERSUS TIME CURVE USED BY PLAST MODEL FLO21H2MS

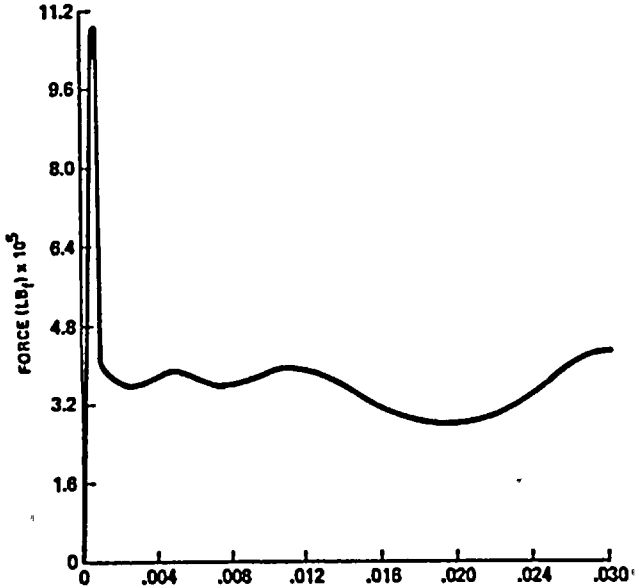

PIPE THRUST FORCE VERSUS TIME CURVE USED BY PLAST MODEL FLO21H2MS

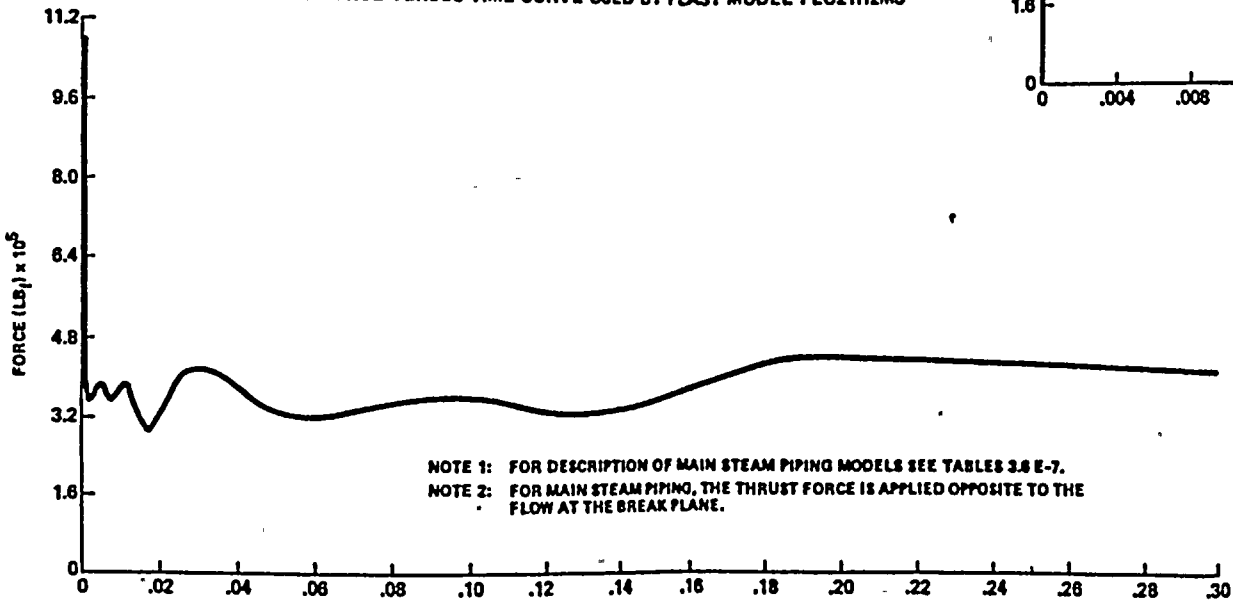

NOTE 1: FOR DESCRIPTION OF MAIN STEAM PIPING MODELS SEE TABLES 3.6 E-7.

NOTE 2: FOR MAIN STEAM PIPING, THE THRUST FORCE IS APPLIED OPPOSITE TO THE FLOW AT THE BREAK PLANE.

AMENDMENT NO. 3 (6/81)

FLORIDA POWER & LIGHT COMPANY
ST. LUCIE PLANT UNIT 2

PIPE THRUST FORCE VS. TIME CURVE USED BY PLAST MODEL FLO21H2MS

FIGURE 3.6E-5

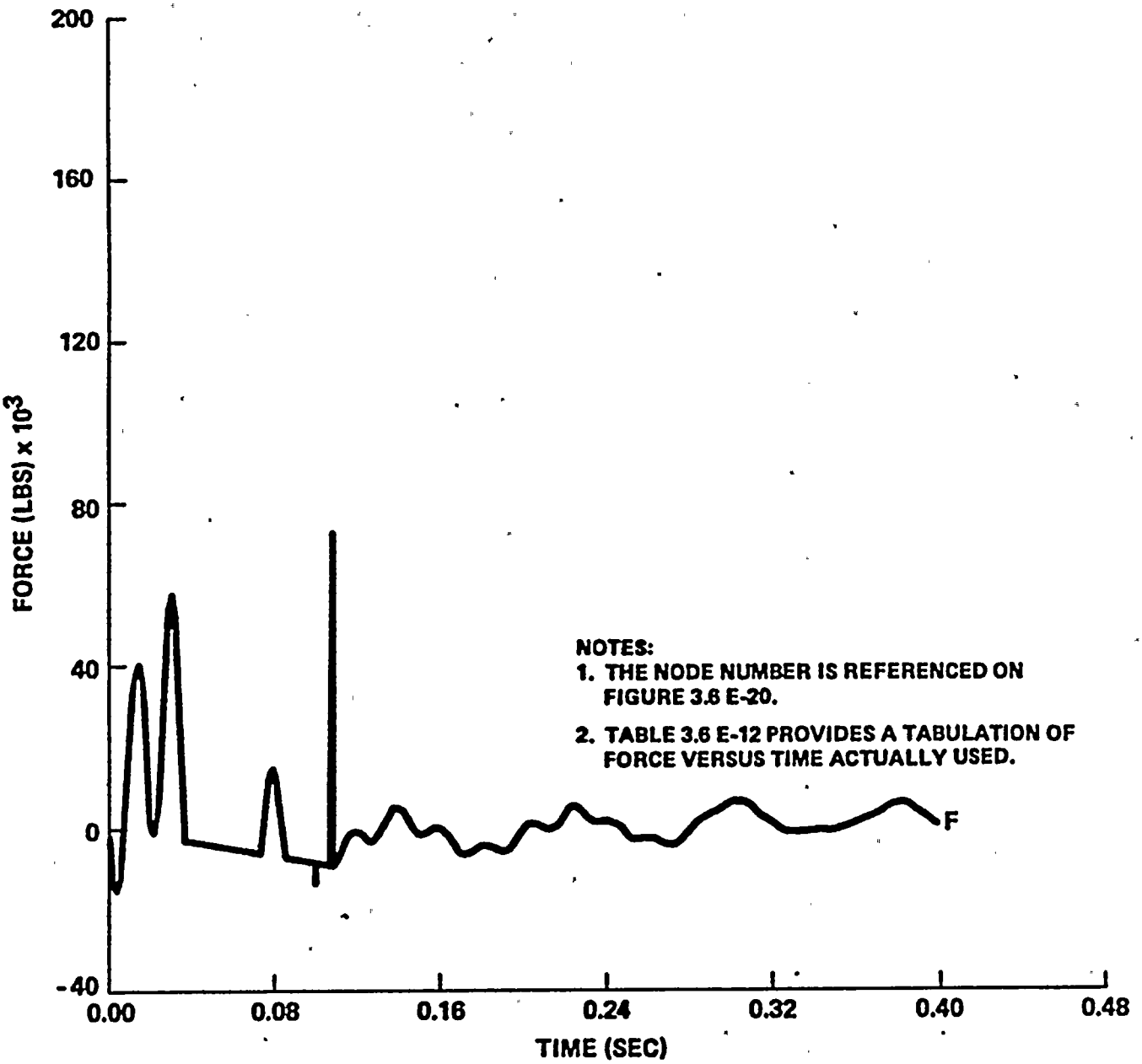

AMENDMENT NO. 3 (6/81)

FLORIDA POWER & LIGHT COMPANY
ST. LUCIE PLANT UNIT 2

FORCE HISTORY APPLIED AT NODE 14 OF BOILER FEEDWATER PIPING MODEL FL021PLASTBF4

FIGURE 3.6E-6

Attachment B

Reference 9 Discussion of a Use of PLAST

3.6.4.3 Pipe Whip Analysis - Main Steam and Feedwater

As shown on Figure 3.6-52, a break location was established at node 12 for the main steam line. A break at node 12 results in the maximum impact at the restraint located at node 9 and the maximum total strain in the pipe.

Span lengths between pipe whip restraints are as shown on Figures 3.6-52 through 3.6-55 for main steam and feedwater piping. The maximum span lengths depicted were established using the design criteria presented in Section 3.6.5.1. As stated in 3.6.5.1, failure stress is limited to that value which corresponds to 50 percent of the true ultimate strain when related to a simplified stress-strain curve (Figure 3.6-9A).

For the steam line break selected (node 12 on Figure 3.6-52), the moment required for full plasticity, for yielding and the actual moment computed for that limiting case are 35.2×10^3 in-kip, 27.8×10^3 in-kip and 35.2×10^3 in-kip, respectively. The actual computed moment and the moment to full plasticity are equal since for this limiting span length the pipe does plastically deform, but does not whip.

Sensitivity studies for the main feedwater line outside containment are summarized for variations in gap length and pipe wall thickness in Table 3.6-1 and Figures 3.6-58, 3.6-60& 3.6-62. A reduction in gap reduces peak restraint reactions while decreasing wall thickness seems to increase reactions.

rev 5

The span method of restraint placement (See Section 3.6.5.1) does not provide for a margin to full plasticity since the method itself assumes the pipe to go plastic. The span method does, however, prevent maximum calculated strain from exceeding one-half of the ultimate strain. For example, at the instance when a pipe is fully plastic, the pipe can still carry moments - only additional strain energy into the pipe will cause further straining up to the ultimate.

If the strain hardening is ignored, as was done in this analysis, then the span method does not predict the strain corresponding to imposed moment since this strain is not unique. However, Figure 3.6-61 shows that the maximum strain does not even approach half ultimate strain values. Since zero strain hardening was employed, it follows that the calculated moment at maximum strain and the moment required for full plasticity are identical, 35.2 in-kip.

At this moment value, the pipe has not collapsed and can continually carry equal or diminishing loads. The moment necessary to yield the outer fibers of the pipe is 27.6 in-kip.

Figures 3.6-52 through 55 provided the span lengths, restraint locations and node locations using nodal breakdown requirements for pipe whip analysis. Nodal breakdown requirements for pipewhip analysis are different than those required for stress analysis as reflected in the piping isometrics of Section 3.6.

Because node points were included in the numbering scheme in Figures 3.6-52 through 55 and since nodes were not shown in other Section 3.6 figures, no correspondence should be expected between the two except that piping dimensions and location of pipe whip restraints are identical.

To illustrate this point refer to Figures 3.6-36 and 3.6-52. Figure 3.6-36 restraint locations MS-2, MS-3, MS-4 and MS-5 correspond to restraint locations 2, 4, 5 and 8 in Figure 3.6-52, respectively. All the related figures have been reviewed for accuracy.

a) Conclusions

Four cases (2 feedwater line breaks and 2 main steam line breaks) of circumferential pipe rupture were analyzed for maximum restraint reactions and maximum pipe strain. All analyses were extended for a period of 0.2 seconds past initiation of pipe rupture when steady state oscillations of the deflection of the rupture point occurred with decreasing amplitude. Strain hardening in the pipe was assumed to be zero for conservatism.

Figure 3.6-56 indicates that blowdown forces for the feedwater line rupture reach a steady state value of 110,000 lbs at 0.034 seconds; for the main steam line, the blowdown forces reach a value of 135,000 lbs at 0.1 seconds, decrease exponentially to 100,000 lbs at 0.15 seconds, and continue to decrease at the same exponential rate thereafter.

Since the steam line is multi-planar, restraint reactions can occur in more than one direction and in more than one restraint. This is evident from the reaction force results plotted on Figures 3.6-57 and 3.6-58. Peak reactions in all cases except two were below the 2 KPA factors applicable to the line under analysis. In the two exceptions (feedwater line break at node 6, Figure 3.6-59, and main steam line break at node 12, Figure 3.6-58), the peak duration is approximately 0.002 seconds or less.

Since the natural periods of the restraint system, consisting of the steel frame restraints, the embedments and the concrete wall are of 0.002 seconds or less, this system was reviewed to determine to what extent, if any, its primary function of pipe restraint during blowdown may be impaired.

A very conservative analysis of the steel frames, in which the stiffening effects of collar plates and webs were ignored and the pipe whip impulse loads were treated as step functions constant in time, revealed that yield would occur in the structure. Since the pipe whip dynamic analysis was based on the assumption of elastic, non-yielding restraints, the effect of yielding would be to reduce the loading peaks shown in Figures 3.6-58 and 3.6-59. However, the non-yielding assumption used in the pipe whip analysis is taken, as the more conservative approach. In either case, yielding or non-yielding, the steel frames will perform their function of adequately restraining the pipes against excessive movement.

Assuming complete rigidity of the steel frame restraints and concrete, the bolts, subjected to a pulse (hat function) loading of 0.002 seconds duration were shown to reach a peak strain of 0.0155 in/in (based on a bilinear stress-strain curve in which Young's modulus $E=30\times10^6$ psi and the strain hardening modulus S-0.05E) for carbon steel. This strain is well below 1/2 ϵ_μ for carbon steel (taken as 0.1) and is confined to the threaded portion of the bolt. Once more it is seen that under very conservative assumptions the bolts do not rupture, and that yielding results in lowering the applied pulse peaks due to pipe whip.

Assuming, once more, that the restraint frames remain rigid, and that a step function load is applied through the bolt anchor plates to the concrete with a peak equal to the applied pipe whip impact-pulse distributed to the embedded bolts, it was shown that the concrete would not fail in shear (i.e., pullout) and that the concrete wall was adequate to resist these loads.

In summary, the design of the pipe whip restraints and embedments is considered adequate to perform their primary function of limiting pipe motion and secondary damage following a pipe break because there will be no intolerable loadings as a result of exceeding the factor 2.0 for the k load factor.

Maximum strains in the feedwater and main steam lines are found by adding the yield strain to the maximum plastic strain. These peak strains, in all cases, are considerably less than half the ultimate strain of the materials (main steam - steel, A 155 GR-KC 65; feedwater - steel, A 106 GRB).

Critical results of these analyses are indicated on Figures 3.6-57 through 3.6-64 and on Table 3.6-2 for the four ruptures considered.

b) Dynamic Analysis

Four different breaks were analyzed, two on a main steam line and two on a feedwater line. The break locations chosen, restraint locations, geometry, material properties, and maximum operating temperatures and pressures for each break condition are shown in Figures 3.6-52 through 3.6-55. The four breaks were chosen as representative of breaks producing maximum impact reactions and pipe strains. In all cases circumferential breaks were analyzed since the greatest potential for whipping a pipe exists. Thrust forces at the break locations were developed by performing a time history, thermal hydraulic analysis of the blowdown with the RELAP-3 code (Reference 14), suitably modified to predict thrust forces.

With the RELAP-3 code the transient energy, momentum, and state equations were solved for an assembly of volumes and flow paths modeling the true piping system. The total thrust out of the break was evaluated as the sum of three components:

a) A Momentum flux component equal to $W^2/g_c \rho A$, representing the outflow of momentum out of the control volume about the break,

b) a pressure force component equal to $(P_e - P_a)A$, representing unbalanced pressure forces on the control volume about the break, such as occurring when flow is choked at the exist plane, and

c) an inertial component equal to $\left[\frac{W_{t+\Delta t} - W_t}{g_c \Delta t}\right] L$

representing the thrust due to acceleration caused by the change of momentum with time within the control volume about the break.

Herein t is the time, W the mass flow rate, A the break flow area, P_e the critical pressure at the exit plan, P_a the ambient pressure, ρ the fluid density, g_c the gravity constant, and L the length of the control volume chosen to represent the break. The velocity used in the calculations is either the inertial velocity (Bernoulli's equation) or the choking velocity as found from Moody's critical flow correlation (Reference 12).

Time dependent blowdown forces are shown by curves in Figure 3.6-56, Empirical functions conservatively approximating this data, shown in heavy lines on Figure 3.6-56, were used in the dynamic analysis pipe whip program "PLAST" as input. Gap data and spring constants for pipe whip restraints are as indicated in Tables 3.6-3 through 3.6-6 for the four breaks chosen.

The "PLAST" program models the pipe run as a lumped parameter system with elastoplastic material properties. The equations of motion of the system are solved by a step by step integration method in the time domain using varying time steps to insure solution stability.

A pipe run is modeled as a lumped parameter system consisting of discretized "masses" and "springs". The "masses" are represented by the physical mass and rotary inertia of the pipe while the "springs" are represented by pipe stiffnesses corresponding to the 6 degrees of freedom for every point along the pipe axis.

A section of pipe bounded by lumped masses at each end is defined as an "element". A 12 x 12, symmetric stiffness matrix may be written for each such element. The individual terms of the matrix may be represented by the symbol "k_{ij}" where the i,j subscripts refer to the row and column locations respectively of the term within the matrix. For a linear pipe element, the non-zero terms are given below:

$k_{11} = AE/L$

$k_{17} = -k_{11} = k_{71}$

$k_{22} = 12\,E\,I/(L^3 + L\,C)$

$k_{26} = k_{62} = -6\,E\,I/(L^2 + C)$

$k_{28} = k_{82} = -k_{22}$

$k_{2,12} = k_{12,2} = k_{26}$

$k_{33} = k_{22}$

$k_{35} = k_{53} = -k_{26}$

$k_{39} = k_{93} = -k_{33}$

$k_{3,11} = k_{11,3} = k_{35}$

$k_{44} = GI_x/L$

$k_{4,10} = k_{10,4} = -k_{44}$

$k_{5,5} = 4\,E\,I/L - \alpha$

$k_{5,9} = k_{26} = k_{9,5}$

$k_{5,11} = k_{11,5} = \beta$

$k_{66} = k_{55}$

$k_{68} = k_{86} = -k_{26}$

$k_{6,12} = k_{12,6} = \beta$

$k_{77} = k_{11}$

$k_{88} = k_{22}$

$k_{8,12} = k_{12,8} = -k_{26}$

$k_{99} = k_{33}$

$k_{9,11} = k_{26}$

$k_{10,10} = k_{44}$

$k_{11,11} = k_{55}$

$k_{12,12} = k_{66}$

When E = Young's modulus

G = Shear modulus

L = Element length

A = Cross - sectional area of pipe metal

I = Cross - sectional moment of inertia in bending

Ix = Torsional moment of inertia

$C = 24\mu(1 + \upsilon)\kappa^2$

υ = Poisson's ratio

μ = Shear factor (2 for pipe)

$r = \sqrt{I/A}$

$$a = \left(3C/L^2 + c\right)\left(EI/L\right)$$

$$\beta = 6EI/\left(L + c/L\right) - \left(4EI/L\right)\left(4L^2 + c/4\,(L^2 + c)\right)$$

This stiffness matrix includes the effect of transverse as well as Torsional shear.

Stiffness matrices have also been developed for curved and "stepped" elements with appropriate "flexibility" factors applied.

The equations of motion for an element are written:

$$[M]\{\ddot{X}\} + [C]\{\dot{X}\} + [K]\{X\} = \{F\} \quad (1)$$

for linear elastic behavior where:

$[M]$, $[C]$, $[K]$ are the mass, damping and stiffness matrices.

$\{X\}$, $\{\dot{X}\}$, $\{\ddot{X}\}$, are the displacement, velocity and acceleration vectors and $\{F\}$ is a vector of forces acting at the element nodes (end masses) that keep the element in equilibrium. Hence in the absence of externally applied forces at a node these represent internal forces.

The equations of motion for the overall structural system are obtained after adding individual element stiffness matrices (referred to overall global axes). The overall equations of motion have the same appearance as (1) but $\{F\}$ represents a vector of forces acting on but external to the structural system.

Damping:

An upper bound damping factor[16] is found for the range of periods between 0.025 seconds and the largest system period. This requires the determination of two constants α and β such that:

$$C_{ij} = 2\beta M_{ij} + \alpha k_{ij} \quad (2)$$

where: C_{ij}, M_{ij}, k_{ij} are the damping, mass and stiffness terms of the i^{th} row and j^{th} column of the $[C]$, $[M]$ and $[K]$ matrices respectively.

The damping matrix represented in (2) represents a conservative estimate of the system damping.

Plasticity:

The materials that make up a piping system are considered to yield according to Von Mises[17] criteria and are either elastic - perfectly plastic (zero-hardening) or harden "isotropically."[18] The constitutive laws are considered to be "incremental" in that they relate increments of plastic deformation to total stress at a point in body as follows:

$$\Delta\epsilon'_{ij} = \frac{\Delta\tau'_{ij}}{2G} + \frac{\partial f(\tau'_{ij})}{\partial\tau_{ij}} \quad (3)$$

where: $\Delta(\ )$ = increment of $(\ )$

G = Shear modulus

ϵ'_{ij}, τ'_{ij} are the tensor components of strain and stress deviators respectively

$f\left(\tau'_{ij}\right)$ is defined by:

$$f\left(\tau'_{ij}\right) - J2 = o \qquad (4)$$

The Von Mises yield criteria are stated in the following way:

If $\left\{ \begin{matrix} f > J2 \\ \Delta f > o \end{matrix} \right\}$ then yielding occurs

If $\left\{ \begin{matrix} f \leq J2 \\ \Delta f < o \end{matrix} \right\}$ then elastic action occurs

Equation (4) may be depicted as a right circular cylinder making equal angles with three principal axes representing principal stresses at a point. [18] When yielding occurs, the plastic strain increment can be plotted on the same set of axes (with an appropriate scale factor) as a vector normal to the cylindrical surface. Isotropic hardening is represented as an expansion of the cylinder cross - section about its origin (i.e., isotropically). In order to establish hardening parameters it is necessary to know the slope and shape of the uniaxial stress - strain curve beyond initial yielding.

The flow rule associated with the Von Mises yield criteria is not applied directly to the framed structures. Instead, use is made of yield surfaces in "force space".[19] derived from the Von Mises yield surface. These surfaces are symmetrical with respect to principal force axes but lack point symmetry. A simplifying approximation to such surfaces may be made by utilizing their circumscribing sphere in force space. The equation of this space is given as:

$$\Phi = \left(\frac{My}{My^P}\right)^2 + \left(\frac{Mz}{Mz^P}\right)^2 + \left(\frac{Fx}{Fx^P}\right)^2 - \kappa^2 \left(1 - \left(\frac{M_x}{M_x^P}\right)^2\right) \qquad (5)$$

Where: Mx, My, M are the internal moments about the designated axes.

$F_x^P, M_x^P, M_y^P, M_z^P$ are the fully plastic values of these forces.

Fx is the internal axial force on a member.

κ is the sphere radius.

The associated flow is then:

$$\Delta X_i^P = \lambda \frac{\partial \Phi}{\partial f_i} \qquad (6)$$

Where: ΔX_i^P = the i^{th} component of plastic displacement increment

F_i = the i^{th} component of internal force (limited to the components in eq. (5))

The total displacement of a point can be broken up into elastic and plastic components:

$$\Delta X_i = \Delta X_i^{(e)} + \Delta X_i^{(P)}$$

Then since only elastic displacement contribute to force at a node, equation (1) becomes: (7)

$$[M]\{\ddot{X}\} + [C]\{\dot{X}\} + [K]\{X\} = \{F\} + \{F^{(P)}\} \quad (8)$$

Where: $\{F^{(P)}\} = [K]\{X^{(P)}\}$

is the "plastic correction force" developed internally for a yielding element, and assembled as a total correction force for the overall structure system. Expressions for λ in equation (9) for cases of one and two nodes of an element yielding are shown in detail in reference (20). These were based on the following assumptions:

a) - Small deformation
b) - Concentrated forces applied only at nodes (masses)
c) - Yielding at a cross - section occurs simultaneously over the entire cross - section or not at all
d) - There is no spread of yielding beyond the node along the beam axis
e) - The flow rule of eq (6) applies

In the case of isotropic hardening, one seeks parameters that indicate the correct yield surface to use (in force space) for the flow rule, eq. (9). Towards this end the following terms are defined for pipe beams:

a) - Effective stress:

$$\sigma_e = \sqrt{3\, J_2}$$

where:

$$J_2 = 1/3\,(\tau_{xx})^2 + (\tau_{xo})^2$$

b) - Effective plastic strain:

$$e^{(P)} = \sum_{i=1}^{n} \left(\Delta e_i^{(P)}\right)$$

Where:

$$\Delta e_i^{(P)} = \sqrt{2/3\left[(\Delta \epsilon_{xx}^{(P)})^2 + 2\,(\frac{\Delta \gamma_{xo}}{2})^2\right]}$$

c) - Effective stress strain curve

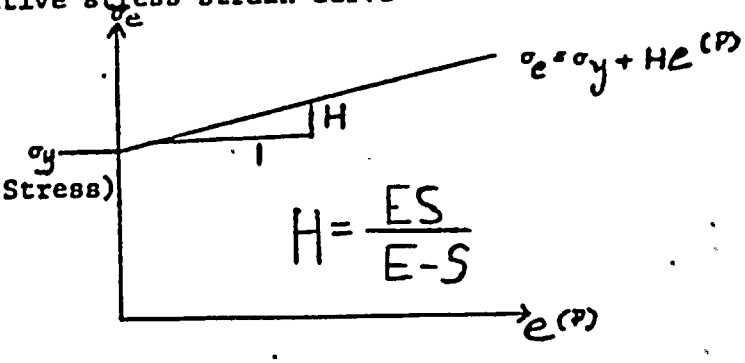

E=Young's modulus
S=Plastic modulus

(Shown for a bilinear material)

Fig 1

The effective stress-strain curve is a plot of stress vs plastic strain for a uniaxial specimen. For a three dimensional analysis, it represents the radius of the yield surface plotted against effective plastic strain. The area under this curve is the plastic work of deformation. Therefore if the forces that give rise to yielding along this curve are known the expression for the yield surface in force space may be used to find plastic displacement increments as in equation (6).

Solution

Solution of equations (8) is by the Newmark "Beta" Method[21] using Beta = 1/6 and a convergence rate of 0.1. The initial integration step is found internally as a fraction of the approximate value of the lowest period of the system. Solution stability is assured by maintaining an upper bound of 1/5 on the value of this fraction. Further improvements in the time step may be made by accounting for the lowering of natural frequencies of the system that result from yielding.

In propagating the solution through the time domain, no modifications are made to the initial stiffness and mass matrices. The problem, in short, is considered to be in the "small deformation" regime. However small deformations give rise to large deflections and rotations. Hence, blowdown forces at severed pipes are made to follow the pipe movements. Gaps at restraints, are treated as step changes in displacement force boundary conditions; i.e. a node initially with a zero force specification in some direction suddenly changes its specification to zero displacement in that direction. Pipe whip restraints are modeled as bilinear, elasto-plastic springs of zero length and negligible mass. These "take a ride" with the whipping pipe until the gap is closed.

As each element of the system is loaded, it deforms according to elastic and then elastoplastic constitutive laws. Unloading occurs elastically leaving a residual "plastic displacement" in each of the yielded elements.

Restraint models consist of one or more "anchors" and elastoplastic external springs with initial gaps; the latter representing the pipe whip restraints. All hangers and earthquake restraints are considered to have failed. Rebound velocities and impact forces are affected by gap size, restraint and pipe material properties and system damping as follows.

Rebound velocities and impact forces at a restraint result from the instantaneous introduction of a displacement boundary condition at the restraint. This boundary condition imposes displacement constraints on a mass which has the effect of applying external forces on the mass. If the boundary condition nullifies displacements in any direction, the restraint is considered "rigid." If displacements are a linear function of themselves, the restraint is considered "elastic." If displacements are governed by laws of one dimensional elastic-plasticity, the restraint is considered as an "elasto-plastic, strain-hardening" restraint. The sum of the rate of change in momentum of the mass due to the introduction of this boundary condition plus the viscous forces in the mass plus the internal force of the attached pipe is the total force acting on the mass. The resultant total momentum change accounts for the instantaneous rebound velocity of the mass. These factors depend on the mass velocity at impact, the type of restraint (rigid, elastic or elasto-plastic), system damping and the stiffness properties of the pipe. Gap size affects the mass velocity at impact.

The analysis, in each break case, was allowed to run until it was observed that the loaded mass point oscillated with decreasing amplitude about some displacement value. It was noted, in all cases, that the first peak in reaction force magnitude was never subsequently superceded, even though displacement peaks were reached after the reaction peaks. Strain hardening in the piping system was taken as zero for conservatism.

The peak plastic strains in each system are indicated in Figures 3.16-3,5,7 and 9. The total strain in each case can be obtained by adding the yield strain to the maximum plastic strain and is seen never to approach $E_u/2$.

Results of pipe whip analyses performed on guillotine breaks in two locations of the feedwater line on either side of the penetration and in two locations of the main steam line inside containment are shown in Table-3.6-2. In addition, sensitivity studies for the feedwater line outside containment are shown for a change in gap and a change in wall thickness. A reduction in gap reduces peak restraint reactions as was expected. Decreasing the wall thickness however seems to have the opposite effect. The results of this sensitivity study are given in Figures 3.6-63 through 3.6-68 and Table 3.6-1.

The coefficients used to calculate the jet thrust force on the ruptured pipe are based on the following:

1) Maximum theoretical values of the thrust coefficients have been predicted by Moody (Reference 12) under steady flow conditions to be 1.26 for steam and flashing water, and 2.0 for subcooled water. These values ignore frictional effects in the pipes and exit effects.

2) In real fluids friction and exit losses are present, therefore the maximum theoretical coefficients have been modified to account for such losses. Thrust forces for several piping breaks involving steam and feedwater were derived by using the RECAP-3 thermal hydraulic code (Reference 14). The results show that at steady state flow conditions peak values of the thrust coefficients are close to unity for steam and 1.1 for flashing water. The particular values listed above of 1.01 and 1.12 respectively for steam and flashing water were derived for conditions typical in power plants using 350 psi exit pressure for saturated steam and low quality ($\approx$1 percent) and 800 psi pressure at the exit plane for feedwater.

3) For subcooled water frictional effects are accounted for by utilizing a resistance coefficient of 1.23 (Reference 11)

4) To account for the more severe contraction present in the case of a slot break, a contraction coefficient of 0.61 has been chosen (Reference 13).

TABLE 3.6-1

SENSITIVITY STUDY FOR 20" FW LINE OUTSIDE CONTAINMENT

Node No. At Restraint	Gap (in)	Wall Thick. (in)	Max. Reaction (lbs)	Max. Plastic Strain in Pipe	Max. Defl. At Loaded Node
5	2	1	$.8221 \times 10^6$	.0065	6.381"
5	2	1.5	$.68 \times 10^6$	.0072	5.446"
5	4	1.5	$.7806 \times 10^6$	.00148	9.255"

TABLE 3.6-2

SUMMARY OF PIPE WHIP ANALYSIS

Line Description	Guillotine Break at Node Number	Active Restraint Node Number	Maximum Deflection at break	Maximum Reaction at Restraint (pounds x 10^6)	Maximum Plastic Strain in Pipe
Feedwater Outside Containment 1.5" wall and 4.00" gap	7	5	9.255"	0.7806	0.00148
Feedwater Inside Containment	7	6	3.502"	1.34	0.00259
Mainsteam Inside Containment	12	9	11.46"	2.72* (+X) 2.34 (+Z)	0.00762
Mainsteam Inside Containment	16	9 13	13.36"	1.0 (+Z) 1.78 (+X) 1.52 (+X,-Z)	0.0000

*Values exceeding 2KPA have a duration of <2 milliseconds

TABLE 3.6-3

MAIN STEAM LINE INSIDE THE CONTAINMENT
GUILLOTINE BREAK AT NODE #12

Node	Restraint I.D. No.	El. Spring Const.	Pl. Spring Const.	Gap (in.)
2	MS-12	8.536×10^6 #/in	3.570×10^5 #/in	6.00
4	MS-13	8.786×10^6 #/in	3.650×10^5 #/in	6.00
5	MS-14	8.786×10^6 #/in	3.650×10^5 #/in	6.00
8	MS-15	8.786×10^6 #/in	3.650×10^5 #/in	5.50
9	MS-16	8.786×10^6 #/in	3.650×10^5 #/in	5.50
11	MS-17	8.786×10^6 #/in	3.650×10^5 #/in	4.00

TABLE 3.6-4

MAIN STEAM LINE INSIDE THE CONTAINMENT
GUILLOTINE BREAK AT NODE #16

Restraint Information

Node	Restraint I.D. No.	El. Spring Const.	Pl. Spring Const.	Gap (in.)
2	MS-12	8.536×10^6 #/in	3.570×10^6 #/in	6.00
4	MS-13	8.786×10^6 #/in	3.650×10^6 #/in	6.00
5	MS-14	8.786×10^6 #/in	3.650×10^6 #/in	6.00
8	MS-15	8.786×10^6 #/in	3.650×10^6 #/in	5.50
9	MS-16	8.786×10^6 #/in	3.650×10^6 #/in	5.50
11	MS-17	8.786×10^6 #/in	3.650×10^6 #/in	4.00
13	MS-18	8.786×10^6 #/in	3.650×10^6 #/in	4.00

TABLE 3.6-5

BOILER FEEDWATER LINE OUTSIDE THE CONTAINMENT
GUILLOTINE BREAK AT NODE #7

Restraint Information

Node	El. Spring Const.	Pl. Spring Const.	Gap (in.)
2	8.536×10^6 #/in	3.570×10^6 #/in	4.00
4	8.536×10^6 #/in	3.570×10^6 #/in	4.00
5	8.536×10^6 #/in	3.570×10^6 #/in	4.00

TABLE 3.6-6

BOILER FEEDWATER LINE INSIDE THE CONTAINMENT
GUILLOTINE BREAK AT NODE #7

Restraint Information

Node	El. Spring Const.	Pl. Spring Const.	Gap (in.)
4	8.786×10^6 #/in	3.650×10^6 #/in	2.50
6	8.786×10^6 #/in	3.650×10^6 #/in	4.00

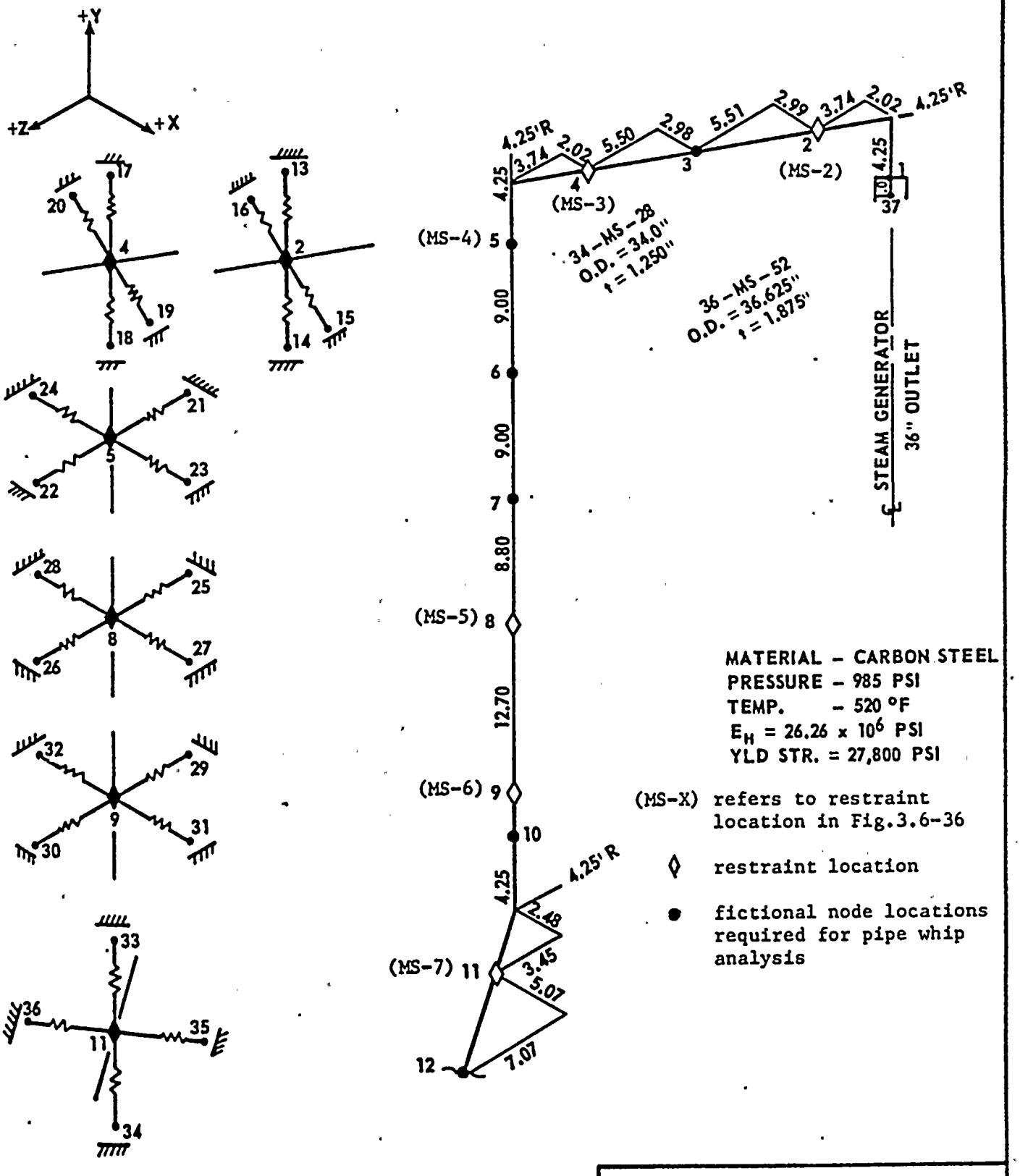

REF. ISOMETRIC: MS - 147-1

FLORIDA POWER & LIGHT COMPANY
ST. LUCIE PLANT UNIT 1

MAIN STEAM LINE INSIDE CONTAINMENT
GUILLOTINE BREAK AT NODE #12

FIGURE 3.6-52

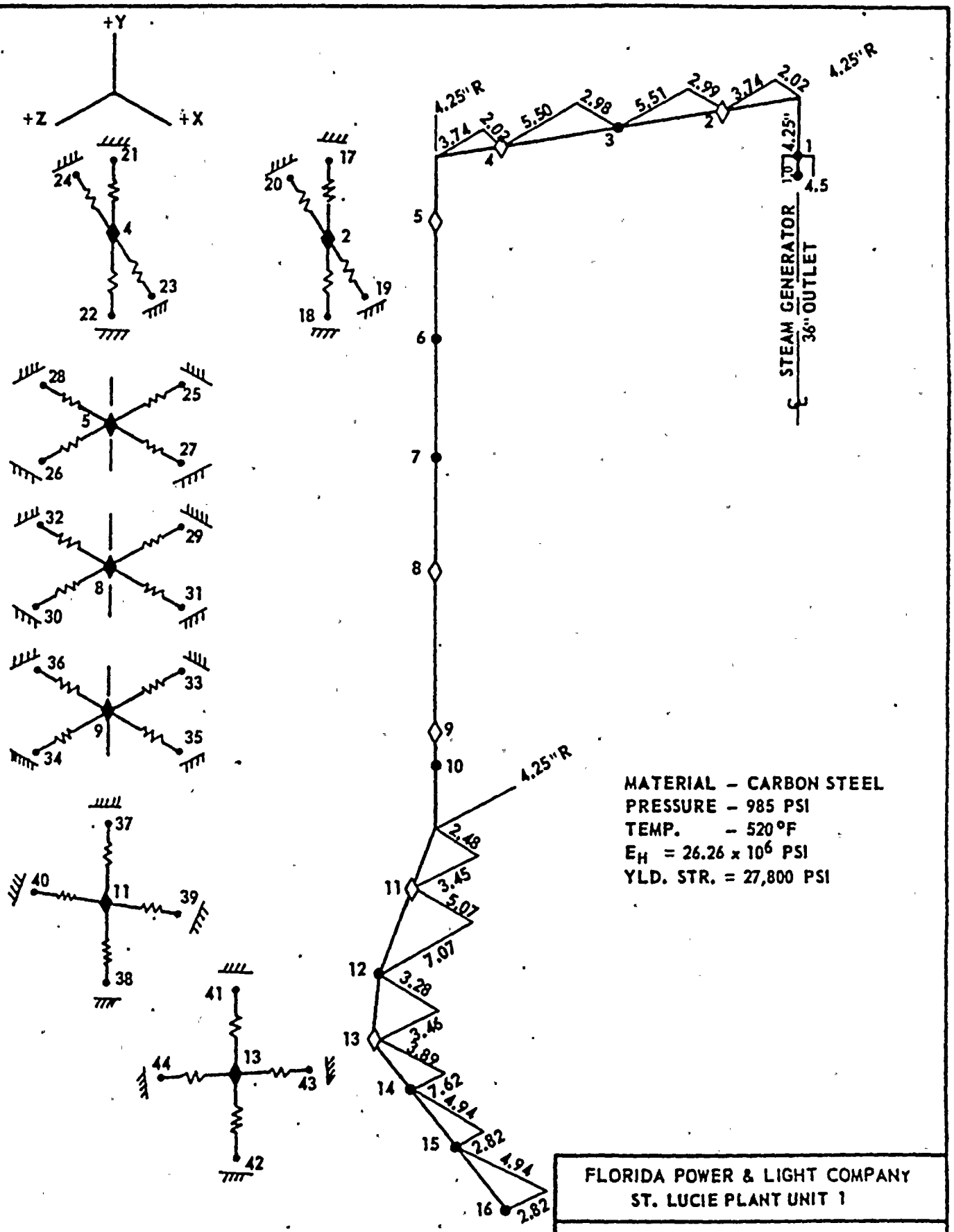

FLORIDA POWER & LIGHT COMPANY
ST. LUCIE PLANT UNIT 1

MAIN STEAM LINE INSIDE CONTAINMENT
GUILLOTINE BREAK AT NODE #16

FIGURE 3.6-53

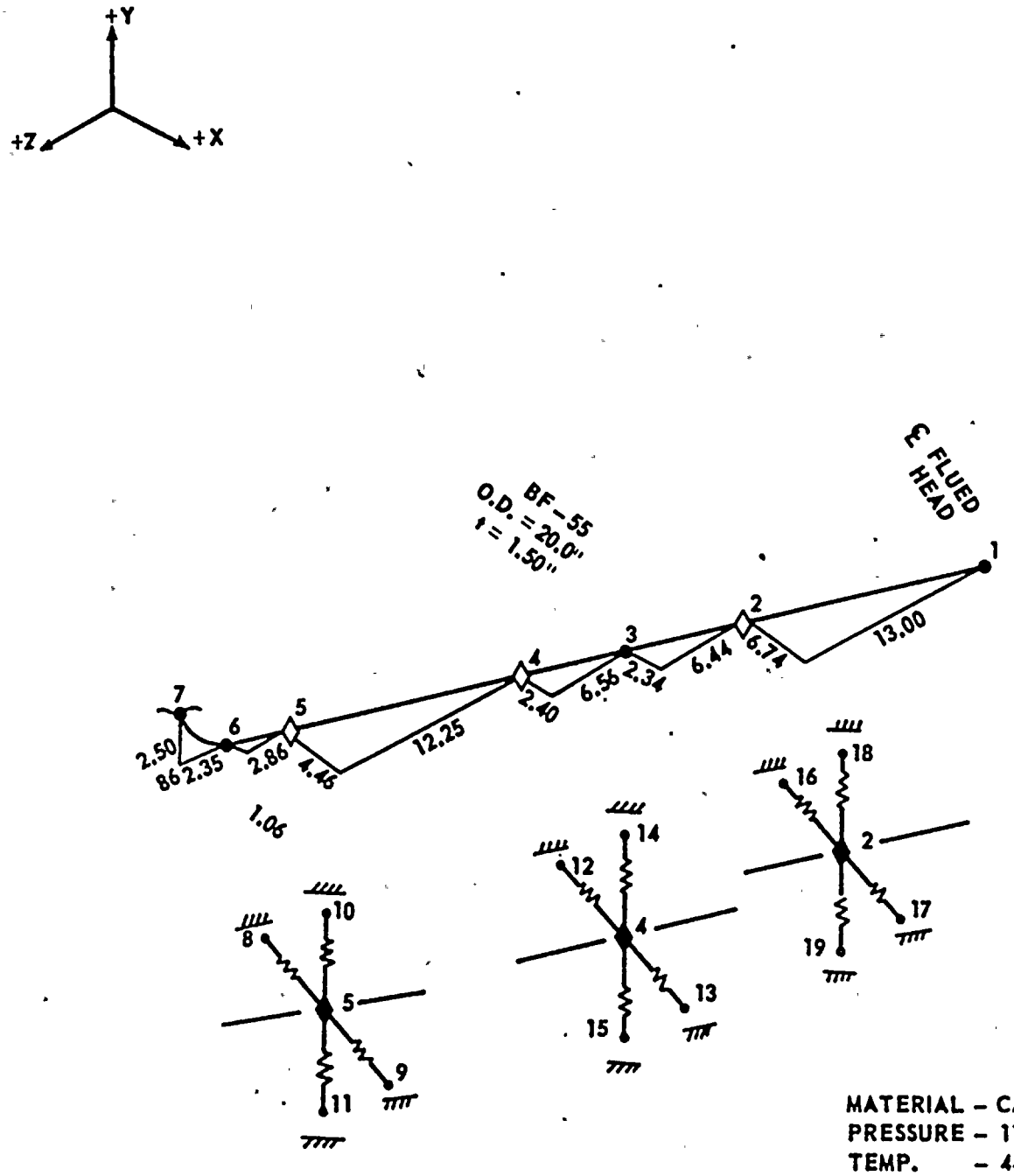

MATERIAL – CARBON STEEL
PRESSURE – 1100 PSI
TEMP. – 440°F
$E_H = 26.76 \times 10^6$ PSI
YLD. STR. = 29,320 PSI

REF. ISOMETRIC: BF-149-1

FLORIDA POWER & LIGHT COMPANY
ST. LUCIE PLANT UNIT 1

BOILER FEEDWATER LINE OUTSIDE CONTAINMENT GUILLOTINE BREAK AT NODE #7

FIGURE 3.6-54

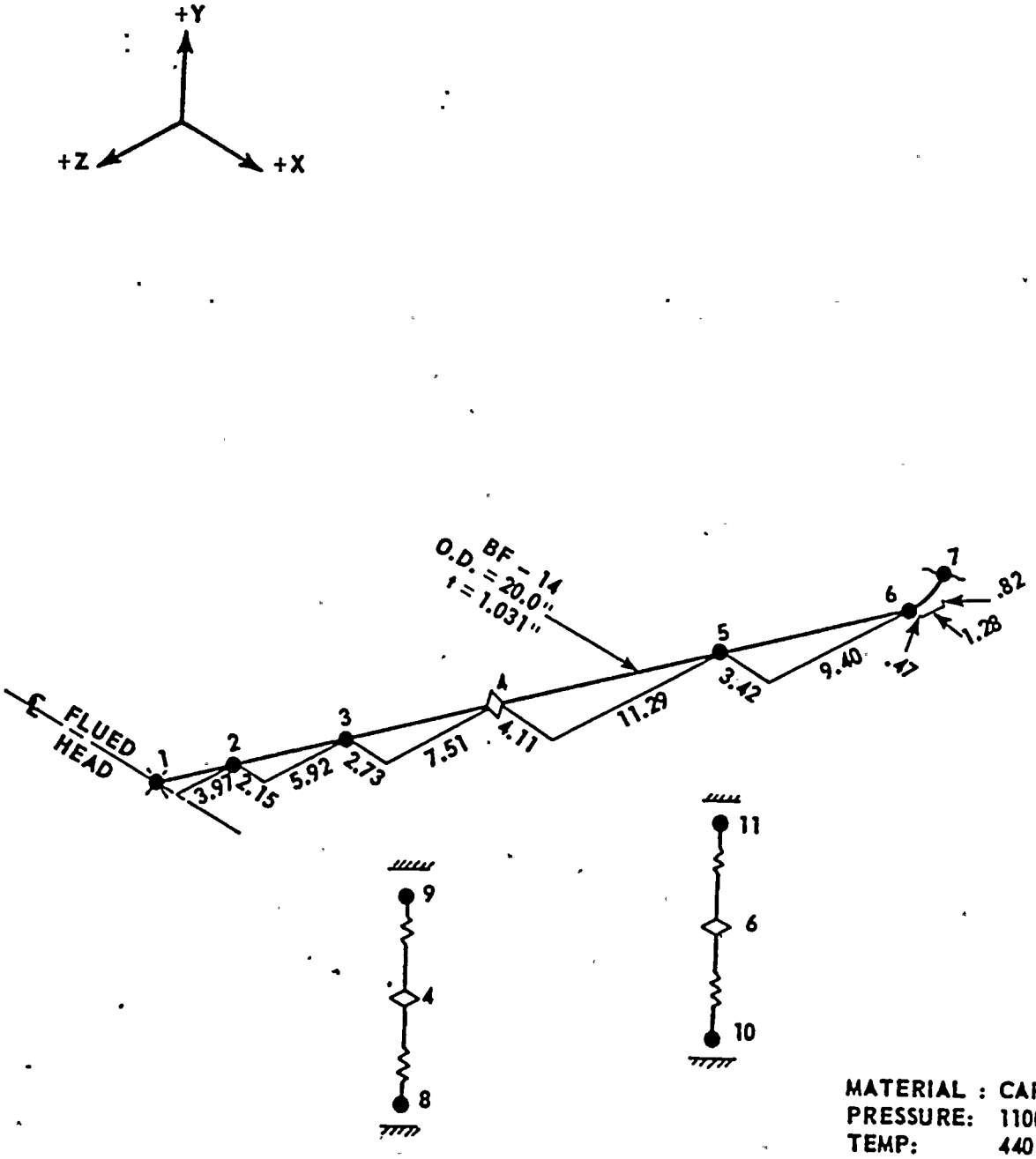

MATERIAL : CARBON STL.
PRESSURE: 1100 PSI
TEMP: 440 °F
E_H = 26.76×10^6 PSI
YLD. STR.= 29,320 PSI

REF. ISOMETRIC: BF-147-1

FLORIDA POWER & LIGHT COMPANY
ST. LUCIE PLANT UNIT 1

BOILER FEEDWATER LINE INSIDE CONTAINMENT GUILLOTINE BREAK – NODE #7

FIGURE 3.6-55

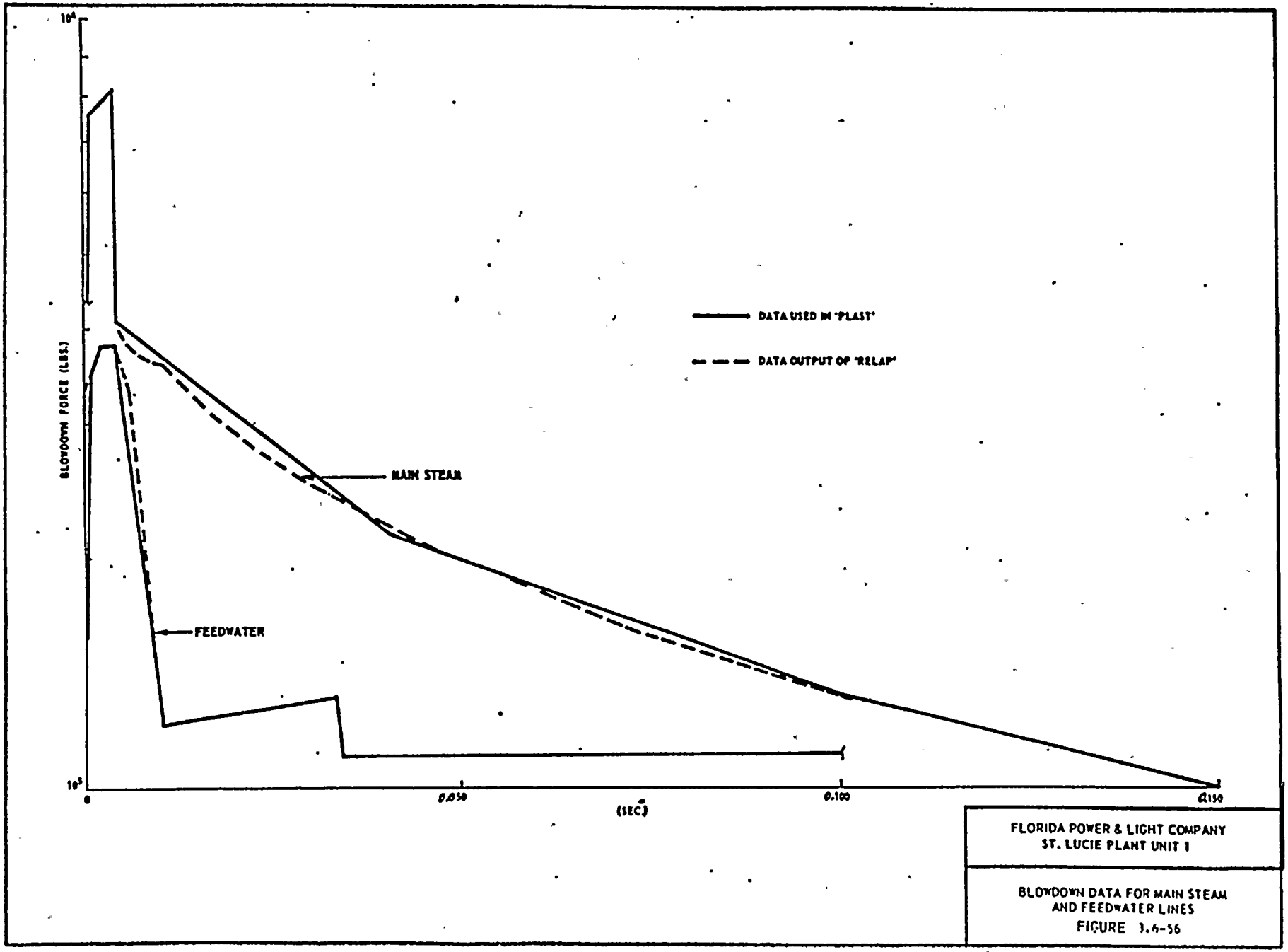

FLORIDA POWER & LIGHT COMPANY
ST. LUCIE PLANT UNIT 1

BLOWDOWN DATA FOR MAIN STEAM AND FEEDWATER LINES
FIGURE 3.6-56

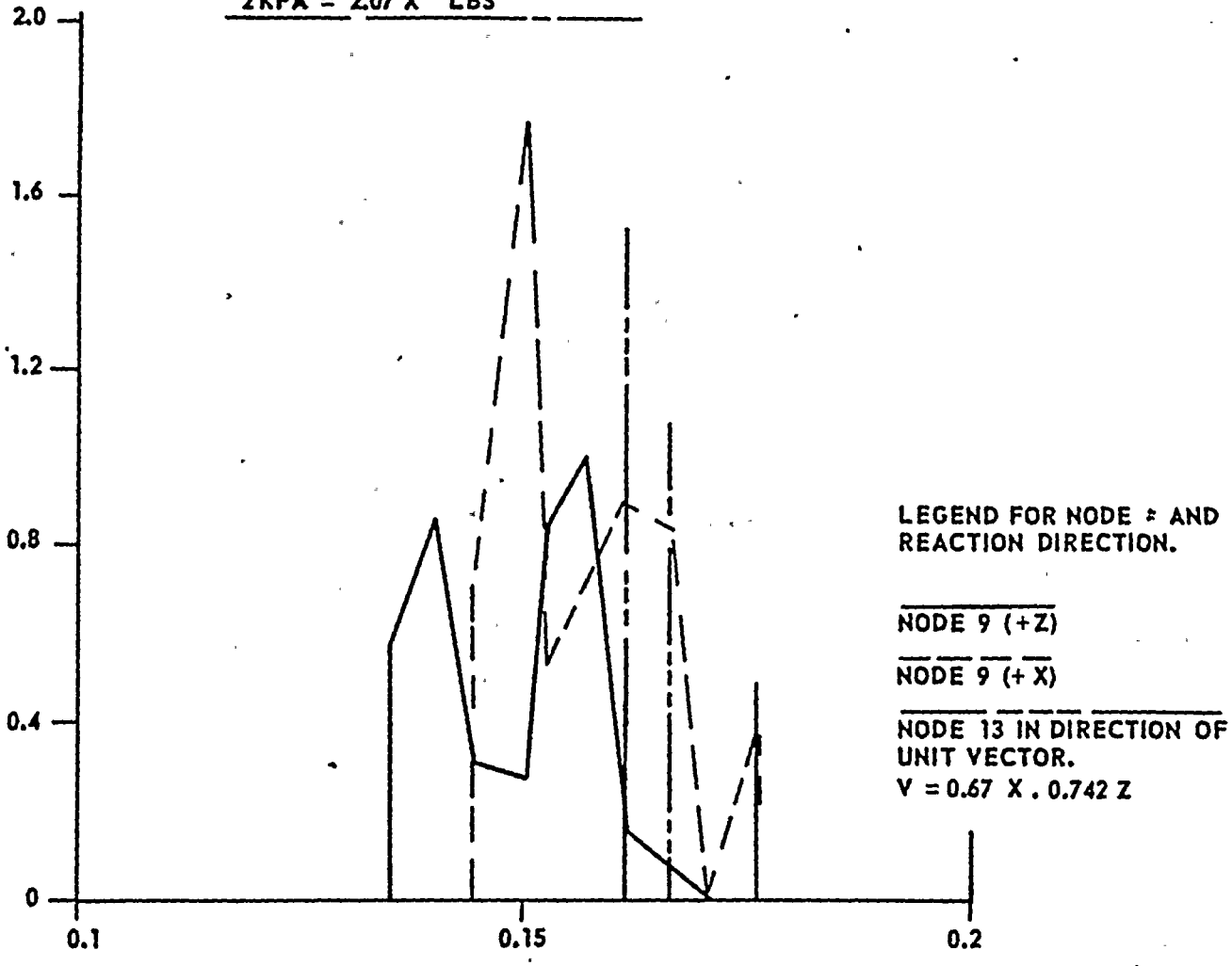

FLORIDA POWER & LIGHT COMPANY
ST. LUCIE PLANT UNIT 1

MAIN STEAM LINE INSIDE CONTAINMENT (BREAK AT NODE 16) REACTIONS AT PIPE WHIP RESTRAINTS (NODES 13 & 9) VERSUS TIME

FIGURE 3.6-57

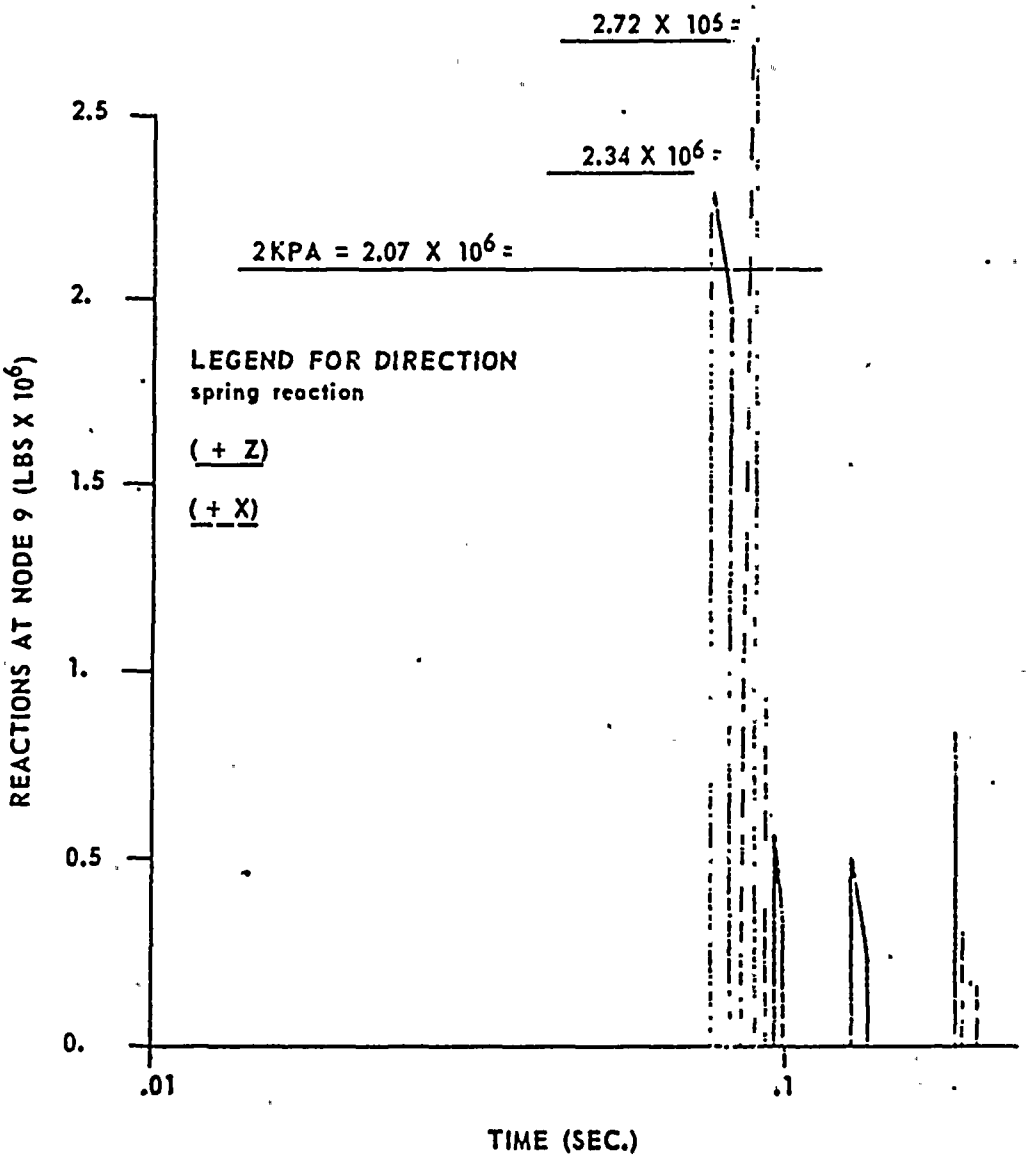

FLORIDA POWER & LIGHT COMPANY
ST. LUCIE PLANT UNIT 1

34" MAIN STEAM LINE INSIDE CONTAINMENT
BREAK AT NODE 12, REACTION AT PIPE
WHIP RESTRAINT AT NODE 9 IN + X & + Z
DIRECTIONS VERSUS TIME

FIGURE 3.6-58

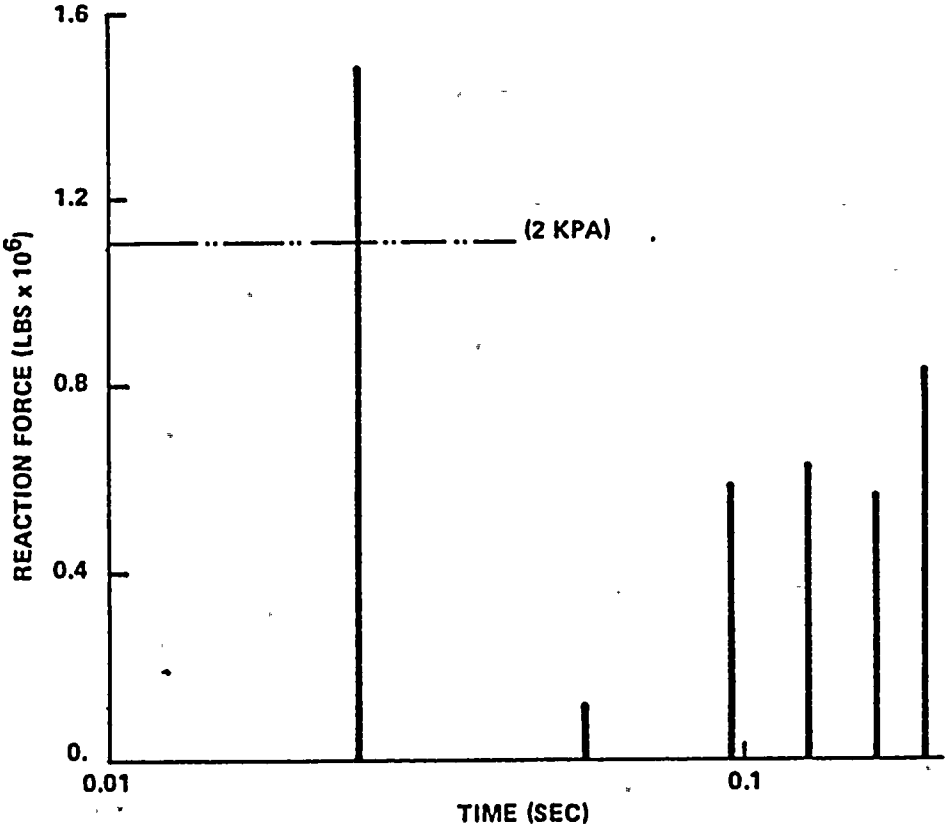

FLORIDA POWER & LIGHT COMPANY
ST. LUCIE PLANT UNIT 1

FW LINE INSIDE CONTAINMENT
REACTION AT PIPE WHIP RESTRAINT
AT NODE 6 VS. TIME
FIGURE 3.6-59

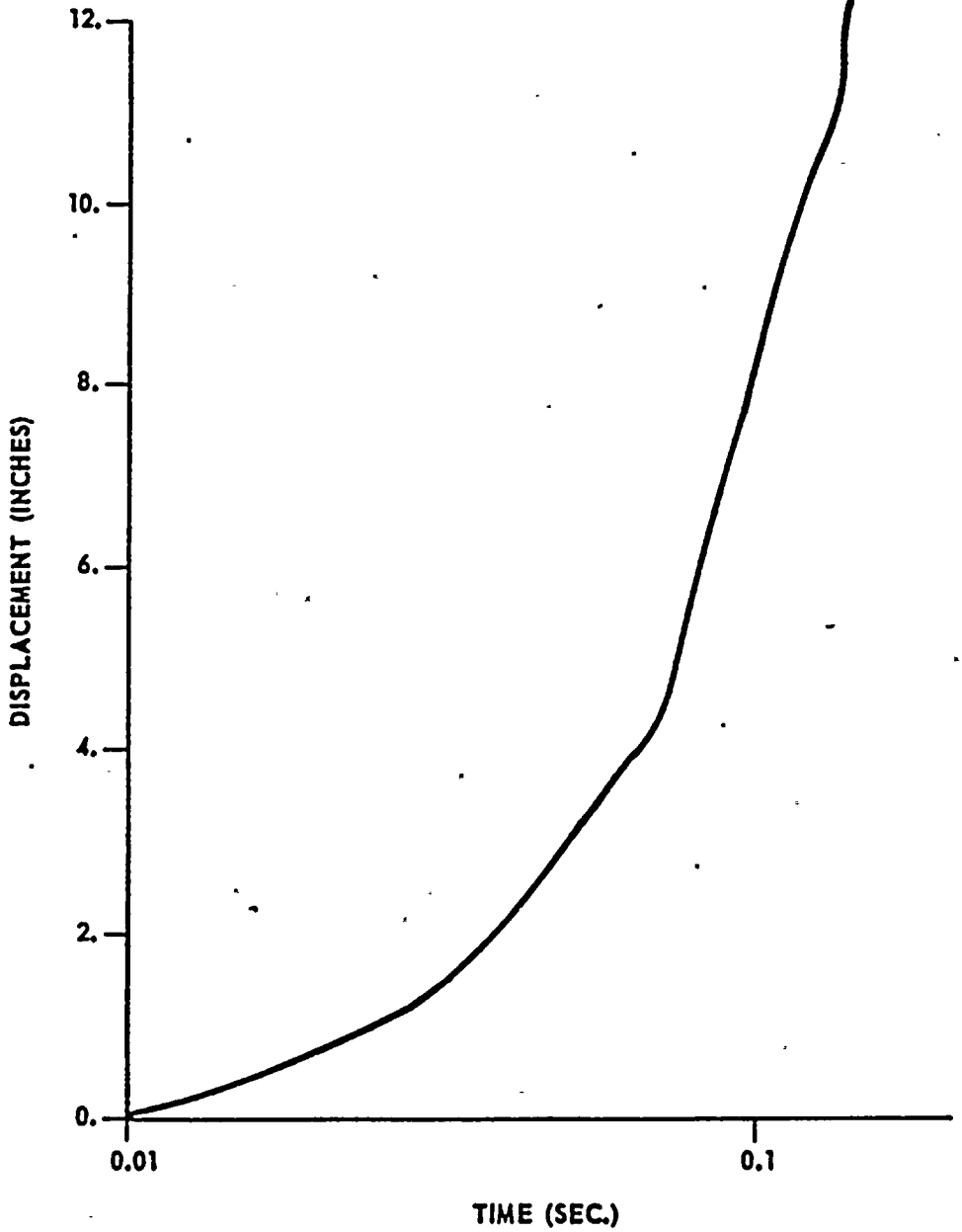

FLORIDA POWER & LIGHT COMPANY
ST. LUCIE PLANT UNIT 1

MAIN STEAM LINE INSIDE CONTAINMENT BREAK AT NODE 16 DISPLACEMENT OF NODE 16 VERSUS TIME MAX. PLASTIC STRAIN = 0.

FIGURE 3.6-60

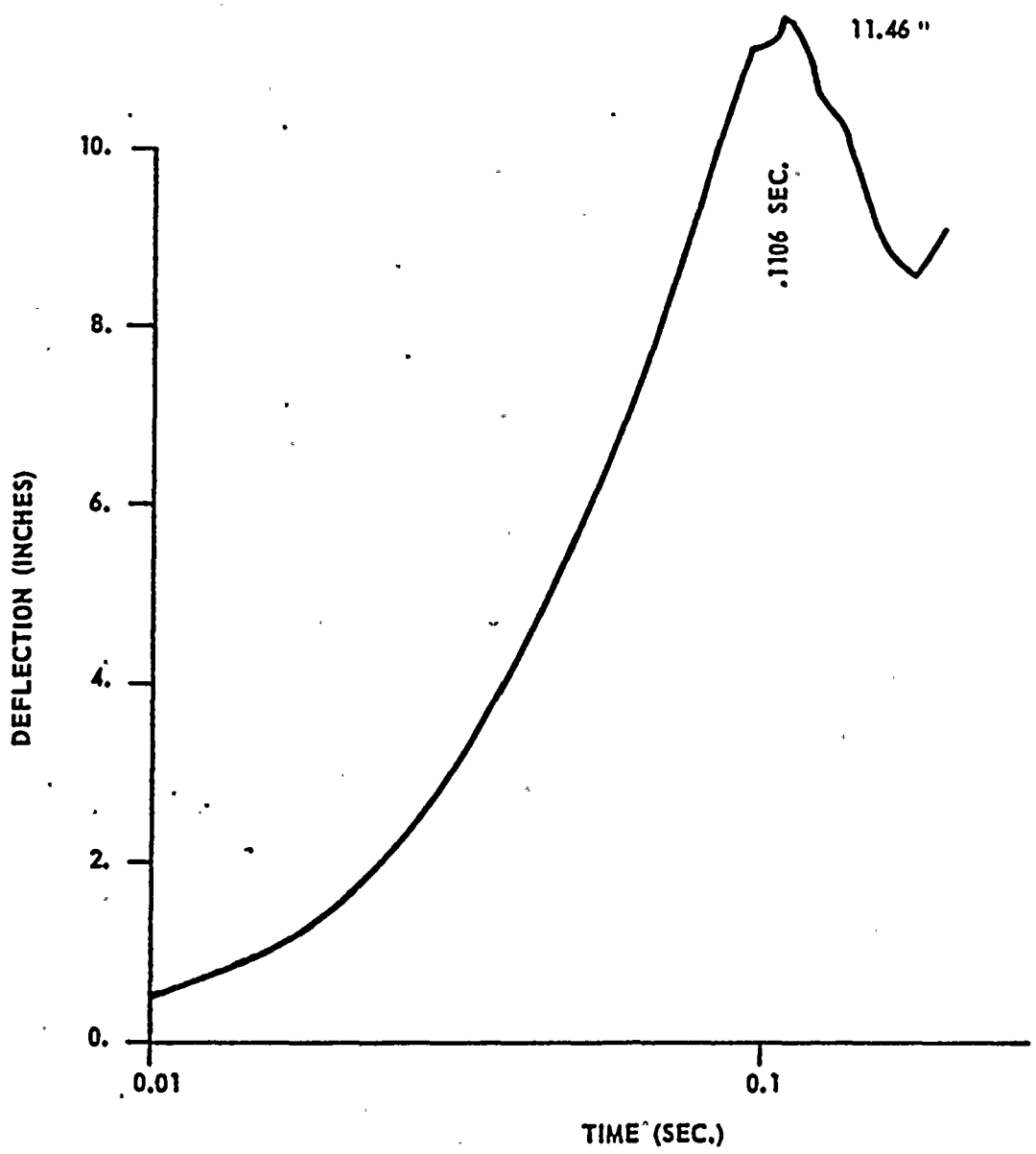

FLORIDA POWER & LIGHT COMPANY
ST. LUCIE PLANT UNIT 1

34" MAIN STEAM LINE INSIDE CONTAINMENT (BREAK AT NODE 12)
DEFLECTION OF NODE 12 VERSUS TIME
MAX. PLASTIC STRAIN = .00762

FIGURE 3.6-61

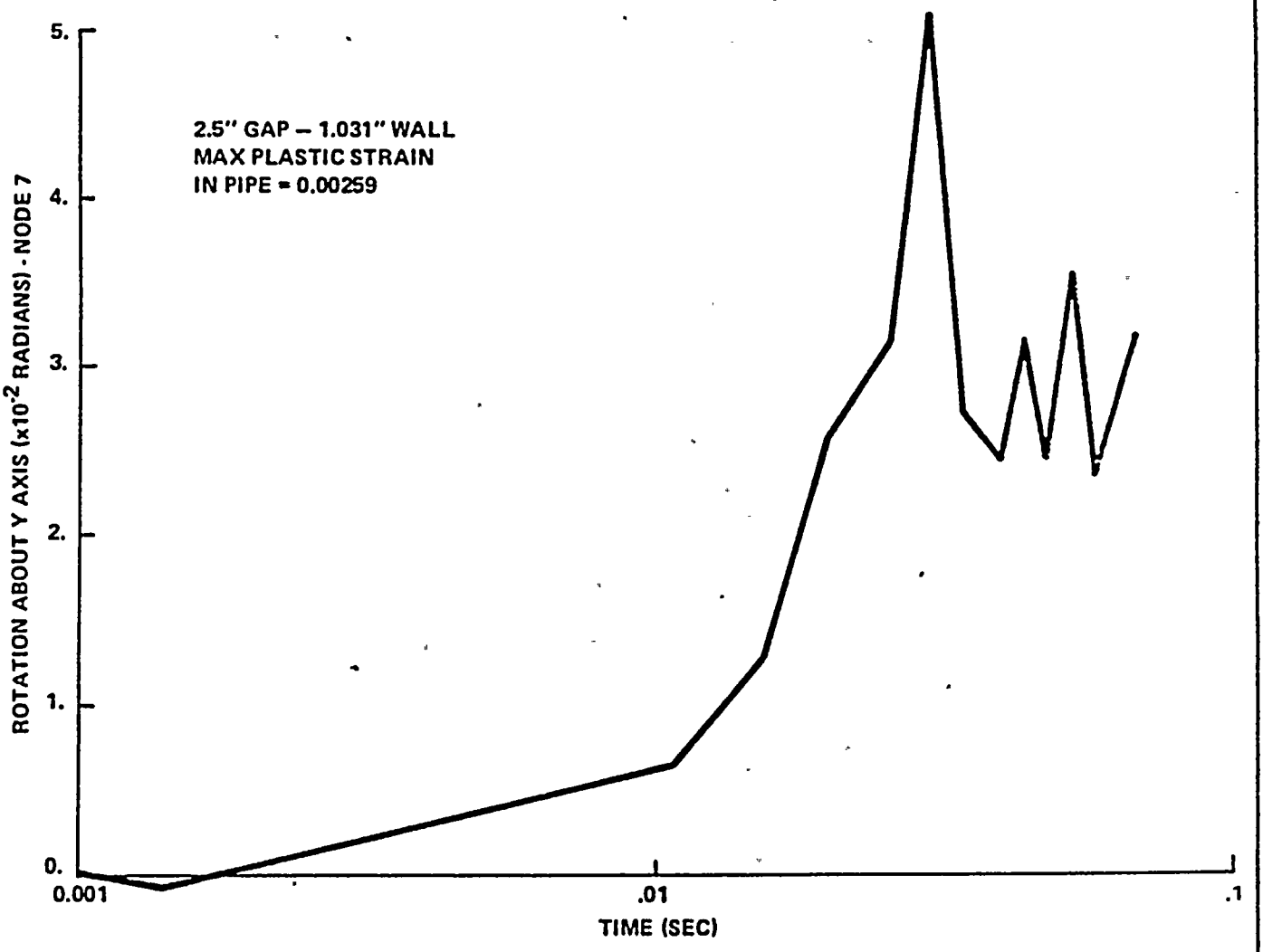

FLORIDA POWER & LIGHT COMPANY
ST. LUCIE PLANT UNIT 1

20" FW LINE INSIDE CONTAINMENT
ROTATION OF NODE 7 VS. TIME
FIGURE 3.6-62

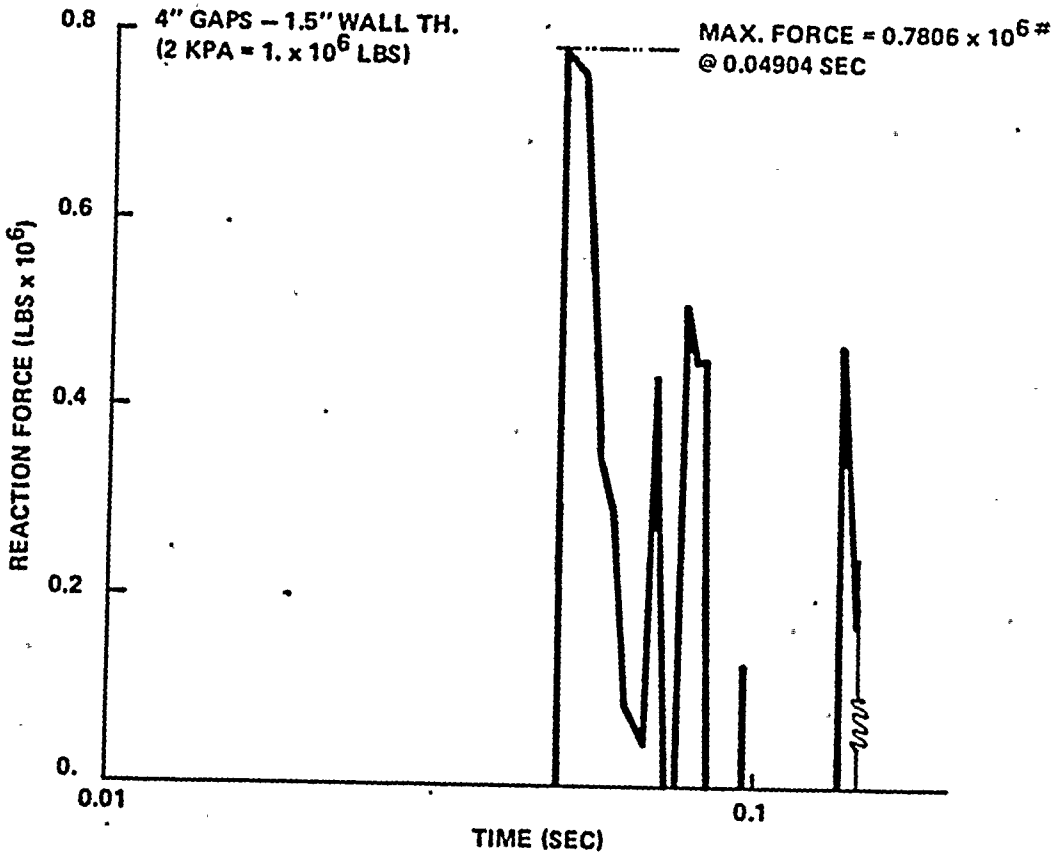

FLORIDA POWER & LIGHT COMPANY
ST. LUCIE PLANT UNIT 1

20" FW LINE OUTSIDE CONTAINMENT
REACTIONS AT PIPE WHIP RESTRAINT
AT NODE 5 VS. TIME
FIGURE 3.6-63

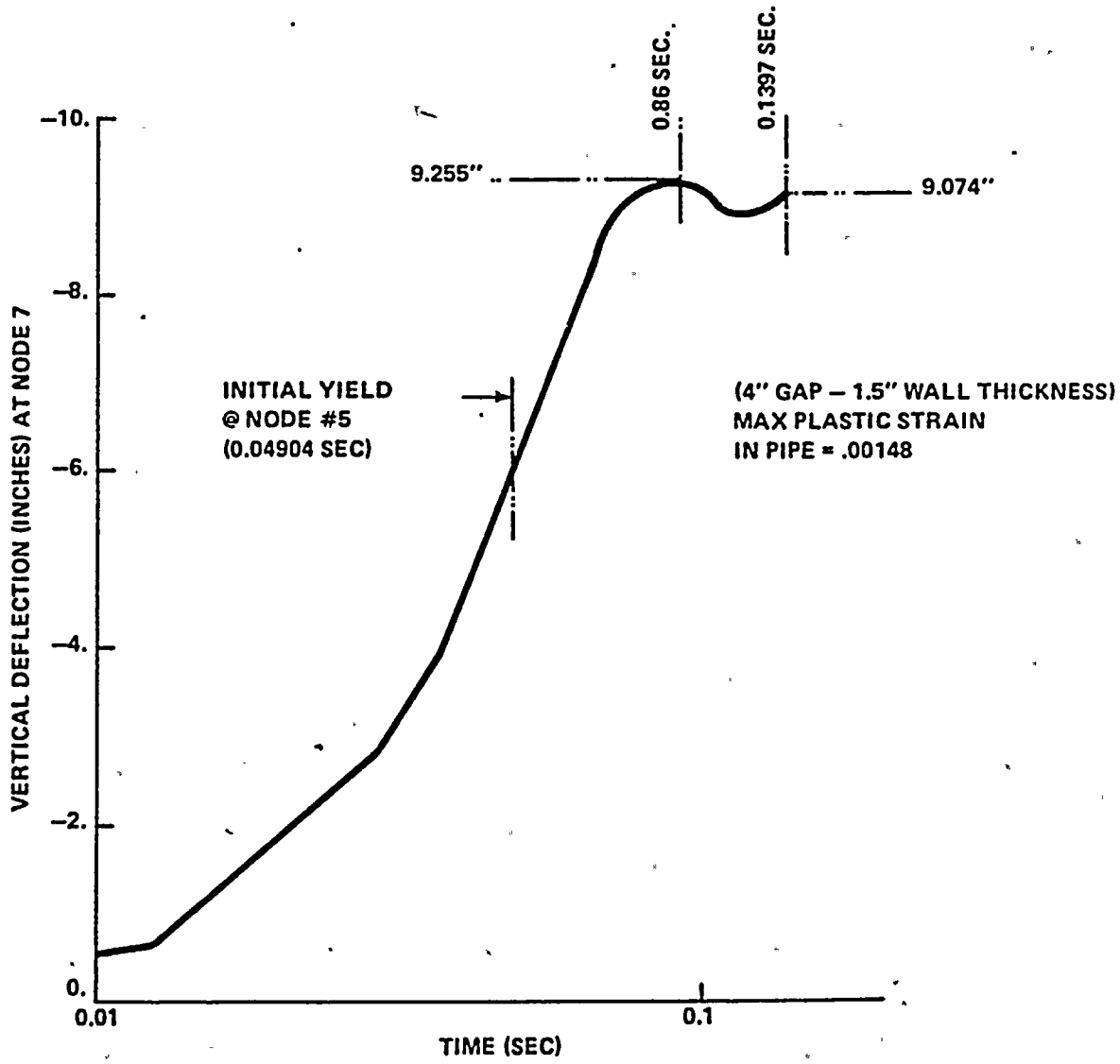

FLORIDA POWER & LIGHT COMPANY
ST. LUCIE PLANT UNIT 1

20" FW LINE OUTSIDE CONTAINMENT
DISPLACEMENT AT NODE 7 VS. TIME
FIGURE 3.6-64

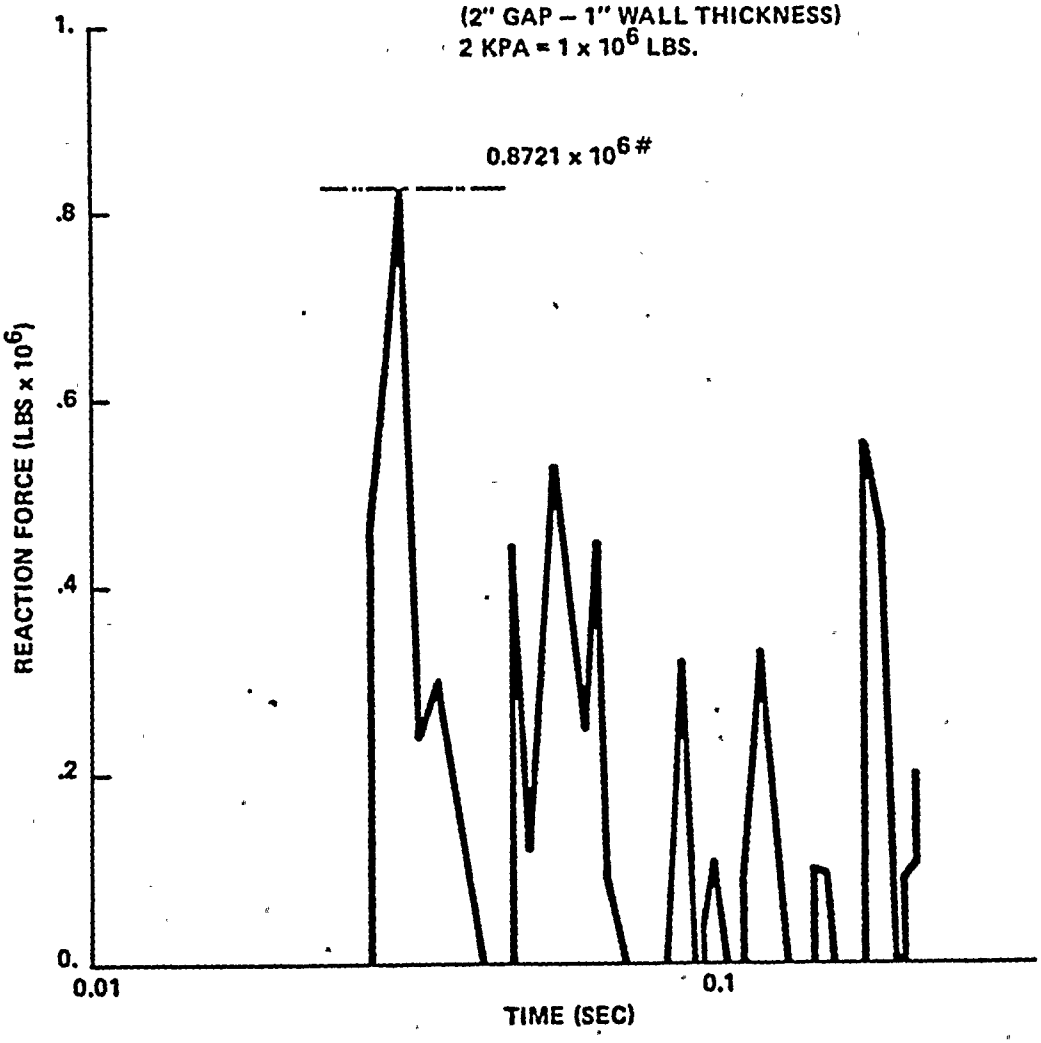

FLORIDA POWER & LIGHT COMPANY
ST. LUCIE PLANT UNIT 1

20" FW LINE OUTSIDE CONTAINMENT
REACTIONS AT PIPE WHIP RESTRAINT
AT NODE 5 VERSUS TIME
FIGURE 3.6-65

(2" GAP – 1" WALL THICKNESS)
MAX. PLASTIC STRAIN IN PIPE - 0.0065

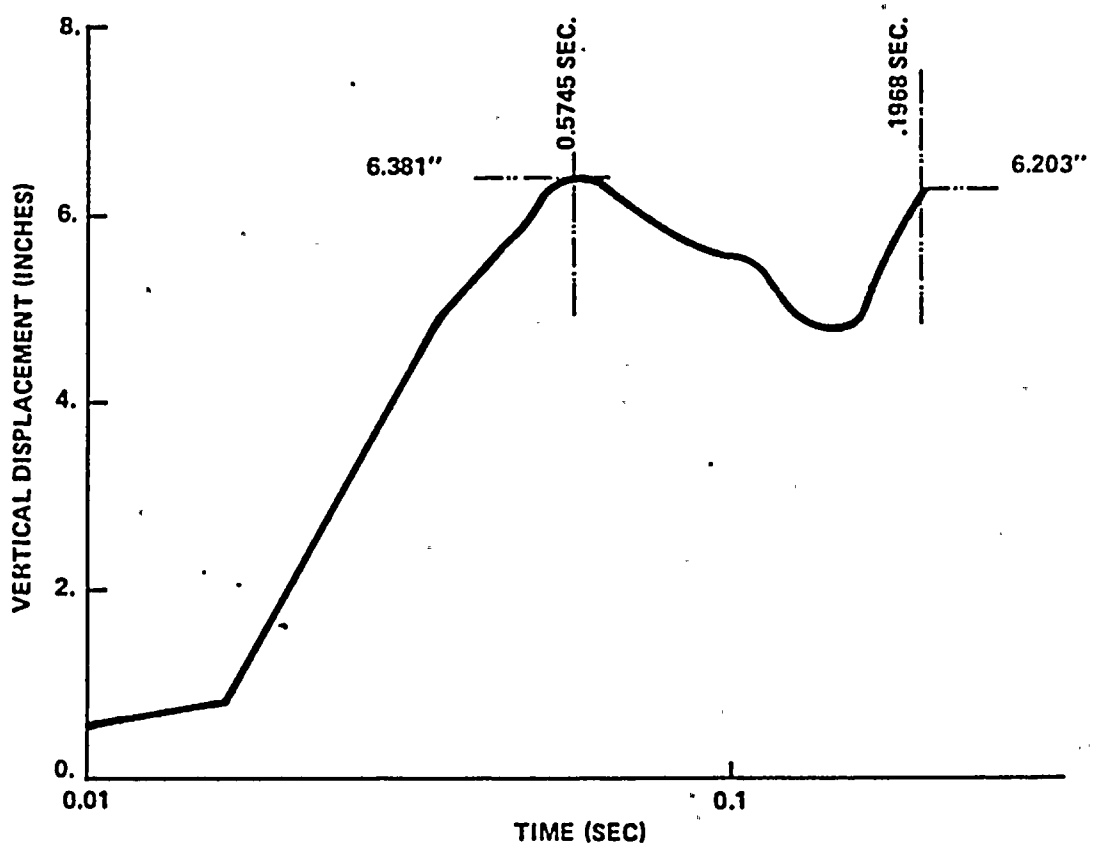

FLORIDA POWER & LIGHT COMPANY
ST. LUCIE PLANT UNIT 1

20" FW LINE OUTSIDE CONTAINMENT
DISPLACEMENT OF NODE 7 VS. TIME
FIGURE 3.6-66

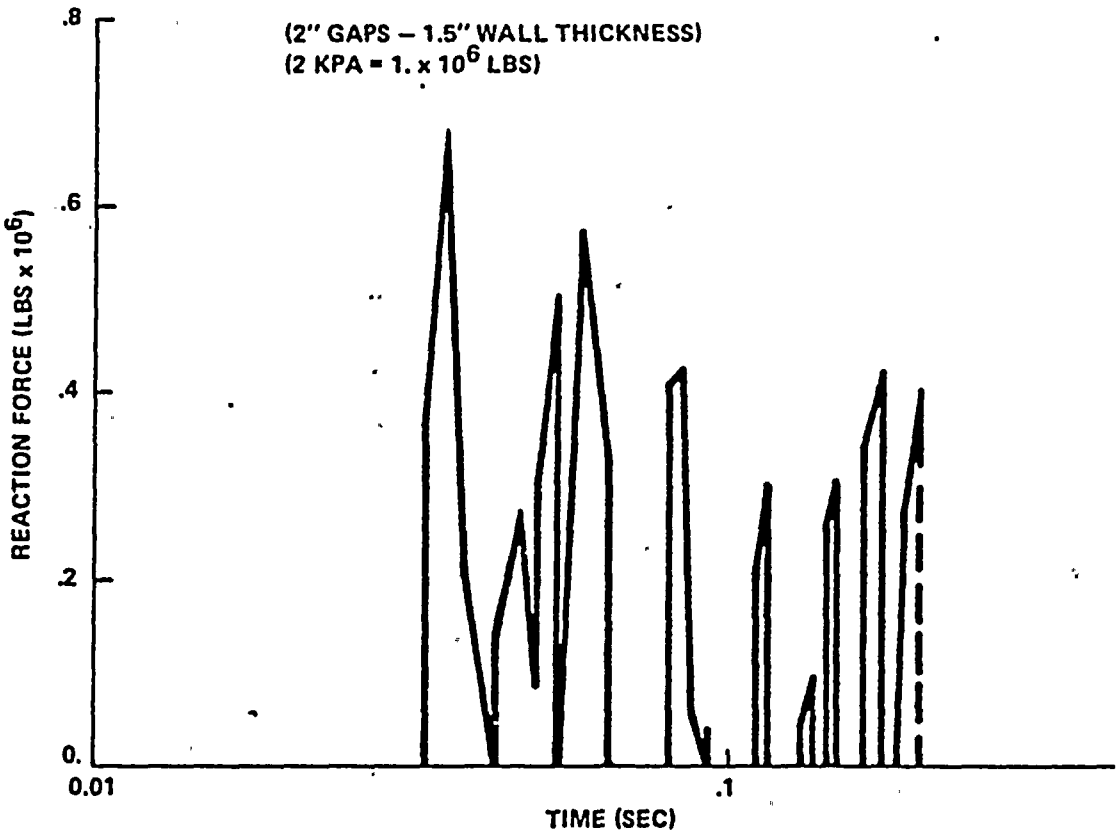

FLORIDA POWER & LIGHT COMPANY
ST. LUCIE PLANT UNIT 1

20" FW LINE OUTSIDE CONTAINMENT
REACTIONS AT PIPE WHIP RESTRAINT
AT NODE 5 VS. TIME
FIGURE 3.6-67

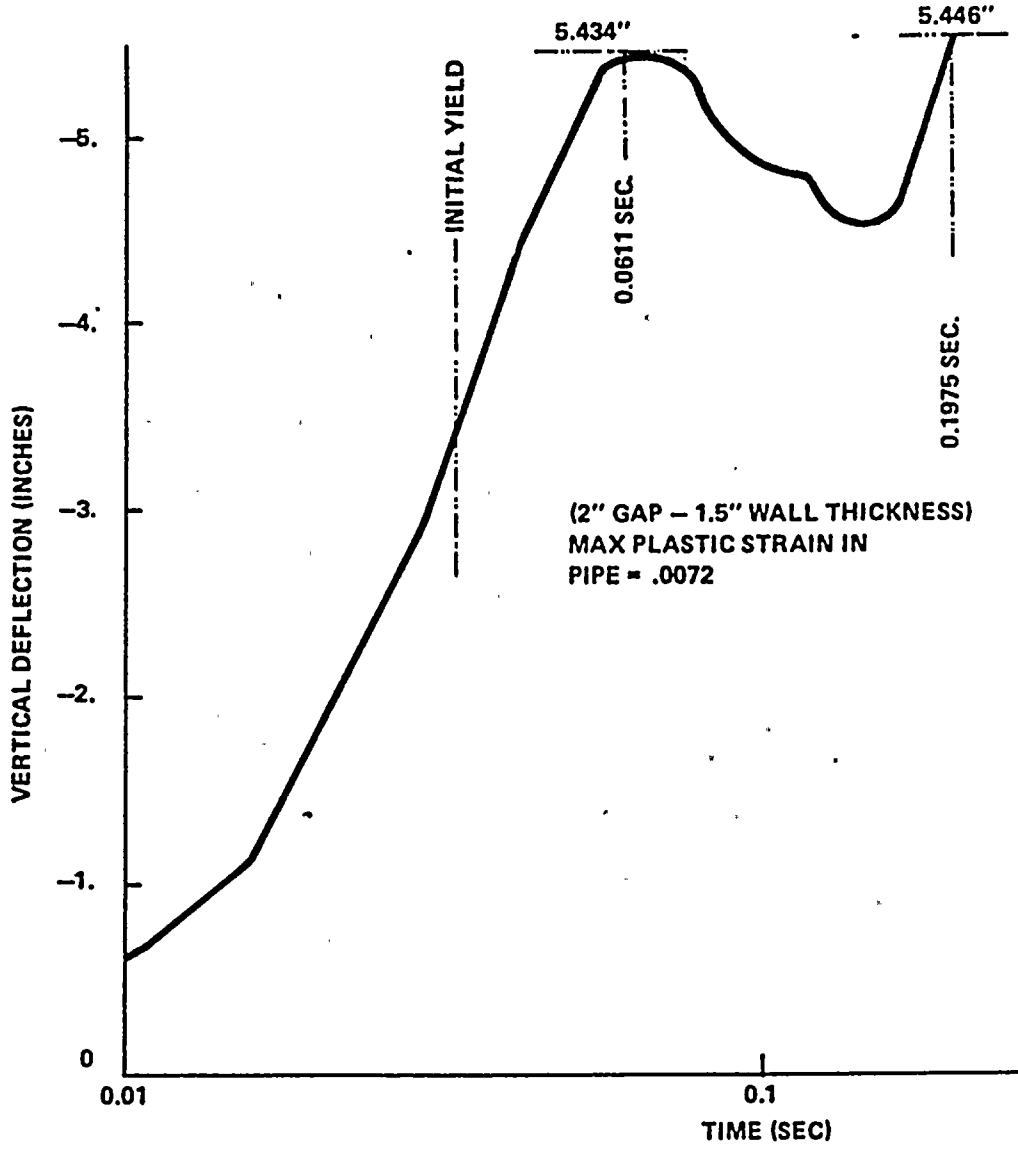

FLORIDA POWER & LIGHT COMPANY
ST. LUCIE PLANT UNIT 1

20" FW LINE OUTSIDE CONTAINMENT
DISPLACEMENT OF NODE 7 VS. TIME
FIGURE 3.6-68

Attachment C

PLAST Information from Reference 9

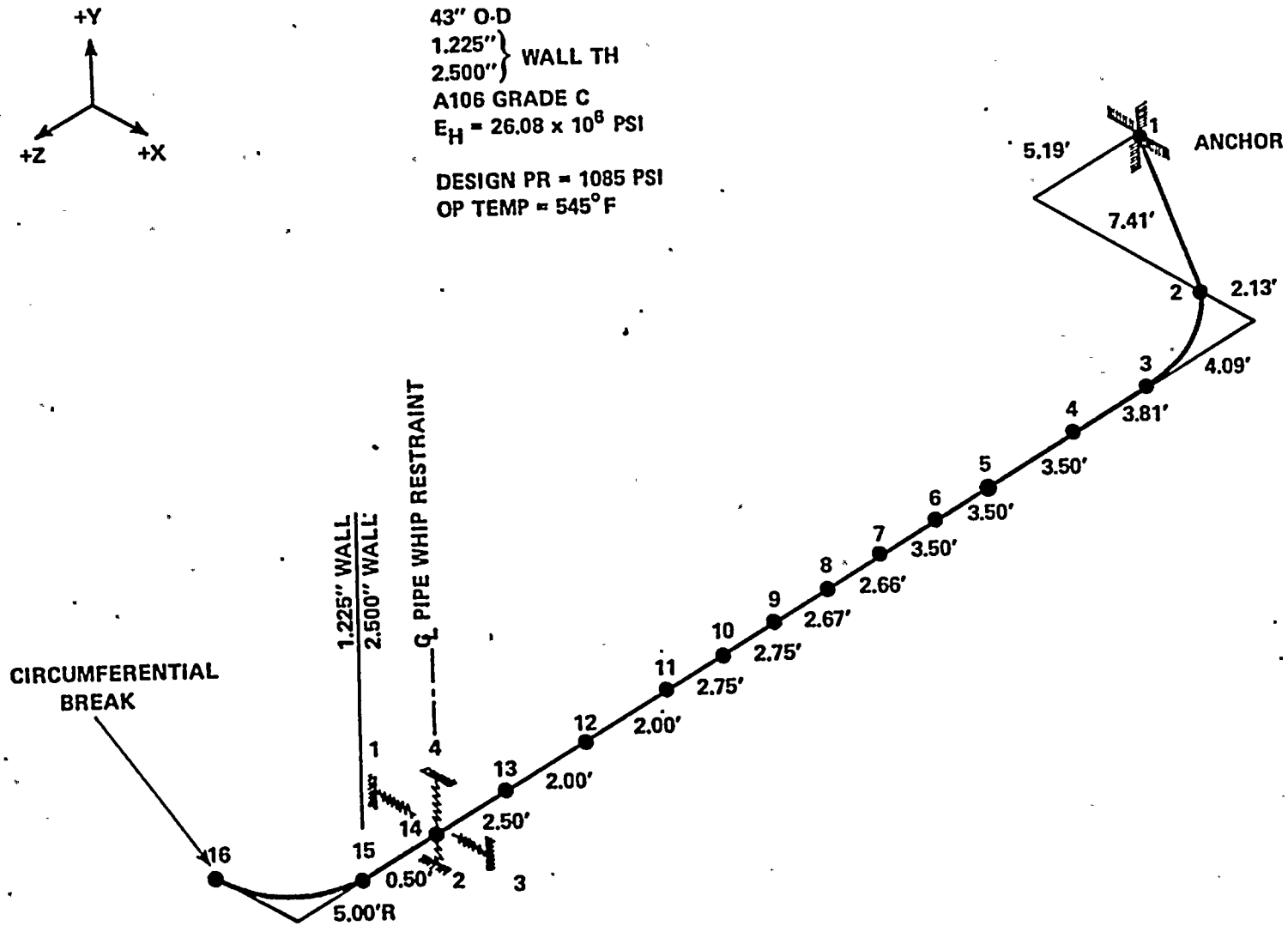

CIRCUMFERENTIAL BREAK IN MAIN STEAM LINE

FIGURE: 2.3.1

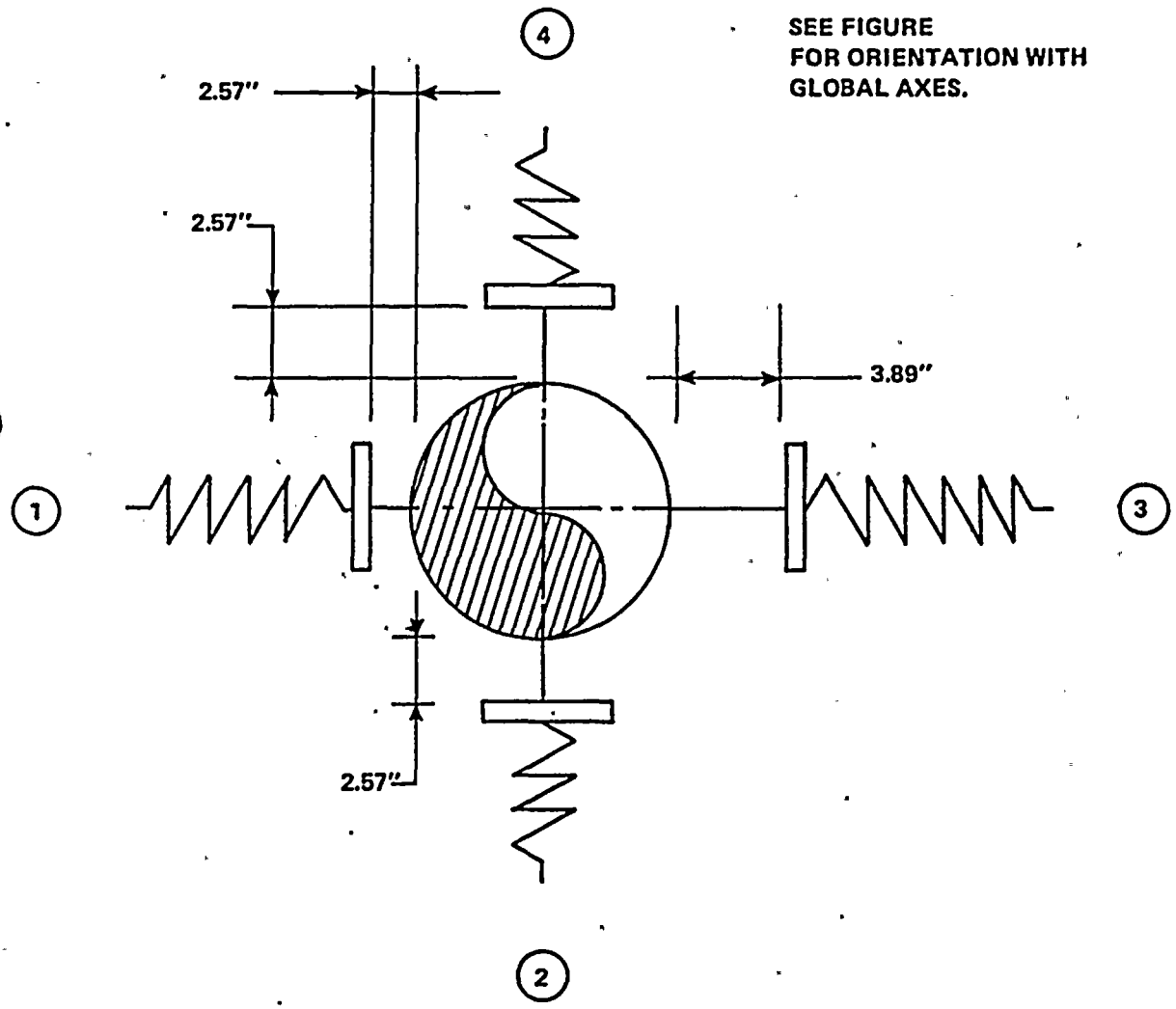

EFFECTIVE GAPS AT RESTRAINT AT NODE 14

FIGURE: 2.3.2

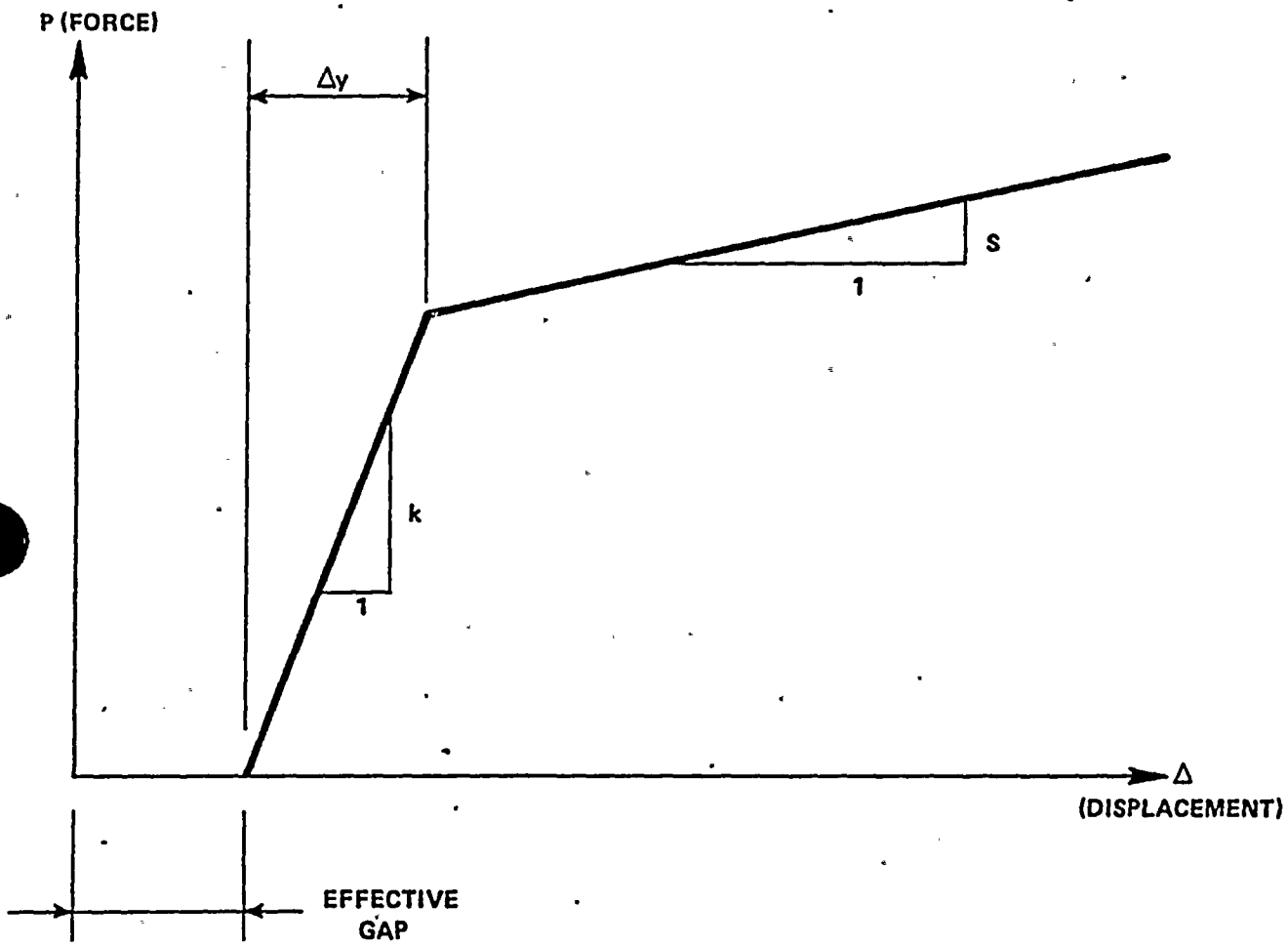

SPRING #	k (psi)	S (psi)	Δy (in)
1	6.95×10^6	2.99×10^4	0.15
2	"	"	"
3	5.95×10^6	"	0.20
4	6.95×10^6	"	0.15

FORCE - DISPLACEMENT DIAGRAM FOR RESTRAINTS

IN 43" MAIN STEAM LINE

FIGURE: 2.3.3

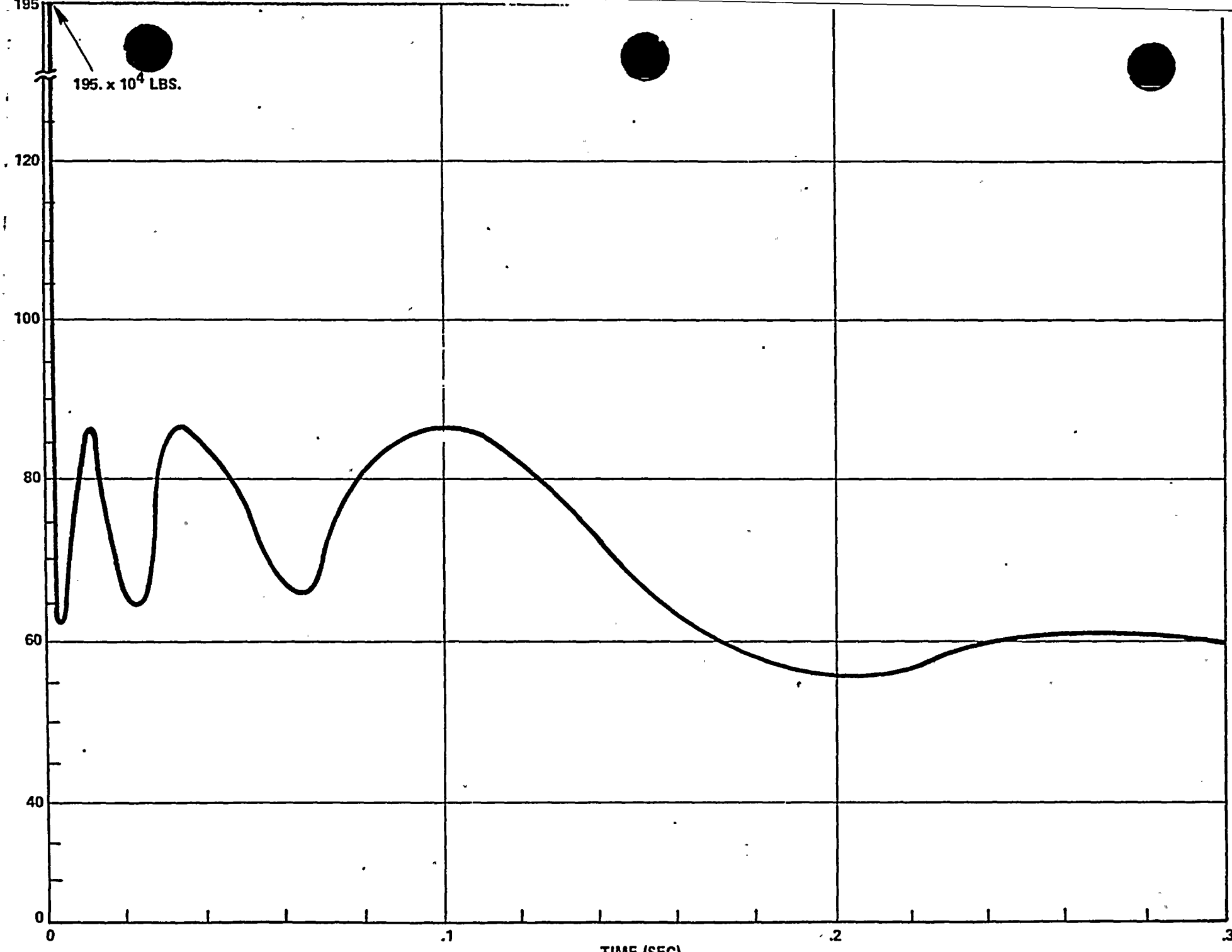

BLOWDOWN FORCE VS. TIME AT NODE 16 IN MAIN STEAM LINE
FIGURE: 2.3.4

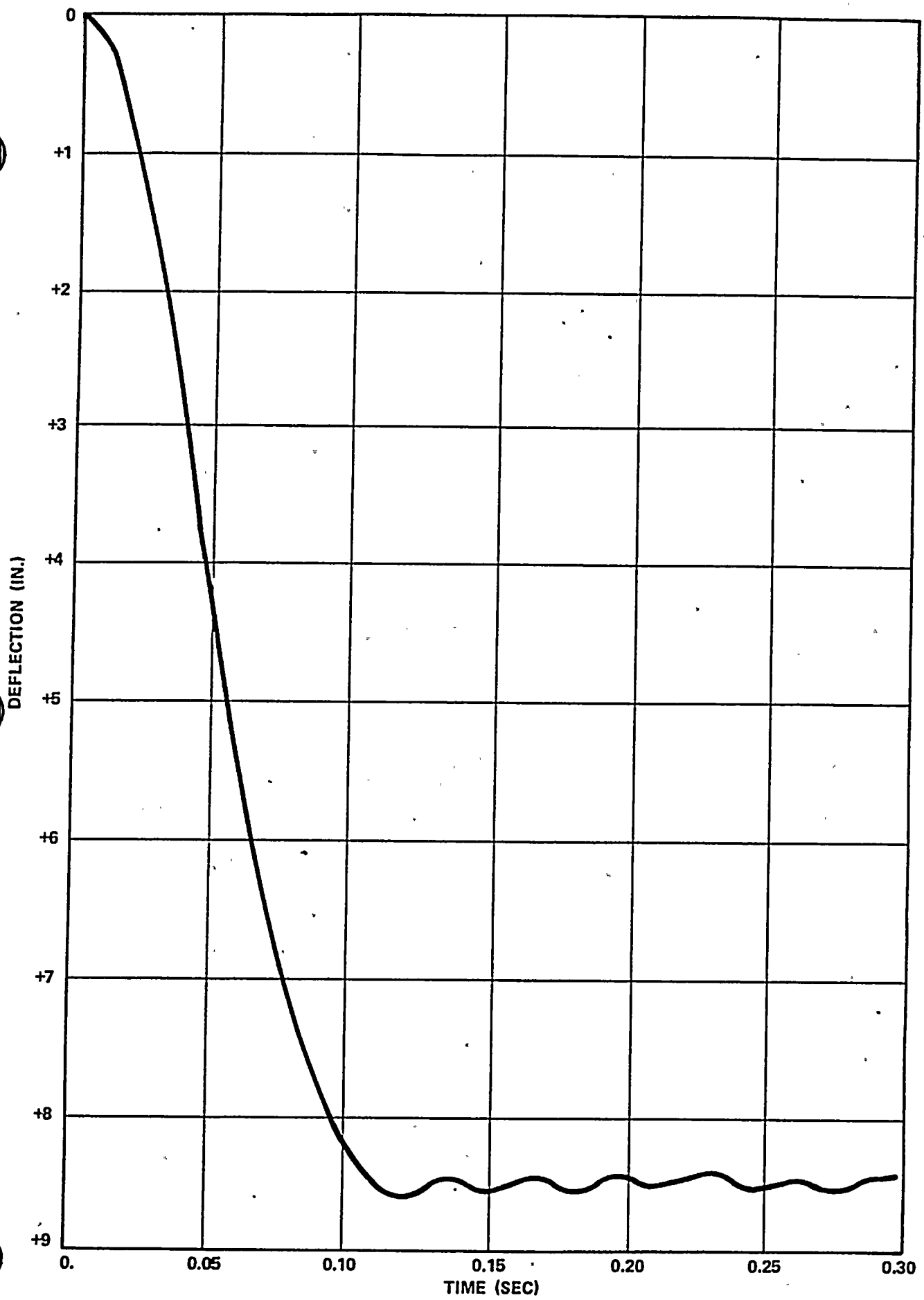

DEFLECTION OF RESTRAINT
(NODE #14)
IN (+x) DIRECTION

FIGURE: 2.3.5

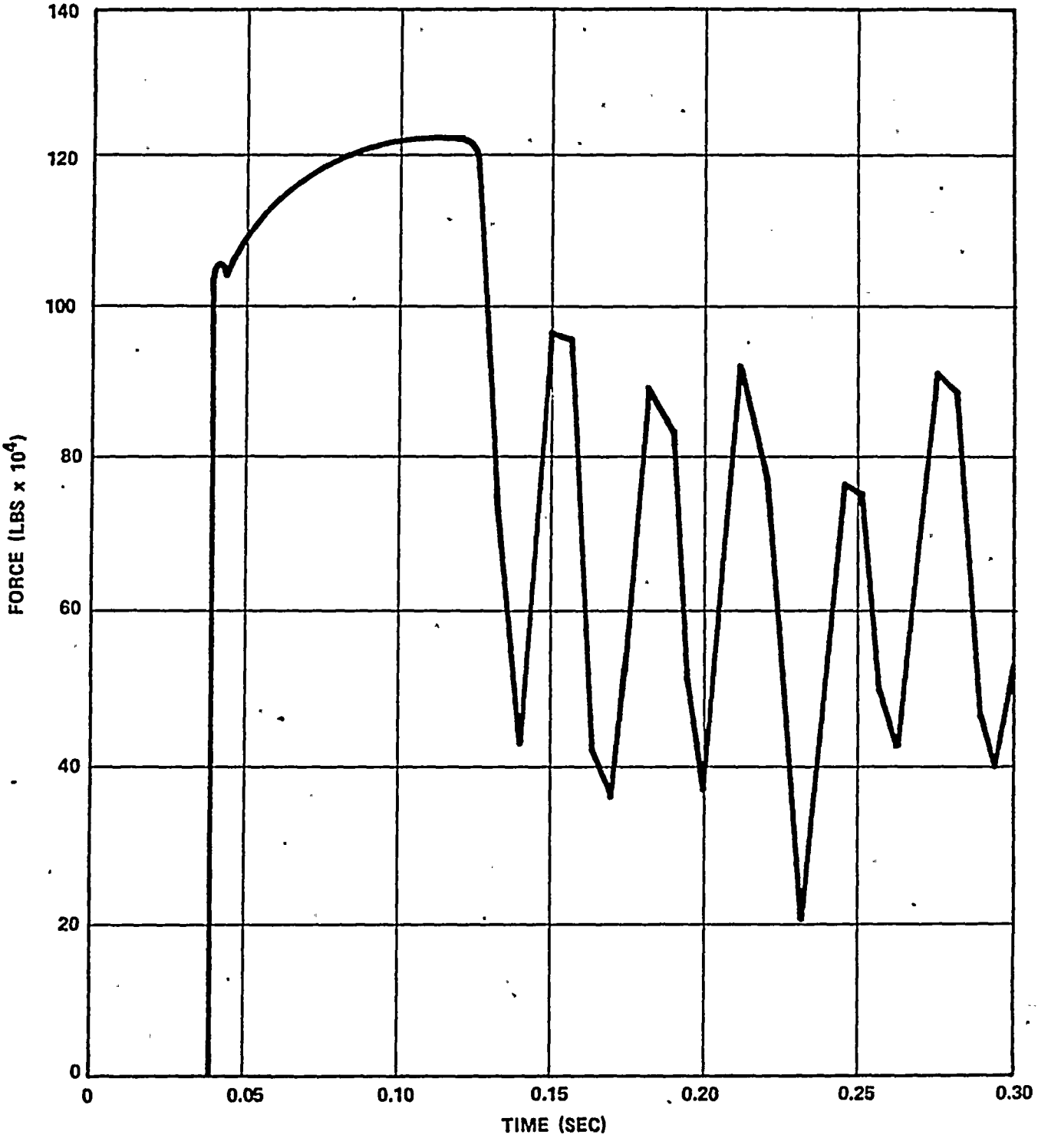

FORCE ON RESTRAINT
AT NODE #14

FIGURE: 2.3.6

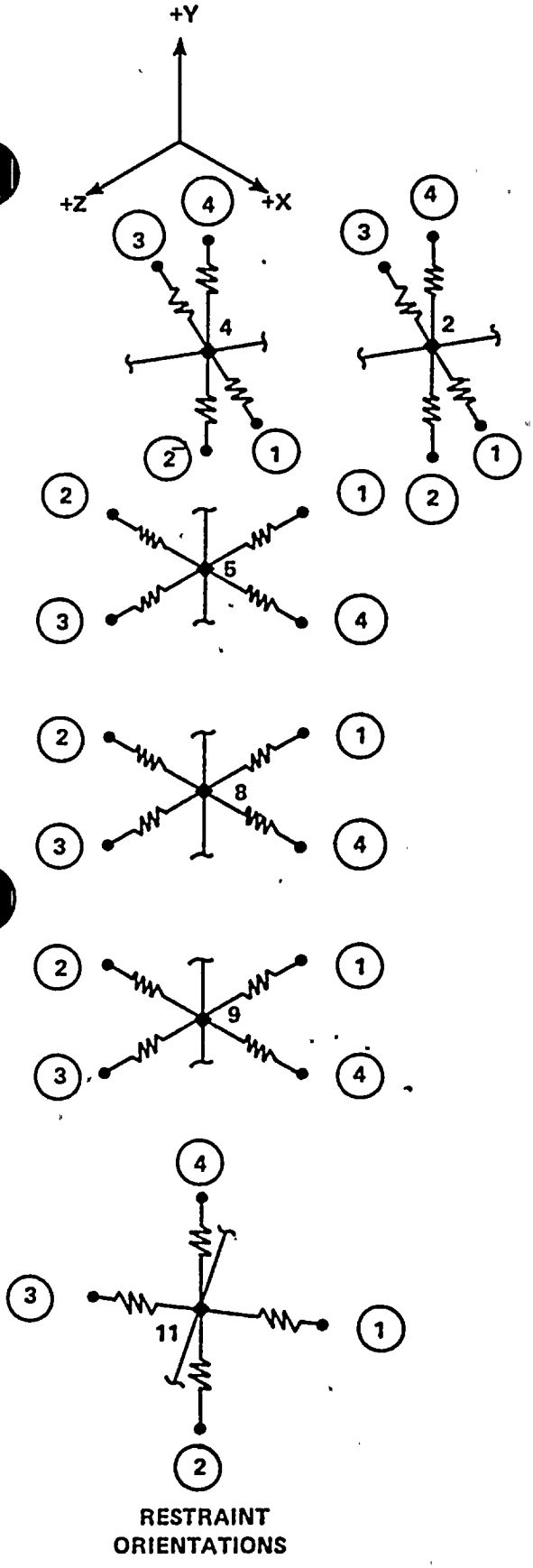

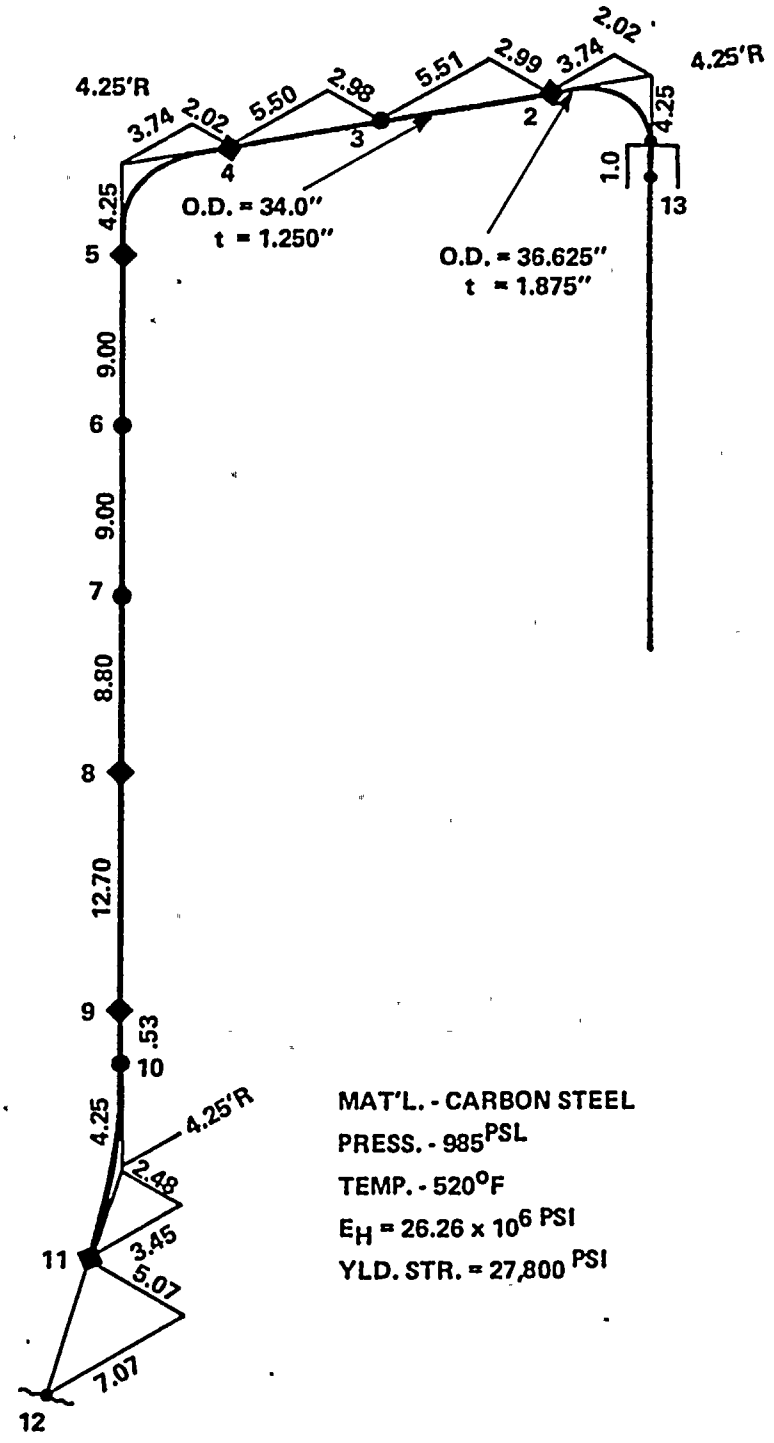

NAIN STM. LINE TRANSVERSE BREAK AT NODE #12

FIGURE: 2.3.7

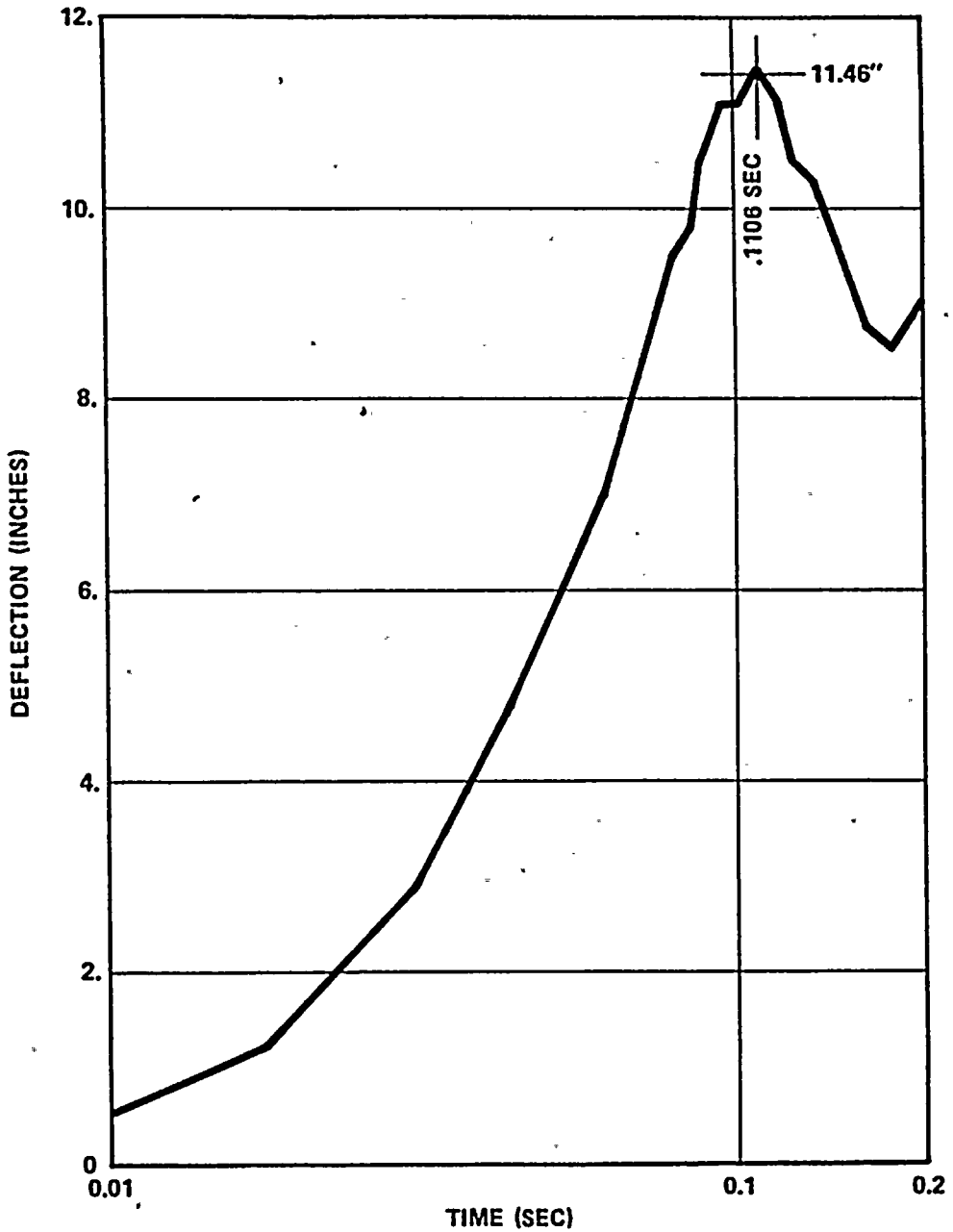

MAXIMUM PLASTIC
STRAIN = 0.0762

MAIN STEAM LINE (BREAK AT NODE 12) DEFLECTION OF NODE 12 VERSUS TIME

FIGURE: 2.3.8

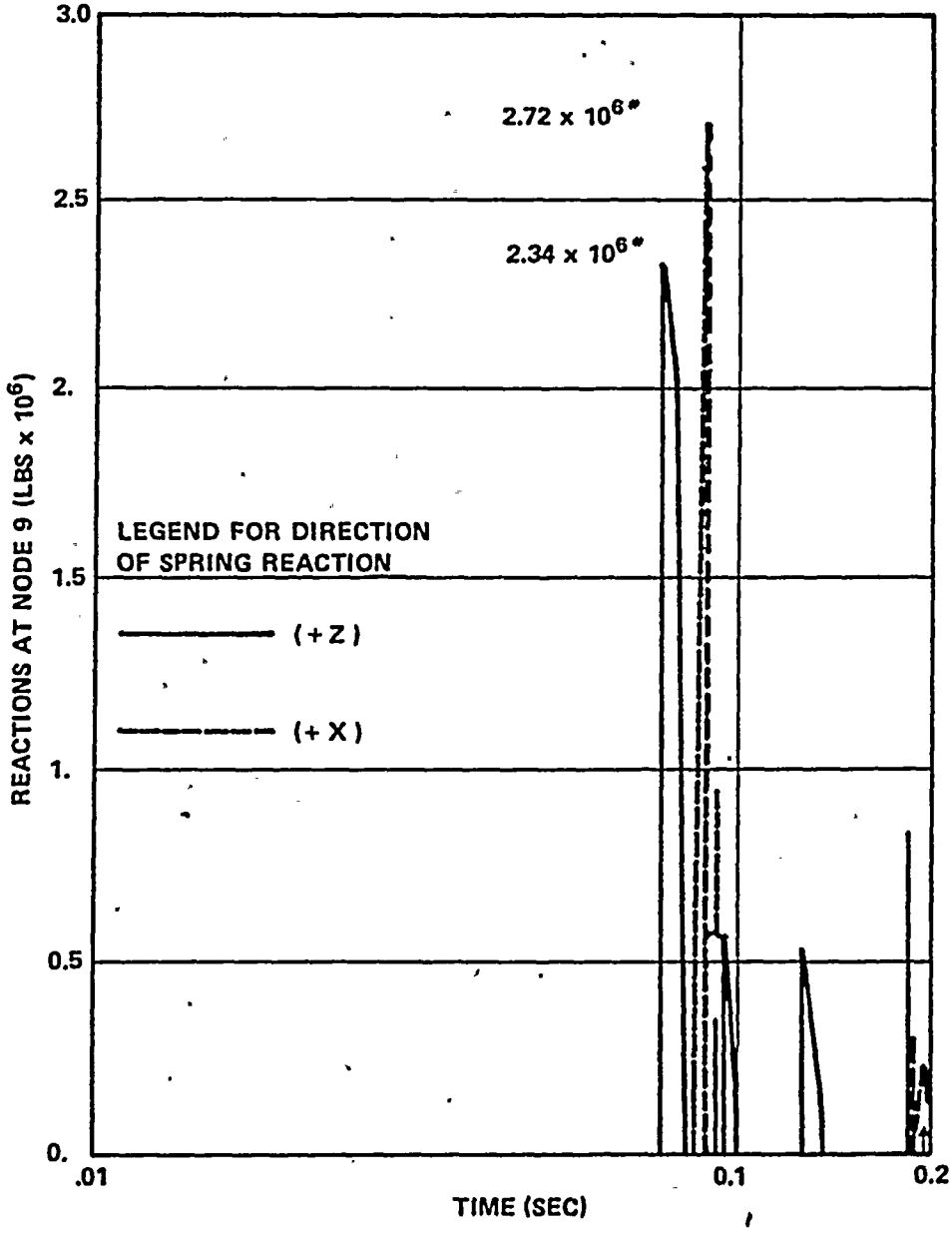

MAIN STEAM LINE BREAK AT NODE 12 REACTION AT
PIPE WHIP RESTRAINT AT NODE 9 IN + X & + Z DIRECTIONS VERSUS TIME

FIGURE: 2.3.9

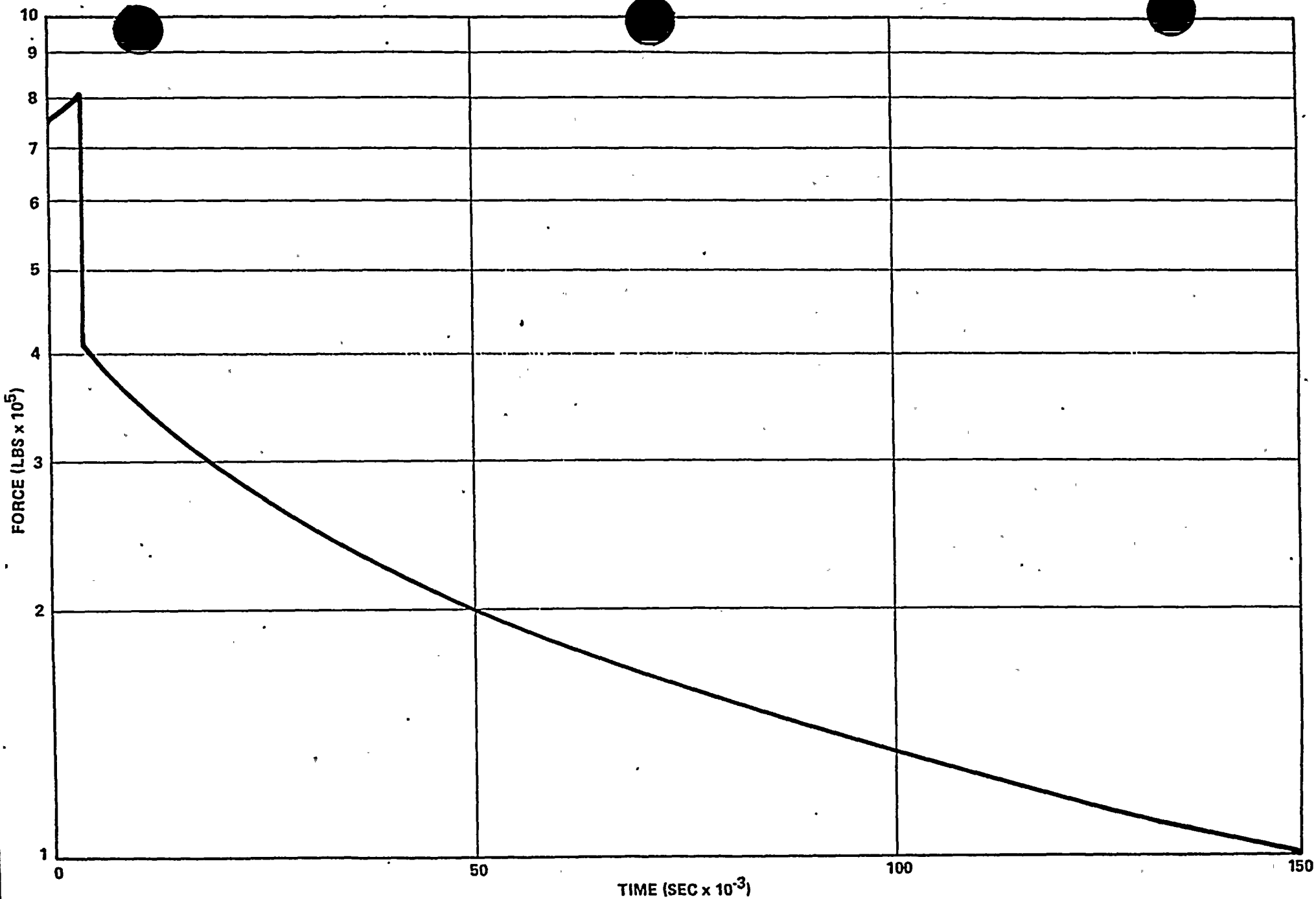

MAIN STEAM BLOWDOWN FORCE

FIGURE: 2.3.10

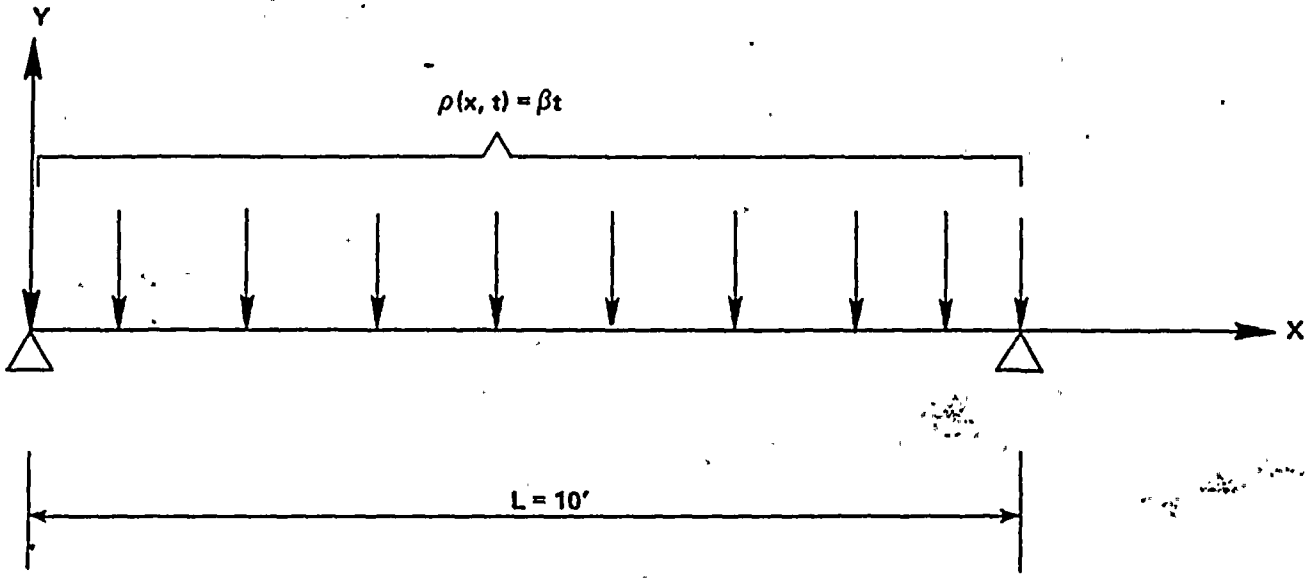

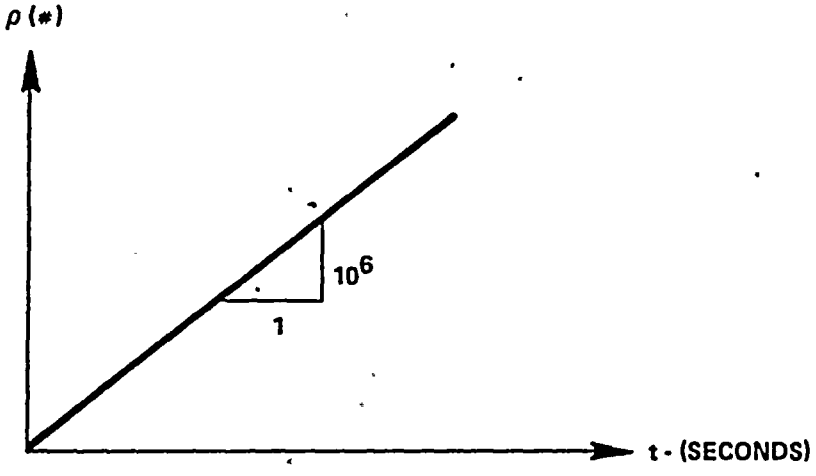

E = 30×10^6 psi

I = 28.1 in^4

β = 10^6 #/SEC.

γ = 0.25

W = 18.9 #/FT.

Mo = $\frac{wL}{8}$

ELASTIC BEAM UNDER UNIFORM DYNAMIC LOAD

FIGURE: 3.1.1

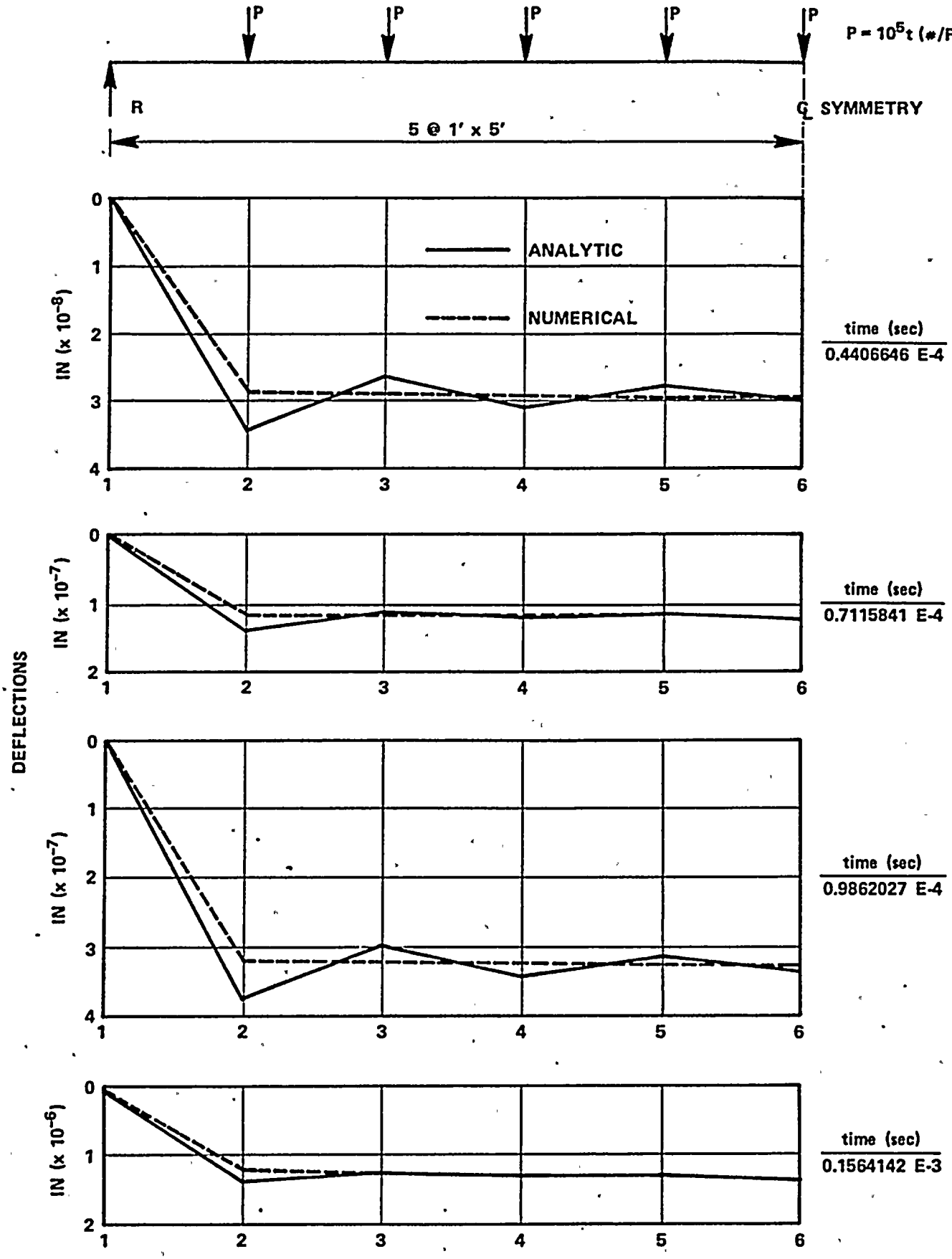

DEFLECTION HISTORY -
UNIFORM SIMPLE BEAM

FIGURE: 3.1.2A

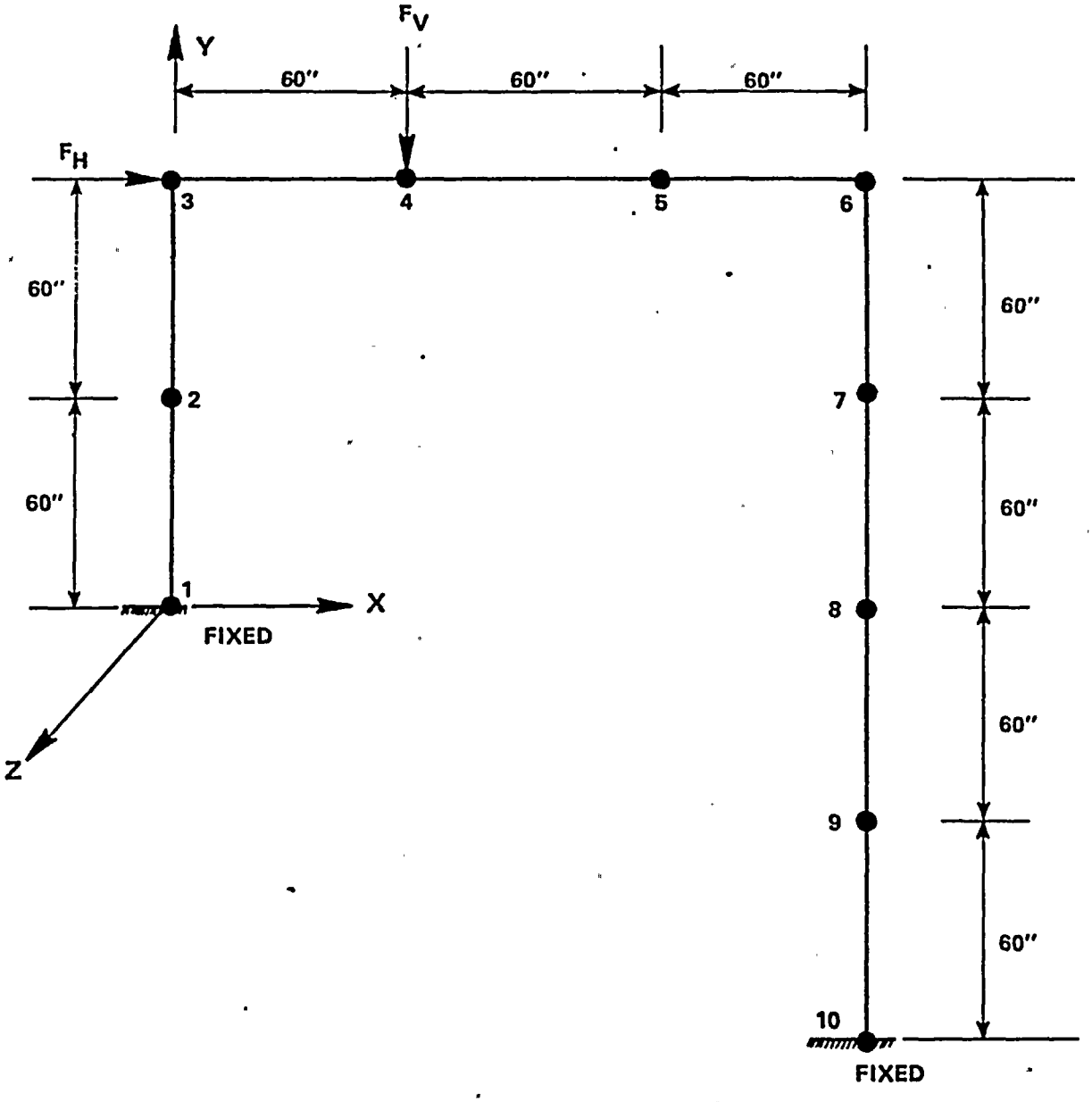

10 MASS PLANE
FRAME

FIGURE: 3.1.3B

ELASTIC-P IC FRAME

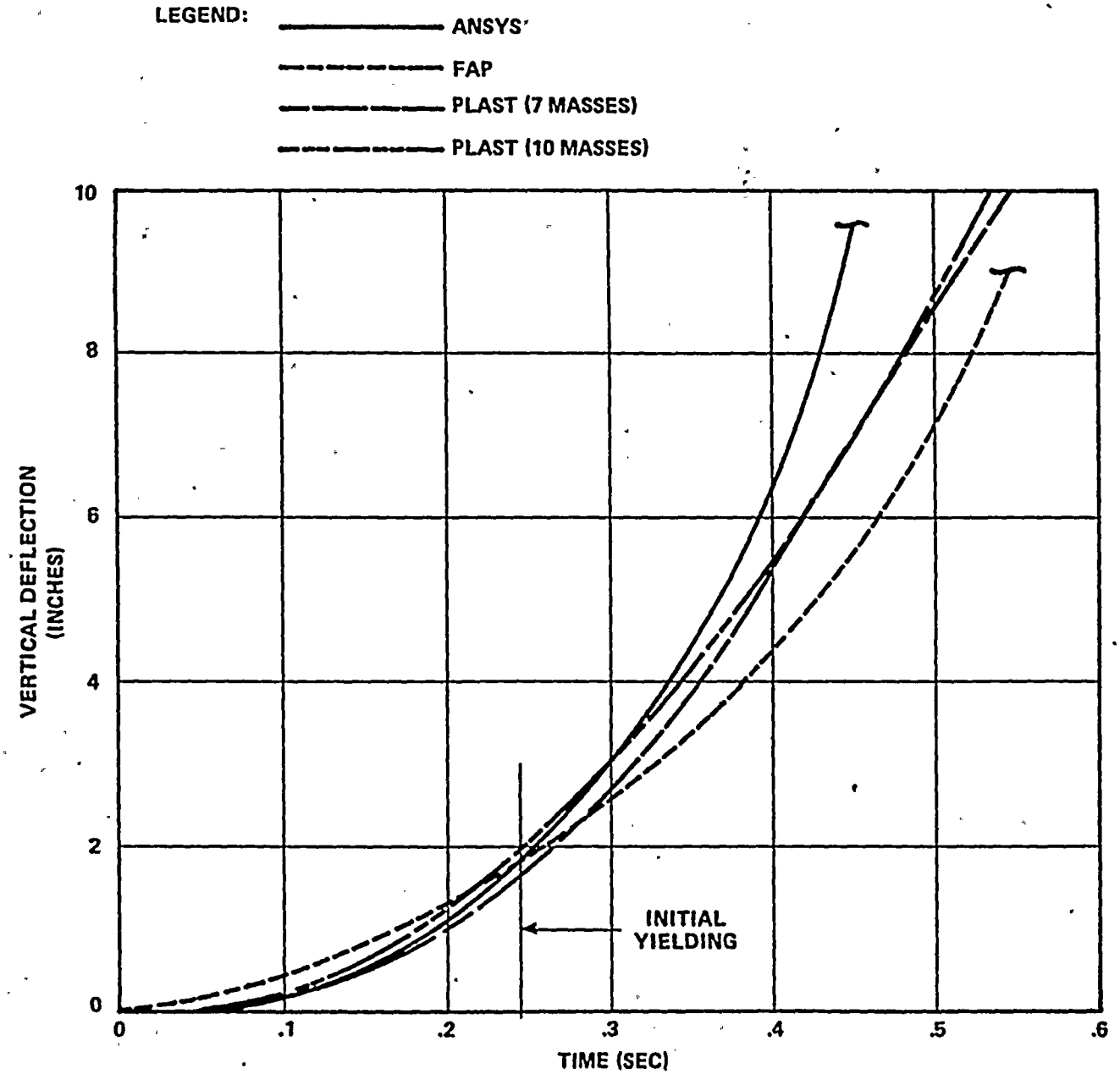

FIGURE: 3.1.5A

ELASTIC-PLASTIC FRAME

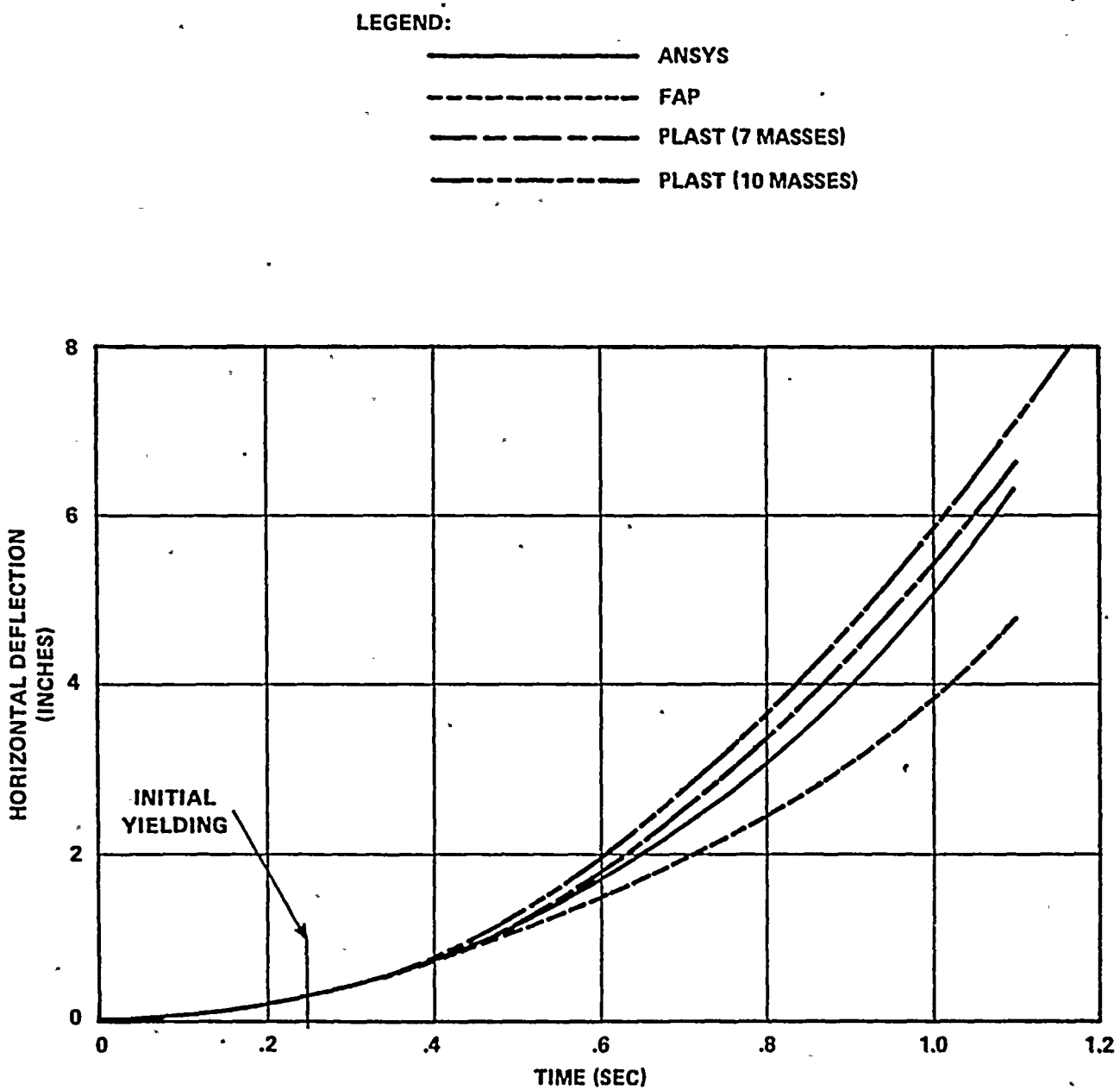

FIGURE: 3.1.5B

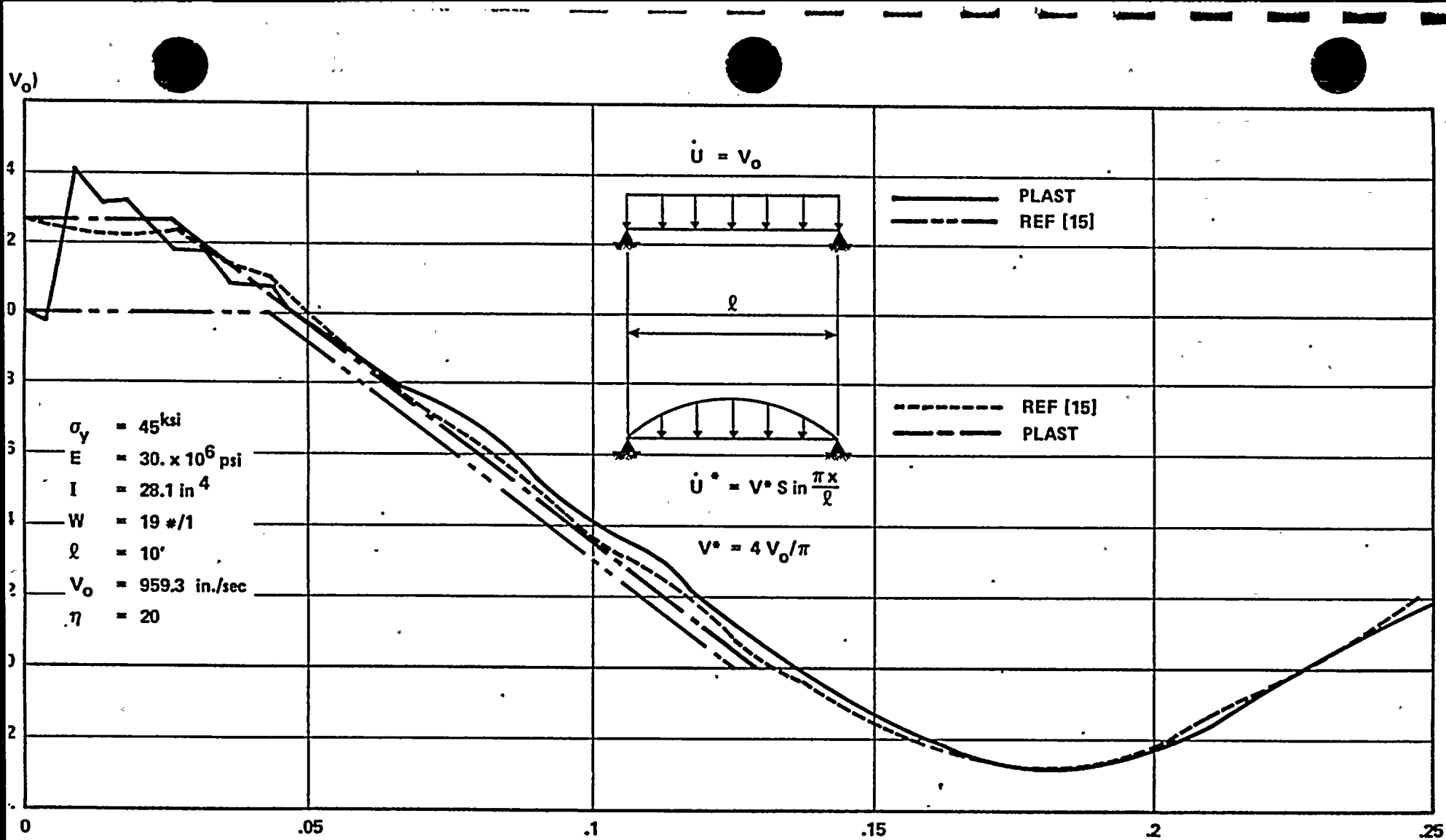

REF 15 above: "Approximate Solutions for Impulsively Loaded Elastic-plastic Beams" J.B. Martin, LSS Lee, J. Appl. Mech. (Paper #68 WA/APM-23)

CENTRAL VELOCITY VS. TIME.

FIGURE:3.1.6A

$$V^* = \frac{-4VO}{\pi}$$

$$\dot{U}^* = V^* \sin\frac{\pi x}{\ell}$$

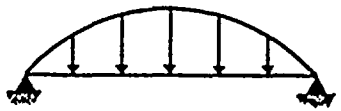

REF [15] & PLAST

PLAST

$\frac{\tau}{H}$ →

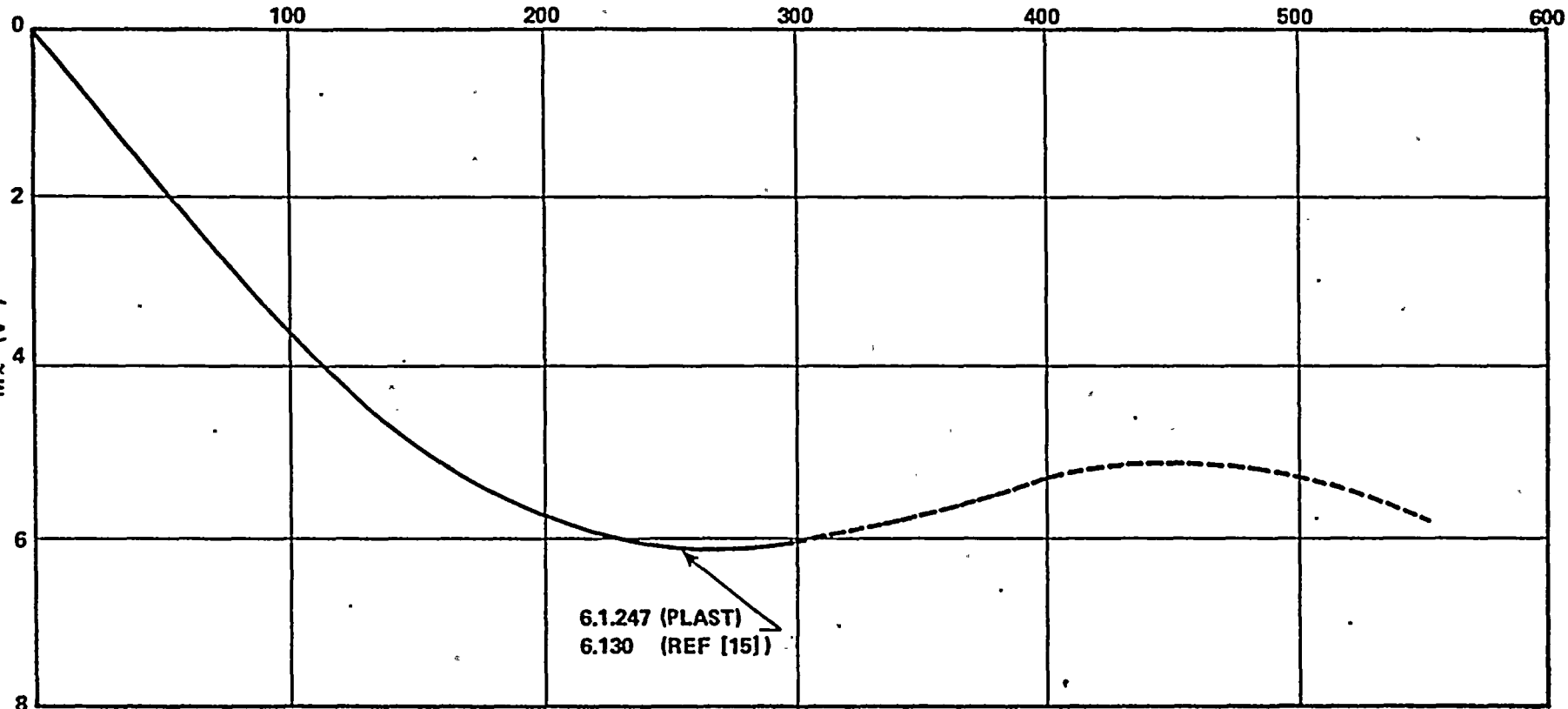

REF 15 above: "Approximate Solutions for Impulsively Loaded Elastic-Plastic Beams" J.B. Martin, L.S.S. Lee, J Appl Mech (Paper #68 WA/APM-23)

$$\tau = \frac{10^2 \, Mo \, t}{MV^*\ell^2}$$

$$H = \frac{1}{1.8\pi\sqrt{\eta^*}}$$

$\eta^* = 20$

CENTRAL DEFLECTION VERSUS TIME

FIGURE: 3.1.6B

Attachment D

Appendix B from Refernce 1

APPENDIX B

DESCRIPTION OF CALPLOTFIII

B-I Mathematical Model

The CALPLOTFIII computer code has been written to convert the transient flow conditions calculated in a piping system by the RELAP5MOD 1 Computer code into transient forces on the piping system. Specifically, CALPLOTFIII calculates and plots the forces on straight lengths of pipe between changes in pipe direction (bends), or between a change in direction and a pipe break. The derivation of the equations used in the code are given below.

B-I-1 Straight Lengths of Pipes between Directional Changes

The force on a straight length of pipe between direction changes (Figure B.1) is calculated using the momentum equation:

$$\bar{F}_s + \iiint_{cv} \bar{B}\rho dv = \oiint_{cs} \bar{V}\,(\rho\bar{V} \cdot d\bar{A}) + \frac{\partial}{\partial t}\left(\iiint_{cv} \bar{V}\,(\rho dv)\right) \tag{B1}$$

If the gravity term is assumed negligible, the following equation results:

$$\bar{F}_s = \oiint_{cs} \bar{V}\,(\rho\bar{V} \cdot d\bar{A}) + \frac{\partial}{\partial t}\left(\iiint_{cv} \bar{V}\,(\rho dv)\right) \tag{B2}$$

Since the force on the straight pipe length only exists in one dimension, the above equation can be written in a scalar form:

$$F_s = \oiint_{cs} V\,(\rho\bar{V} \cdot d\bar{A}) + \frac{\partial}{\partial t}\left(\iiint_{cv} V\rho dv\right) \tag{B3}$$

Since the RELAP5 MOD 1 Computer code calculates the pressures and the flowrates at different physical positions in the piping system, it is necessary to subdivide a piping length into two control volume types for application of the momentum equation. The first division creates the pressure control volumes. The divisions for the pressure control volumes are the positions in the pipe length where the pressures are calculated by the computer code, and serve as the boundaries across which the control volume surface forces are calculated. The second control volume divisions are due to flow conditions. The boundaries of the flow control volumes are located at the pipe length locations where flows are calculated by the computer code. The forces in the pipe length which are due to the rate of efflux of momentum across a control volume and the change of momentum in a control volume are calculated using the flow boundaries as flow control volume divisions.

The resultant force on the fluid across the boundary of the pressure control volumes 1, 2, and 3, shown in Figure B.1, are:

$$F_{S1} = -(P_A - P_a)\ A_A + R_1 \tag{B4}$$

$$F_{S2} = P_A\ A_A - P_B\ A_B + P_a\ (A_B - A_A) + R_2 \tag{B5}$$

$$F_{S3} = (P_B - P_a)\ A_B + R_3 \tag{B6}$$

The net surface force on the straight pipe length is obtained by summing equations B4, B5, and B6:

$$F_{S1} + F_{S2} + F_{S3} = R_1 + R_2 + R_3 \tag{B7}$$

$$F_S = R \tag{B8}$$

Therefore, the force on the straight pipe length due to surface forces is equal to the net normal and shear stresses on the pipe wall length.

The right side of equation B3 can now be evaluated for each of the flow control volumes A and B:

$$F_{S1} = \frac{\rho_2\ V_2^2}{g}\ A_A + \frac{\partial \dot{M}_A}{\partial t}\ \Delta A \tag{B9}$$

$$F_{S2} = \frac{-\rho_2\ V_2^2\ A_A}{g} + \frac{\partial \dot{M}_B}{\partial t}\ \Delta B \tag{B10}$$

Since the RELAP5 computer code calculates non thermal equlibrium conditions for two phase flow conditions and allows the two phases to possess different velocities, the parameters of equations (B9), (B10) are defined as:

$$\dot{M}_A = (\rho_{1A} V_{1A}\ (1-\alpha_A) + \rho_{gA} V_{gA} \alpha_A)\ A_A \tag{B11}$$

$$\dot{M}_B = (\rho_{1B} V_{1B}\ (1-\alpha_B) + \rho_{gB} V_{gB} \alpha_B)\ A_B \tag{B12}$$

$$\rho_2 V_2^2 = \rho_{12} V_{12}^2\ (1-\alpha_2) + \rho_{g2} V_{g2}^2 \alpha_2 \tag{B13}$$

Summing equations B9 and B10, and using equation B8, the net fluid force on the pipe length can be obtained:

$$K = -F_S = -R = \frac{-\partial \dot{M}_A}{\partial t} \Delta A - \frac{\partial \dot{M}_B}{\partial t} \Delta B \qquad (B14)$$

If the straight length of pipe considered is bounded by a directional change and an open end, a break, the forces obtained using equation B11 must be modified to accoun' for the force developed at the pipe exit plane. Consequently, using the momentum equation, the force on the straight pipe length shown on Figure B.2, for unchoked break flow, can be written as:

$$K_{unc} = \frac{-\rho_2 V_2^2 A_2}{g} - \frac{\partial \dot{M}_A}{\partial t} \Delta A \qquad (B15)$$

If choked break flow is determined to exist by the fluid transient computer code, then equation B15 must be modified to account for the pressure unbalance that occurs at the pipe exit plane. A rederivation of the equation for the straight pipe length for this case results in the following relation:

$$K_{ch} = -(P_2 - P_a) A_2 \frac{-\rho_2 V_2^2}{g} A_2 \frac{-\partial \dot{M}_A}{\partial t} \Delta A \qquad (B16)$$

or

$$K_{ch} = K_{unc} - (P_2 - P_a) A_2 \qquad (B17)$$

where:

$$P_2 = P_A + \frac{\rho_A V_A^2}{2g} - \frac{\rho_2 V_2^2}{2g} - \Delta P_f - \Delta P_{acc} - \Delta P_{el} \qquad (B18)$$

$$P_2 \simeq P_A + \frac{\rho_A V_A^2}{2g} - \frac{\rho_2 V_2^2}{2g} \qquad (B19)$$

$$\rho_A V_A^2 = \rho_{1A} V_{1A}^2 (1-\alpha_A) + \rho_{gA} V_{gA}^2 \alpha_A \qquad (B20)$$

Nomenclature

A	flow area
B	body force of a control volume
F_s	surface force resultant on a control volume
g	gravitational constant
K	force of fluid in piping
M	control volume flowrate
P	pressure
P_a	pressure outside pipe control volumes
R	normal and shear stresses in a control volume
t	time
v	volume of a control volume
V	velocity of fluid in a control volume

Greek Letters

ρ	density in control volume
α	void fraction

Subscripts

acc	acceleration
f	friction
ch	choked flow
cs	control surface
cv	control volume
el	elevation
unc	unchoked
l	liquid
g	gas

Figure B.1

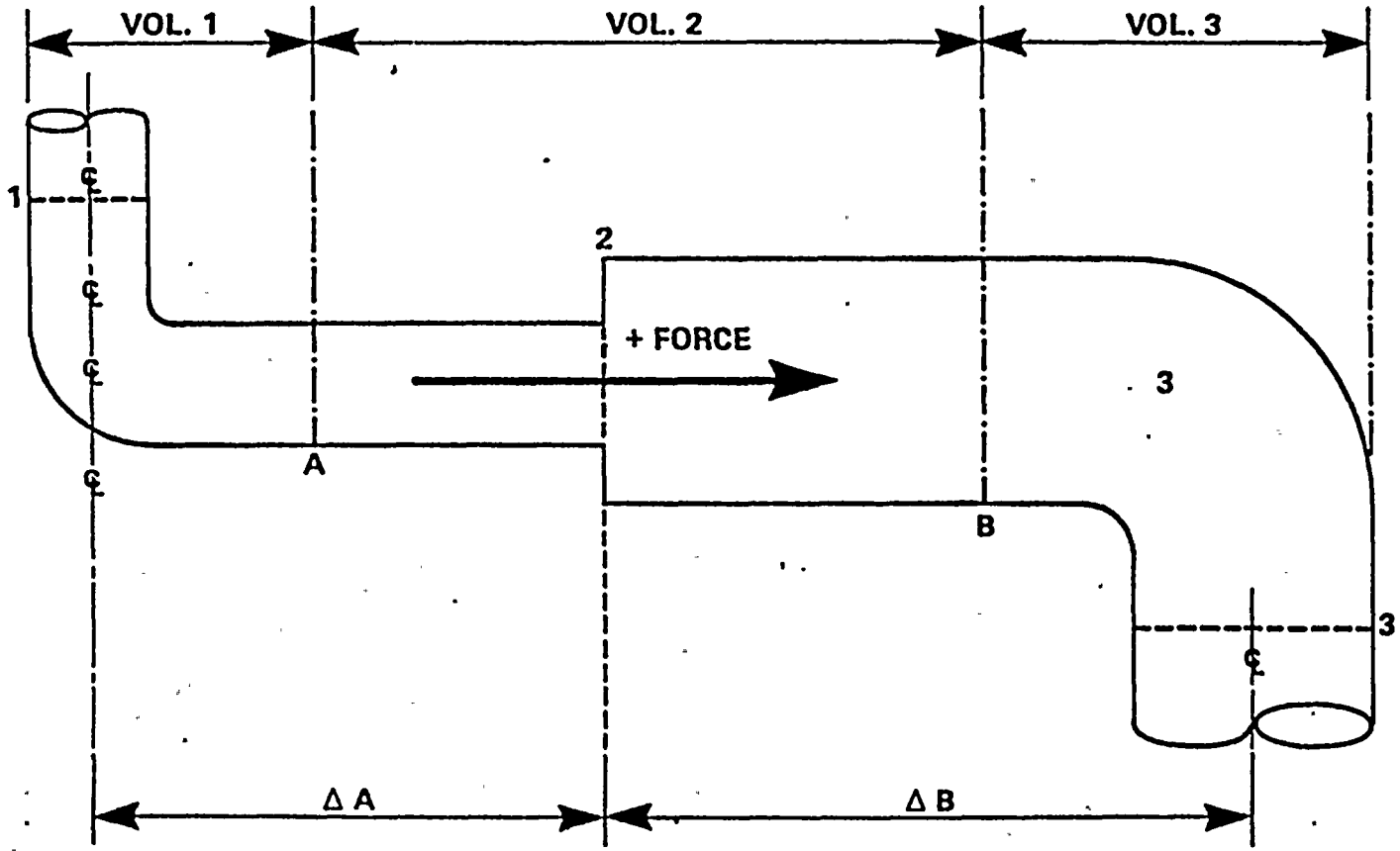
VOL. 1
VOL. 2
VOL. 3
1
2
3
3
A
B
+ FORCE
ΔA
ΔB
LEGEND:
PRESSURE BOUNDARY
FLOW BOUNDARY

Figure B.2

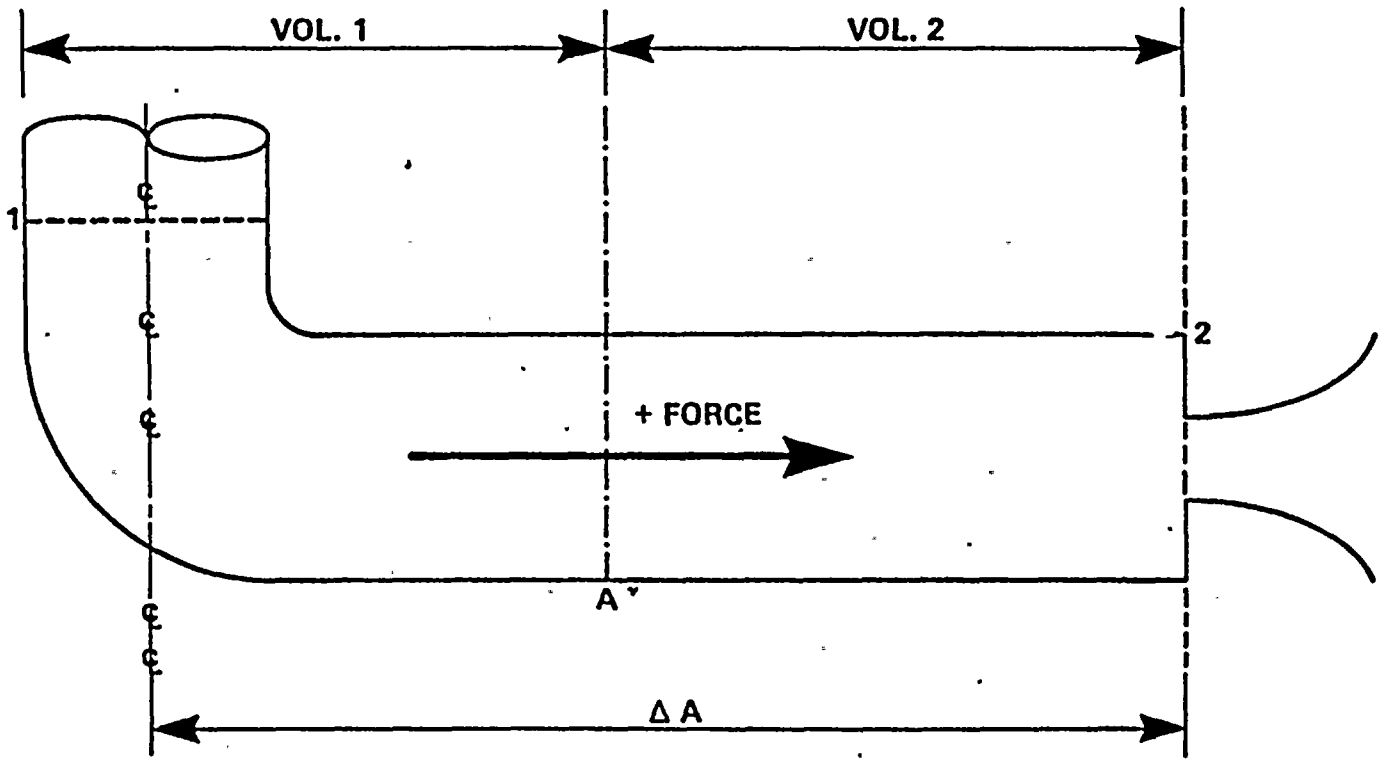

LEGEND:

—·—·— PRESSURE BOUNDARY

------- FLOW BOUNDARY

QUESTION NO. 8

The submittal does not explain what loading combinations were considered in the analysis to determine acceptability of the piping system, therefore, identify the load combinations performed together with allowable stress limits for piping and supports both upstream and downstream of the valves. The letter of September 1, 1982, indicates that the ANSI B31.1 code was used to evaluate stresses in the piping and supports unique to the PORV's. Identify all other governing codes and standards (with date of edition) used to determine piping and support adequacy.

RESPONSE

The load combinations and stress allowables which are used to determine the adequacy of the Turkey Point pressurizer relief piping system are identical to the criteria specified in the Turkey Point FSAR by which the plant was designed, specifically that is the non-seismic ANSI B31.1 (1955) criteria (for comparison purposes the calculated loads which are shown in Tables 4.3.1 and 4.3.2, attached to the response to Question 9, were combined according to the EPRI recommended load combination as provided in Reference 13 and shown in Table 2. Tables 4.3.1 and 4.3.2 were developed for piping upstream and downstream of the PORVs subjected to PORV actuation. The stress allowables for these tables correspond to References 5 and 6, accordingly and are included in Table 2).

The load combinations used to analyze the piping subjected to SRV actuation correspond to EPRI recommended load combinations as shown in Table 2. For

piping upstream of the SRV valves the stress allowables are as shown in Table 2. For piping downstream of the SRVs and subjected to SRV actuation, the moment developed in the piping is compared to 70 percent of the ultimate moment carrying capacity of the pipe. The ASME code itself allows use of this value to satisfy integrity criterias. For a further discussion of this point see the response to Question No. 9.